STUDIES IN THE CATALYTIC PROPERTIES OF SUPPORTED TRANSITION METAL COMPLEXES

THESIS

submitted for the degree of

DOCTOR OF PHILOSOPHY

of the

UNIVERSITY OF GLASGOW

by

JOHN ROBERTSON, B.Sc.

February, 1974

ProQuest LLC.
789 East Eisenhower Parkway
P.O. Box 1346
Ann Arbor, MI 48106 – 1346

ACKNOWLEDGEMENTS

I should like to express my gratitude to Dr. G. Webb for suggesting this problem and for his interest, advice and encouragement throughout the course of the work.

I should also like to thank Professor S.J. Thomson, Dr. K.C. Campbell and Dr. R.J. Cross for helpful discussion and suggestions.

I acknowledge also the assistance given by members of this Department. In particular, I should like to thank Mr. J. Connelly and his colleagues for their assistance with glassblowing; Mr. J. Hardy for designing and constructing both electronic integrators; Mrs. F. Lawrie for her help with the infra-red work; and Miss Frances Green for her assistance in the laboratory. My thanks also go to the boys of Room 276 for their moral support and camaradie.

Thanks are due to my mother for her assistance with the typing.

Finally, I gratefully acknowledge a Science Research Council Award for the duration of this work.

John Robertson

SUMMARY

The object of this research was to investigate possible relationships between homogeneous and heterogeneous catalysis at the interface by examining complexes of potential homogeneous catalytic activity, supported on an "inert" carrier, and by studying the catalytic activity of these complexes in the heterogeneous phase.

Attempts have been made to support a number of transition metal complexes on silica. From the observation of colour changes and changes in the infra-red spectra of the supported systems, it has been shown that some complexes, viz. ethylene palladous chloride, potassium ethylene trichloroplatinate and triiron dodecacarbonyl, decompose to the metal when supported by impregnation on the carrier from solution. Titanocene dichloride and rhodium trichloride retain their structures when so supported, while tristriphenylphosphine rhodium(I)chloride, when supported on silica, undergoes a structural rearrangement which is believed to involve the formation of a metal-hydride bond. Supported triruthenium dodecacarbonyl and triosmium dodecacarbonyl, although retaining their structures at ambient temperature and in an inert atmosphere, undergo chemical change on exposure to light, heat or air. By studying the ^{14}CO labelled dodecacarbonyls, it has been shown that this chemical change involves

the loss of carbon monoxide. It is postulated that such structural changes are due to the influence of hydroxyl groups on the surface of the support material.

The catalytic properties of titanocene dichloride, tristriphenylphosphine rhodium(I)chloride, rhodium trichloride, triruthenium dodecacarbonyl and triosmium dodecacarbonyl supported on silica have been investigated by studying their activities for the hydrogenation and isomerisation of but-1-ene in a pulse-flow reactor system.

Titanocene dichloride and tristriphenylphosphine rhodium(I)chloride when supported on silica possess negligible catalytic activity for these reactions.

Silica supported rhodium trichloride is active in the isomerisation of but-1-ene to cis and trans but-2-ene in the absence of molecular hydrogen. It has not been possible to determine whether this reaction proceeds via a 1-methyl-π-allyl or a 2-butyl intermediate.

Catalysts active in the hydrogenation and isomerisation of but-1-ene have been prepared by heating silica-supported triruthenium and triosmium dodecacarbonyl in helium and in vacuo, whereby the complexes undergo an irreversible transition with the loss of some carbon monoxide. It is believed that this activation involves the reaction of the complex with surface hydroxyl groups of the support, thereby forming a new cluster complex which possesses

sites capable of coordinating olefin molecules in a reactive form.

From investigations of the kinetics and energetics of the reactions of but-1-ene with hydrogen and deuterium over the supported ruthenium complex in a static system, and from the product distributions of these reactions, as determined by gas chromatography and mass spectrometry, it is concluded that the isomerisation reaction proceeds via a 1-methyl-π-allyl intermediate. It is also concluded that the hydrogenation and exchange reactions occur by a Rideal-Eley mechanism. Finally, evidence is presented to suggest that two distinct sites are present on this catalyst, probably the result of asymmetry induced in the molecule by its interaction with the surface.

INDEX

CHAPTER 1

I N T R O D U C T I O N

1.1 General Introduction

A catalyst is a substance which increases the rate of approach to equilibrium of a given chemical process with only slight modification of the free energy change of the process. Reactions over heterogeneous catalysts occur at the phase boundary between gases or liquids and solids, whereas in homogeneous catalysis the reactants and the catalytic species exist in the same phase.

In heterogeneous catalysis, supported metal systems, in which there is a high dispersion of metal crystallites on the support, are especially important, as the active metal catalyst has a very large surface area available for reaction. In the homogeneous system, the catalytic species is uniformly dispersed throughout the solvent as single molecules, each being available for attack by reactant molecules.

1.2 Adsorption

The modern theories of heterogeneous catalysis have developed from the work of Langmuir (1), who first postulated that gaseous atoms or molecules could adsorb on to a metal surface and there form an intermediate species.

Both physical and chemical adsorption have been recognised and these were first described semi-quantitatively by Lennard-Jones (2) in terms of a potential energy diagram.

Molecules which are physically adsorbed are held to the surface of the metal by weak dispersion forces. The process, which is random and non-activated, usually occurs at temperatures near the boiling point of the gas and the heat of adsorption, $-\Delta H_a$, is generally similar to the heat of liquefaction, this value being normally less than 6 Kcal. $mol.^{-1}$. In physical adsorption, the formation of multi-layers of gas molecules is possible.

Chemisorption, on the other hand, involves the formation of a chemical bond between the adsorbate and a surface site. This is the activating process which leads to reaction on heterogeneous catalysts (3). The heat of adsorption is normally in the range 10 - 100 Kcal. $mol.^{-1}$ and the bond lengths are in the range 1.5 to 3 $\mathring{A}$, comparable with the lengths of chemical bonds. As chemisorption occurs at a special surface site, the extent of adsorption depends on the number of surface sites available, the limit being monolayer coverage.

The adsorption process can be described by the potential energy curves shown in Fig. 1.1, which describes the case of hydrogen on a clean metal surface. If the

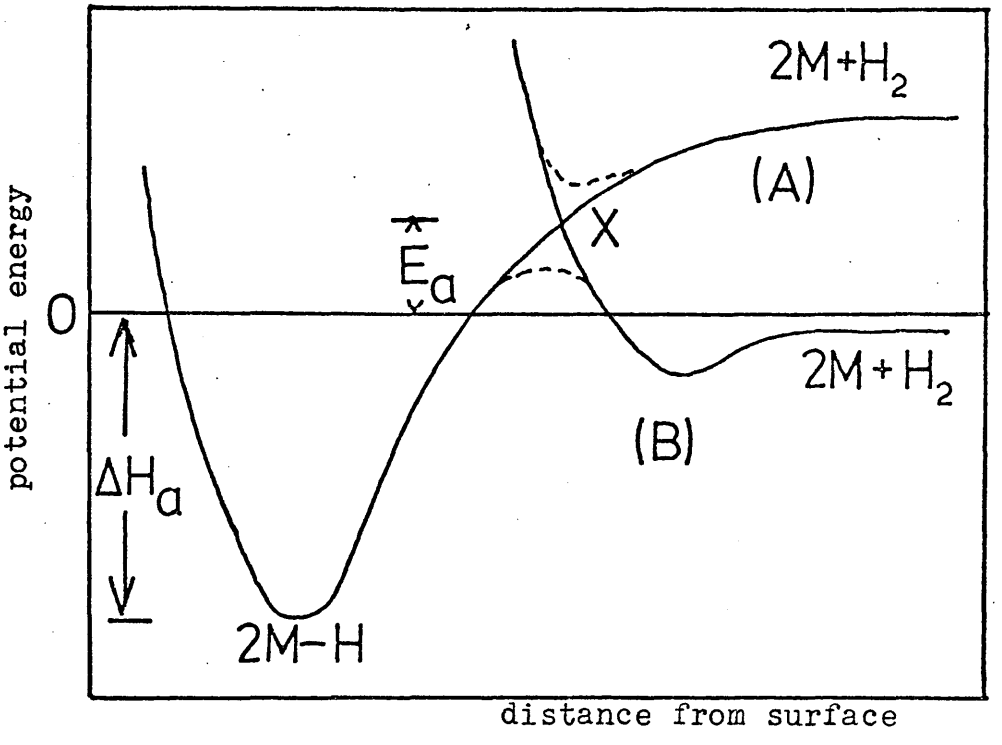

Fig. 1.1 Potential energy curves for (A) the chemisorption and (B) the physical adsorption of hydrogen on a metal surface.

physically adsorbed hydrogen molecule (curve B) can reach X, then, having attained the required activation energy, E_a, it may dissociate and become adsorbed. The heat of adsorption would then be $-\Delta H_a$.

At temperatures near the boiling point of the adsorbate, both physical and chemical adsorption may occur. By raising the temperature, the physically adsorbed species may be provided with the activation energy either to be converted to the chemisorbed state or to be removed from the surface.

1.3 Surface Heterogeneity, Geometric and Electronic Factors

The hypothesis that on the surface of a metal catalyst there would be occasional groups of atoms fixed in metastable positions associated with high energy and chemical unsaturation relative to the atoms of the regular lattice was first advanced by Taylor (4) in 1925. Such active centres might have exceptional catalytic and adsorptive power. This theory helped to explain the phenomena that the heat of adsorption generally decreases with increasing surface coverage, θ, (5) and that catalysts are often poisoned by much less poison than is required to form a monolayer, as had been observed by Pease (6,7). Although a number of concepts have been advanced to explain these

phenomena (8), that based on the heterogeneity of the surface itself (5), due to point imperfections, dislocations and impurities, is the most useful.

Because the d-character of a metal is related to the interatomic spacing (9), it is not possible to distinguish clearly between the concepts of the geometric and electronic factors when the electronic factor is expressed in terms of d-character.

That the activity of a catalyst is largely dependent on the presence of suitably spaced groups of atoms to accommodate reactant molecules was advanced by Balandin (10) in his multiplet theory of catalysis. He claimed that the catalytic decomposition of a relatively large molecule involves simultaneous adsorption at several points. In the dehydrogenation of cyclohexane and the hydrogenation of benzene, he proposed that the benzene ring would lie flat on the surface, adsorbed at six centres and that only a crystal face with the correct hexagonal symmetry and having suitable interatomic distances in the range 2.84 Å (nickel) to 2.77 Å (platinum) would be active in these reactions. More recent work on iron catalysts (11,12,13), however, has both supported and cast doubt upon the validity of the original hypothesis.

The use of oriented metal films of high and reproducible activity (13,14,15) and of single metal crystals

(16,17) has made it possible to study reactions on definite crystal planes. Such experiments have shown that for any one catalyst the activity depends on the crystal face exposed at the surface. In the recombination of hydrogen on copper, for instance, the order of activity of the principal faces is (110) > (100) > (111), so that the reaction occurs most readily on the surface where the inter-atomic spacing will allow the adsorbed intermediate to be relatively strain-free. Bond (18) has shown that the adsorption of acetylene on f.c.c. metals is expected to occur on the (100) and (101) faces but not on the (111) face, which has shorter inter-atomic spacings.

Bond (19) and Van Hardeveld and Hartog (20) have discussed the influence of the size of supported metal crystallites on their adsorptive and catalytic properties. By considering models of different regular metal crystals, they calculated the variation in the relative numbers of atoms at the corners, edges and surface planes of the crystals with crystal size. The results of these calculations gave quantitative evidence that it was those atoms with very low coordination numbers which gave special adsorptive and catalytic properties to small crystallites. Thus, when the edges or corners of a crystal are more active than the faces, the specific activity will decrease with increasing particle size. Conversely, when the faces

rather than the edges or corners of the crystal are more active, as may be the case with aromatic molecules, then the specific activity will increase with increasing particle size. Experiments on the infra-red spectra of adsorbed carbon monoxide (20) have given information about the relative number of atoms with different coordination numbers.

From their study by infra-red spectroscopy on the adsorption of nitrogen on various metals, Van Hardeveld and Van Montfoort (21) have produced evidence of an effect of particle size on the properties of supported metal catalysts. They observed that nitrogen was adsorbed to a measurable extent only on crystallites with diameters between 15 and 70 Å. By considering a number of crystal models, they showed that crystallites within this size range had a large number of a special type of sites which occurred much less frequently on crystallites outside this range. These sites, called B_5 sites, can accommodate a nitrogen molecule which is coordinated by five metal atoms. They also produced evidence (22) that these sites were responsible for the infra-red active form of adsorbed nitrogen. Taking the incomplete cubo-octahedron as his model, Bond (19) has shown that at least four types of B_5 sites may be distinguished. From studies of the infra-red spectra of adsorbed nitrogen (22), it is possible

to estimate the number of B_5 sites on the metal surface per unit surface area.

Of all the metals, only those of group(VIII), which, according to Pauling's theory (9), are said to have incomplete d-bands, show appreciable activity in adsorption and catalysis. Boudart (23) showed that the variation in catalytic activity of a number of transition metals for the hydrogenation of ethylene could be related to the percentage d-character of the metals. This was also observed by Beeck (14) and is illustrated in Fig. 1.2.

Earlier work by Schwab (24) on the chemisorptive and catalytic properties of a copper catalyst in the decomposition of formic acid showed that the activation energy for the reaction increased when the copper was doped with small quantities of cadmium. This work also showed a relationship between the d-character of the alloy and the activation energy of the reaction.

More striking was the work by Couper and Eley (25) on palladium/gold alloys in ortho-para hydrogen conversion. They had calculated that a decrease in catalytic activity of the Pd/Au would occur when the gold-content of the alloy reached 60%, when the d-band of palladium would be filled. They found that a plot of activation energy against percentage gold content of the alloy showed excellent agreement with the theoretical calculation. (Fig. 1.3)

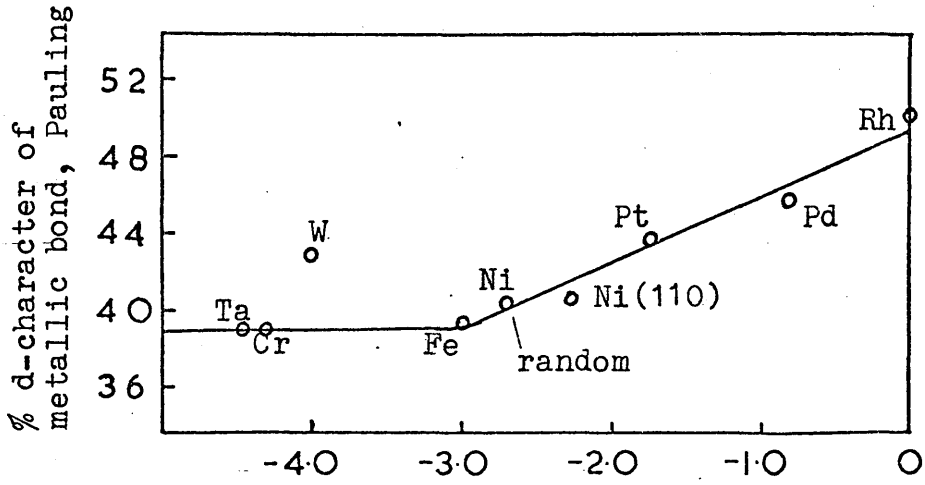

Fig. 1.2 Variation of percentage d-character of a range of metals against the logarithm of the activity of the metals per unit area for the reaction:

$$C_2H_4 + H_2 \rightleftharpoons C_2H_8$$

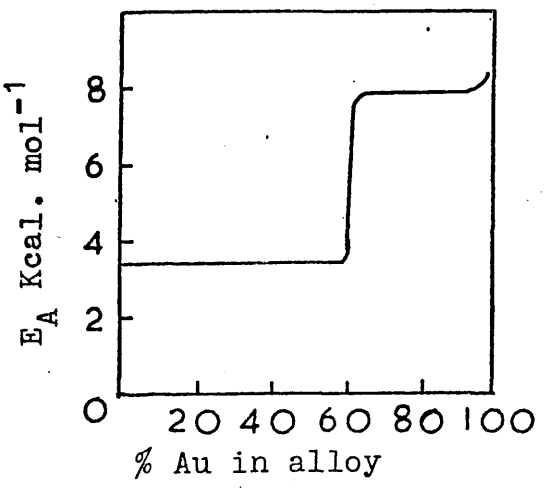

Fig. 1.3 Activation energy for p-H_2 conversion on Pd/Au alloys

Despite these observations, however, there is still considerable doubt about the validity of the correlation of the properties of the bulk metal and the surface and Sachtler (26) has proposed that the regularities in catalysis could be attributed to the properties of metallic compounds rather than directly related to the electronic properties of the bulk metal.

1.4 Catalytic Reactions of Unsaturated Hydrocarbons in an Heterogeneous System

1.4.1 Introduction

Of all catalytic reactions, those undergone by unsaturated hydrocarbons are among the most frequently studied. Not only are they of great importance in industrial processes but they also provide much information which is useful in the mechanistic studies of surface phenomena. The hydrocarbons most often studied are the olefins, diolefins, alkynes and aromatic and alicyclic compounds. Despite the work which has already been done, however, there is still a great deal of controversy concerning the mechanisms of these reactions.

The processes undergone by an unsaturated hydrocarbon when it reacts at the surface of a metal generally fall into one or more of the following categories. Any or all

of these may occur simultaneously.

1. Hydrogenation of the olefinic or acetylenic bond.
2. Cis/trans isomerisation and/or double bond migration.
3. Exchange of one hydrogen atom of the hydrocarbon with another hydrogen in the system.
4. The cracking of large molecules into smaller units or the polymerisation of small molecules into larger units.

One of the most important sources of information for the elucidation of the reaction mechanism is the kinetics of the reaction, which are characteristically governed by complex rate laws. For example, many reactions have been explained by the Langmuir-Hinshelwood mechanism (27), which postulates that the rate is controlled by the reaction of adjacently adsorbed molecules, and others by the Rideal-Eley mechanism (28), which envisages reaction between a chemisorbed and a weakly adsorbed species.

However, reaction mechanisms cannot be fully explained by these hypotheses. When an olefin such as but-1-ene undergoes hydrogenation over a metal catalyst such as rhodium/silica (29), it is converted into cis and trans but-2-ene as well as n-butane. Also, if the reaction is carried out using deuterium instead of hydrogen, there is a fairly wide distribution of deuterated products as well as HD and H_2. Thus, the separation and identification

of the reaction products is of prime importance in gathering the information required to postulate a mechanism.

1.4.2 The Adsorbed Species

Two kinds of adsorption have been identified: dissociative and associative. The chemisorption of ethylene has been studied volumetrically on various evaporated metal films (14,30,31,32). The results of these experiments show that the first few increments of ethylene are completely adsorbed but that after the addition of several doses, ethane and subsequently ethylene appear in the gas phase.

These results have been interpreted in terms of the dissociative adsorption mechanism, viz.,

$$4* + C_2H_4 \longrightarrow C_2H_{2(ads)} + \underset{*}{\overset{|}{2H}}$$

and then $$\underset{*}{\overset{|}{2H}} + C_2H_4 \longrightarrow C_2H_6 + 2* \qquad (14,30)$$

or $$\underset{*}{\overset{|}{4H}} + C_2H_{2(ads)} \longrightarrow C_2H_6 + 6* \qquad (31)$$

Both of the latter processes would create fresh sites for the adsorption of ethylene.

From Selwood's work on supported nickel (33), evidence was found for an associative attachment of ethylene to the metal surface, while a small fraction existed in

a dissociative form which required four or more surface sites:

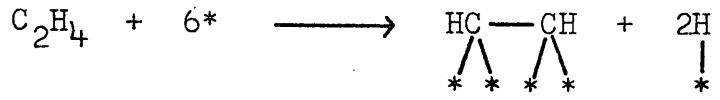

Further evidence for the dissociative intermediate has been found from work by Taylor and co-workers (34,35).

The associative adsorption of ethylene was first postulated in 1934 by Horiuti and Polanyi (36,37). This mechanism involves the opening of the unsaturated bond and the formation of an adsorbed alkane intermediate:

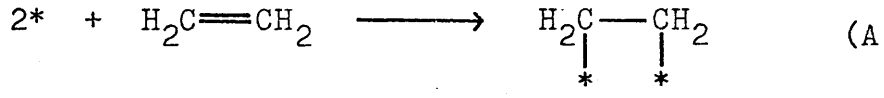

Species (A) could then react with an adsorbed hydrogen atom to give the ethyl radical (B) which could then either add hydrogen and desorb as ethane or alternatively lose a hydrogen to give ethylene exchange:

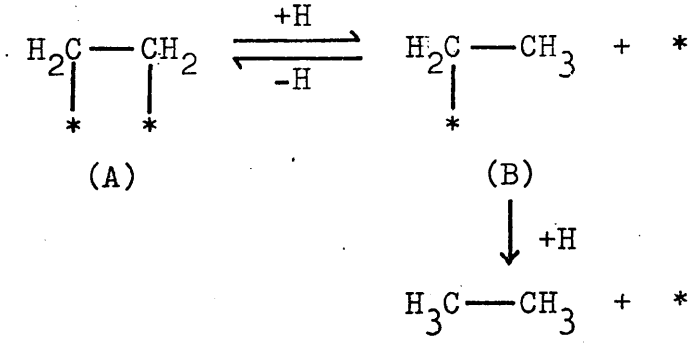

Further evidence for this mechanism came from the work of Conn and Twigg when they observed that no isotopic

mixing occurred when ethylene and deutero-ethylene were exposed to a nickel surface (38).

In 1960, Bond (39,40) calculated that, since the formation of the diadsorbed intermediate (A) would involve adsorption on two adjacent metal atoms, molecules such as ethylene and acetylene would not be expected to adsorb on the same sites. He found, however, that acetylene generally inhibits the reaction of ethylene and concluded that the same sites may adsorb both ethylene and acetylene. Other results, such as the exchange reactions of cyclo-alkanes (41), could not be explained by the mechanism involving the diadsorbed species. It was such evidence which led Rooney and Webb (42,43) to postulate the existence of a π-adsorbed intermediate, envisaging the same kind of bonding as is found in olefinic transition metal complexes (44,45) and as is shown in Figs. 1.6. In this kind of system, only one metal atom would be required for adsorption.

Although no direct evidence has been obtained for either the π-adsorbed or diadsorbed intermediates, the indirect evidence of Bond's calculations (39,40,46) tends to support the former, as many hitherto unexplained reaction mechanisms are explicable in terms of the π-bonded intermediates.

1.4.3 The Isomerisation of Olefins

The chemisorption of olefins as the π-bonded species suggests two possible mechanisms for double-bond isomerisation, viz., interconversion between olefinic and alkyl intermediates and interconversion between olefinic and π-allylic complexes (43). These mechanisms are shown in Figs. 1.4 and 1.5 respectively. Although it may be possible for both of these mechanisms to occur simultaneously, their relative importance must depend upon the experimental conditions and the catalyst used.

Further evidence for the occurrence of the π-allyl mechanism has come from studies of the hydrogenation of pent-1-ene over nickel (47) and of the isomerisation of cis and trans but-2-ene over silver (48).

1.4.4 The Hydrogenation of Mono-olefins

It is now generally accepted that the hydrogenation of ethylene proceeds by the mechanism first postulated by Horiuti and Polanyi (36,37) and that the reaction proceeds by the addition of an hydrogen atom to an adsorbed ethylene molecule to form a relatively stable adsorbed ethyl radical - the "half-hydrogenated state". Evidence for this mechanism has been obtained from the use of equilibrated and non-equilibrated hydrogen/deuterium mixtures (49,50,51).

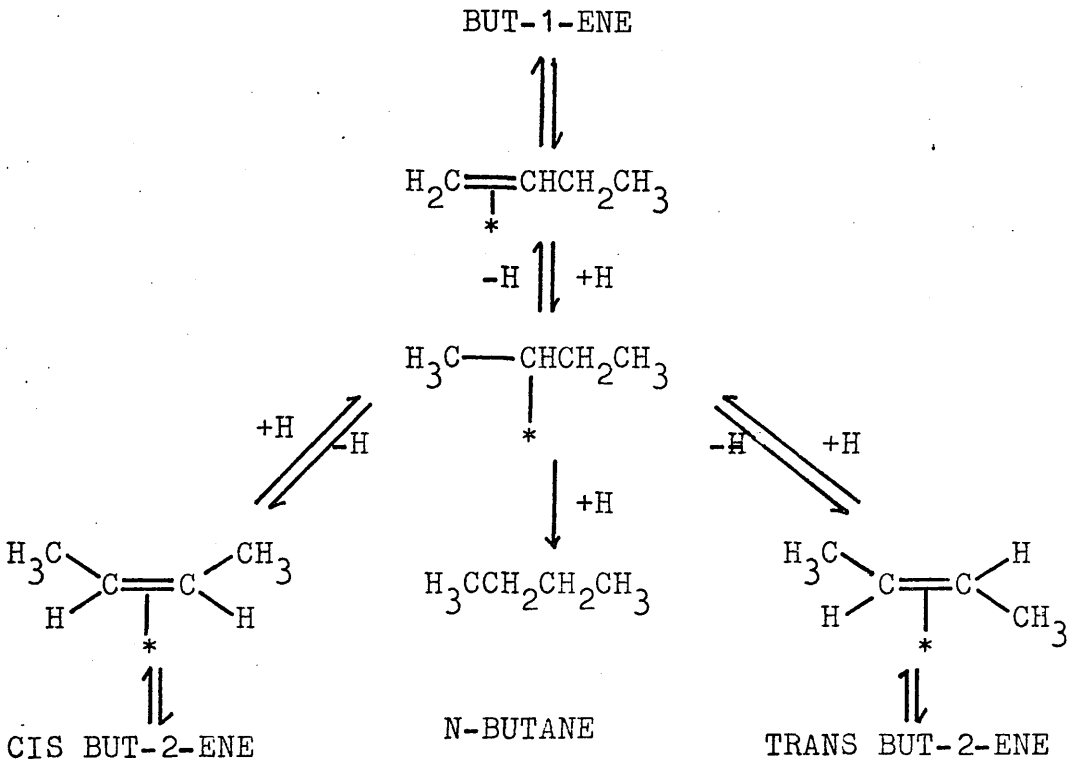

Fig. 1.4 The double-bond isomerisation of but-1-ene by interconversion between olefinic and alkyl intermediates.

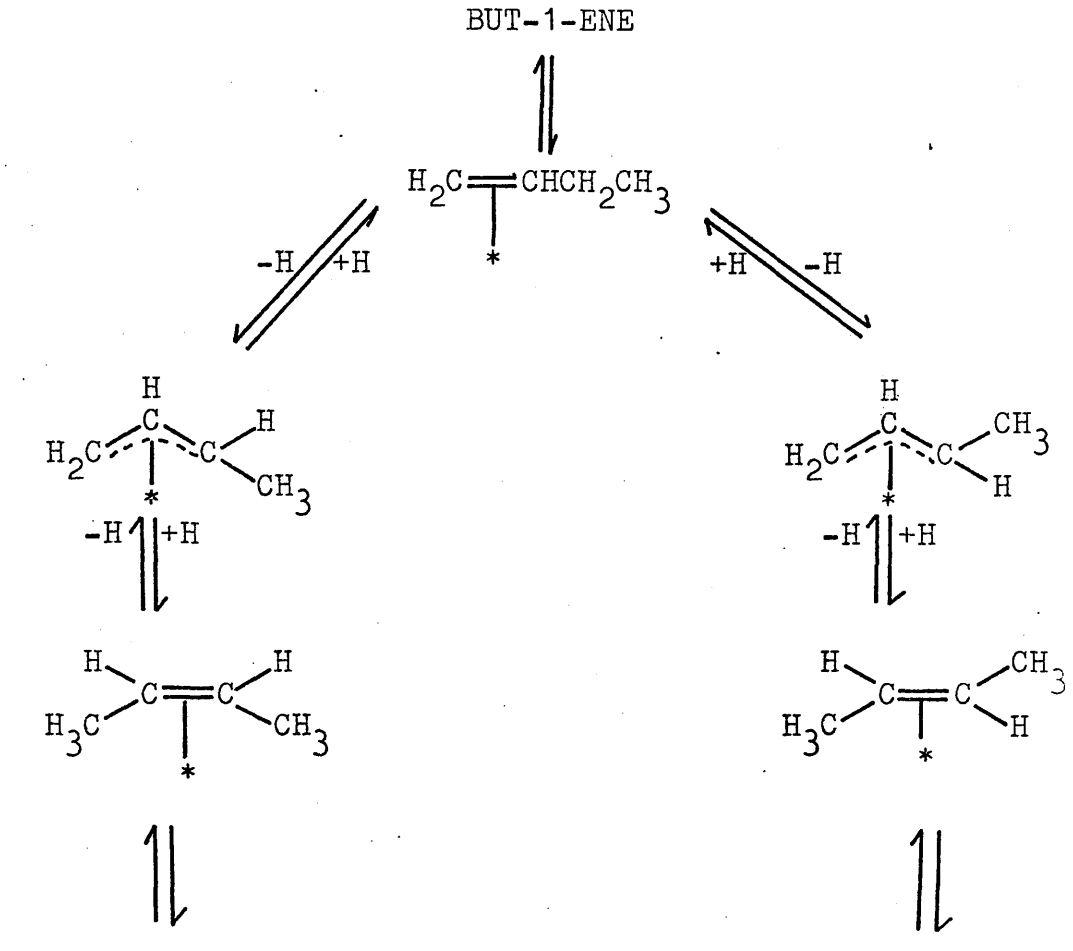

Fig. 1.5 The double-bond isomerisation of but-1-ene by interconversion between olefinic and π-allylic intermediates.

The "half-hydrogenated" intermediate may be formed from the diadsorbed species first envisaged by Horiuti and Polanyi (A), although work on the homogeneous reduction of olefins by Halpern et al. (52,53) has shown that the alkyl species may be produced by the addition of hydrogen to a π-adsorbed complex (B).

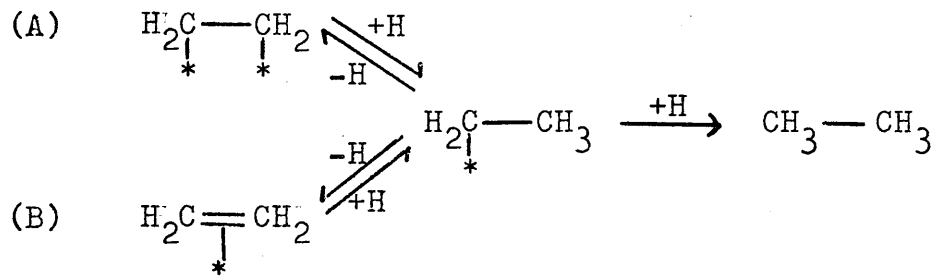

The further addition of a hydrogen atom to the adsorbed alkyl radical produces ethane, which is released into the gas phase.

This mechanism can also explain the production of C_2H_6 rather than the expected $C_2H_4D_2$ in the early stages of the reaction of ethylene with deuterium:

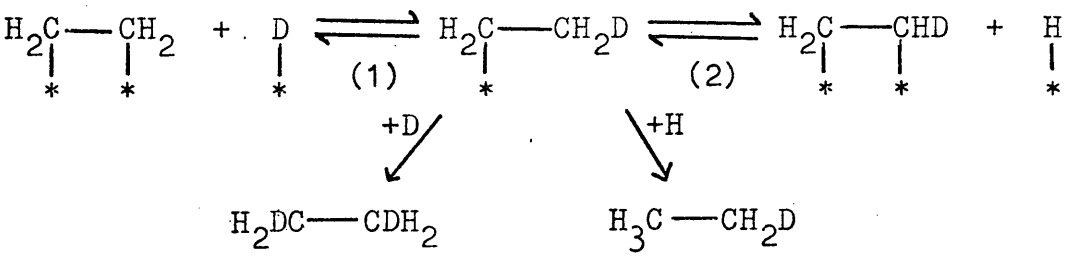

If the equilibria (1) and (2) are fast relative to the addition of the second "hydrogen" atom, then a pool of hydrogen, as opposed to deuterium, atoms can build up on the surface. These can then react to give C_2H_6 or can

combine with themselves or with adsorbed deuterium atoms to form H_2 and HD respectively.

A similar mechanism, as outlined in Fig. 1.4, can account for the isomerisation and exchange of C_4 and higher olefins. It is unlikely, however, that the π-allyl intermediate shown in Fig. 1.5 takes part in the hydrogenation reaction and it is generally assumed that the same mechanism operates for the hydrogenation of larger olefins as for ethylene. Studies by MacNab and Webb on poisoned catalysts (54) tend to substantiate this view.

1.5 Catalytic Reactions of Unsaturated Hydrocarbons in an Homogeneous System

1.5.1 Introduction

Whereas heterogeneous catalysis has been studied for more than seventy years, the serious study of homogeneous catalysis began only just over fifteen years ago. However, because of the relative ease of detecting intermediates by spectroscopic methods and because the reproducibility of homogeneous systems is high, many homogeneous reactions are better understood after only a few years of study than heterogeneous reactions after a much longer time. It is, therefore, in this field that

many new catalytic reactions have been discovered and most of these have been recently reviewed (55,56,57). Examples of these reactions are: the hydrogenation of olefins catalysed by complexes of ruthenium (58), rhodium (59), cobalt (60), platinum (61,62,63) and other metals; the isomerisation of olefins catalysed by complexes of rhodium (64,65), palladium (65), cobalt (66), platinum (61,62,63,67) and other metals (68); the dimerisation of ethylene(69) and polymerisation of dienes (70) catalysed by complexes of rhodium; the hydroformylation of olefins (71) catalysed by rhodium and cobalt complexes; the oxidation of olefins catalysed by palladium chloride (72); the hydration of acetylene catalysed by ruthenium chloride (53);and many others. Table 1.1 (56) lists some of these reactions together with examples of possible active forms of the catalysts.

The complexes most often used as catalysts are those of d^8 and d^{10} configuration having particularly "soft" ligands such as tris-triphenylphosphine, which, because they are excellent π-electron acceptors, are capable of stabilising low oxidation states. Because these complexes are often able to coordinate small molecules reversibly (73,74), they are often used as models for "active centres" for adsorption on transition metals and it is from such comparisons that some of the recent advances in heterogeneous

TABLE 1.1

Examples of Catalysts Active in the Catalysis of Homogeneous Reactions of Olefins

A. $RuCl_6^{4-}$

B. $RuCl_2(PPh_3)_4$

C. $Co(CN)_5^{3-}$

D. $Fe(CO)_5$

E. $FeH(CO)_4^-$

F. $CoH(CO)_4$

G. $RhCl(PPh_3)_3$

H. $RhCl_3(olefin)^{2-}$

J. $RhCl_2(C_2H_4)_2^-$

K. $RhCl(CO)(PPh_3)_2$

L. $IrI(CO)(PPh_3)_2$

M. $PdCl_4^{2-}$

Reaction	Active Catalysts						
	Ru(II)	Co(II)	Fe(0)	Co(I)	Rh(I)	Ir(I)	Pd(II)
Hydrogenation	A	C	D	F	G	L	
Isomerisation			E	F	H		M
Dimerisation					J		
Hydroformylation	*B			F	K		
Oxidation							M

* Active form of catalyst uncertain

catalysis have come.

A large number of factors, however, contribute to the ability of transition metal complexes to catalyse various reactions. Of these factors, some of the most important are as follows.

(1) Transition metals are able to coordinate as ligands a number of otherwise unstable reaction intermediates in more stable, yet still reactive complexes. Among these intermediates are σ-bonded ligands such as hydrides (75) and alkyl groups (64,68) and π-bonded species such as allyl groups (76, 77,78).

(2) Because of the ability of certain transition metal complexes to have two or more stable configurations differing in coordination and/or oxidation number, they also have the ability to promote rearrangements within their coordination shells (64,68). This allows reactions such as the isomerisation of butenes, described in section 1.5.3 to occur.

(3) Some transition metal atoms can assemble and/or orient several components for reaction within the framework of their coordination shells. One elegant example of this is the cyclo-oligomerisation of 1,3 butadiene to cyclododecatriene (C.D.T.) catalysed by the (C.D.T.)nickel complex, first reported by Wilke (79).

1.5.2 The Olefin-Metal Complex

When simple olefins are considered, Zeise's salt of formula $K[Pt(C_2H_4)Cl_3].H_2O$ or analogous compounds of Pt(II), Pd(II) and Rh(I) are often taken as the model for the coordination of an olefinic molecule to a metal atom (80). This is shown in Figs. 1.6. The central metal atom is in a square planar configuration with the axis of the C=C bond lying perpendicular to the plane. (Fig. 1.6(a))

The illustration in Fig. 1.6(b) shows the two carbon p_z orbitals combined to form a π-bonding and a π^*-antibonding molecular orbital. The metal d orbitals are also hybridised. One of the unfilled metal hybrid e_g orbitals, in this case the d_{z^2} orbital, is able to overlap with the filled π-bonding molecular orbital of ethylene to give a σ-bond, while a filled metal t_{2g} orbital, in this case the d_{xz} orbital, can interact with the empty π^*-antibonding molecular orbital of the ligand. Thus the metal-olefin bond consists of two components: σ-donation from the ligand to the metal and simultaneous π-donation from the metal to the ligand. A model similar to this has been envisaged for the π-adsorbed species on a metal.

1.5.3 The Isomerisation of Olefins

Many transition metal complexes have been found

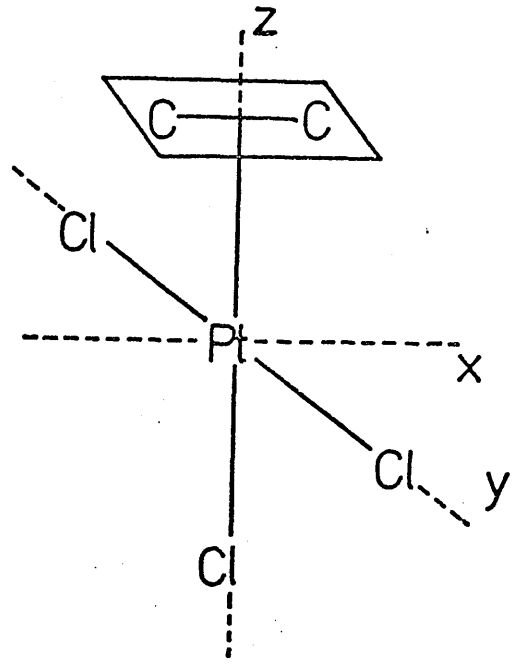

Fig. 1.6(a)

Structure of the anion

$[(C_2H_4)PtCl_3]^-$

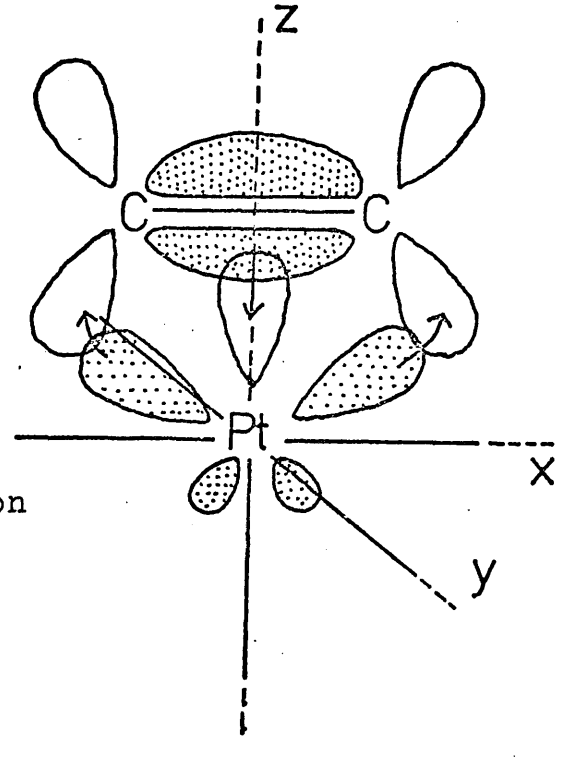

Fig. 1.6(b)

Conventional representation

of the metal-olefin bond.

to catalyse the migration of the double bond in terminal olefins. Harrod (65) has obtained evidence for an alkyl-type intermediate for the rhodium chloride catalysed isomerisation of terminal olefins, illustrated in Fig. 1.7. The hydrogen ion in this case would be provided by a co-catalyst, usually ethanol.

Mechanisms involving a labile π-allyl intermediate have also been postulated to explain the isomerisation of olefins in the presence of transition metal complexes such as iron pentacarbonyl or palladium chloride (69,70, 71).

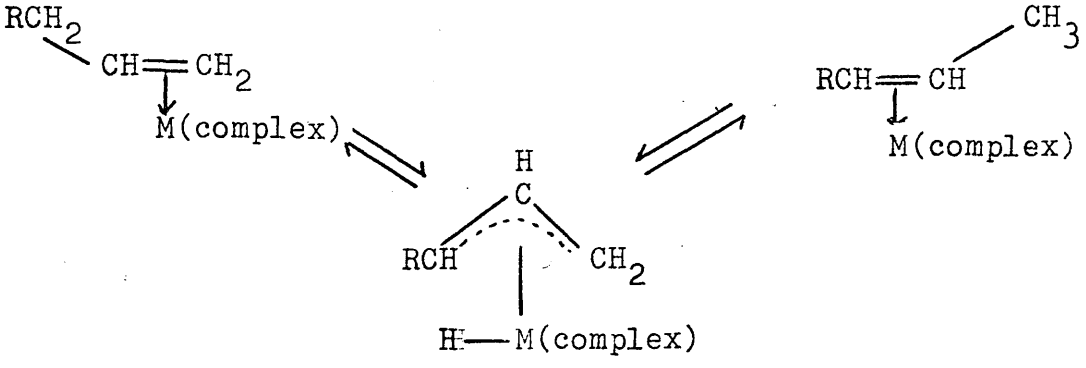

These mechanisms are analogous to those postulated for the isomerisation of but-1-ene over various metals, as described in section 1.4.3.

1.5.4 The Activation of Molecular Hydrogen and the Catalytic Hydrogenation of Mono-olefins

Just as the group (VIII) metals may activate molecular hydrogen heterogeneously, so the ability to activate

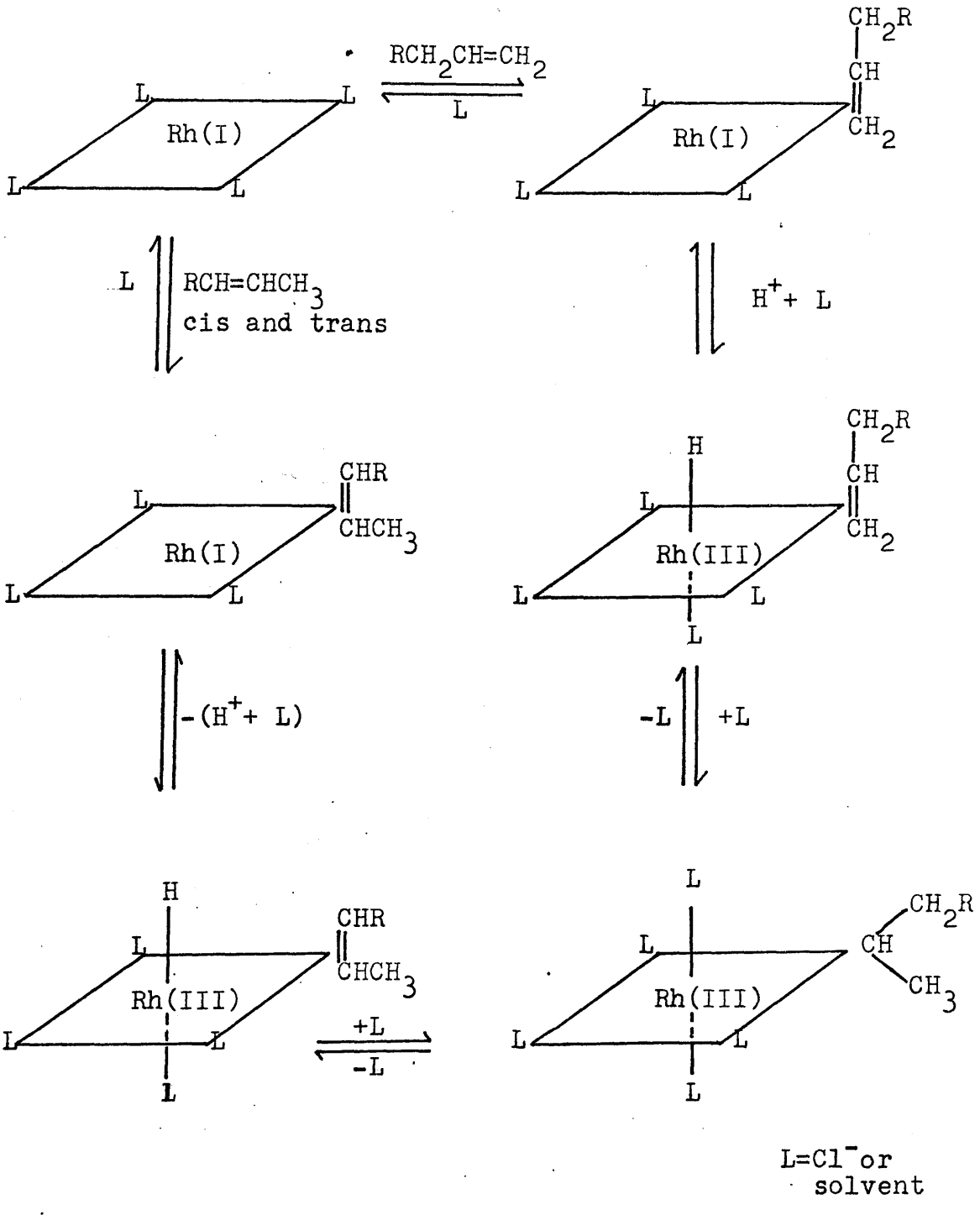

Fig. 1.7 Reaction mechanism for the homogeneous isomerisation of terminal olefins by rhodium trichloride.

hydrogen in a homogeneous system has been demonstrated for many of their ions and complexes (75). Three distinct mechanisms by which the hydrogen molecule may be split to form a reactive metal hydride complex as an intermediate have been recognised, and these are listed below.

(1) Heterolytic Fission

This mechanism involves the splitting of the hydrogen molecule into a hydride ion, which is bound to the metal atom, and a hydrogen cation. This probably occurs in the presence of $Ru(III)Cl_6^{3-}$ (81):

$$Ru(III)Cl_6^{3-} + H_2 \rightleftharpoons Ru(III)HCl_5^{3-} + H^+ + Cl^-$$

It has also been proposed by Halpern and co-workers (58) that heterolytic fission operates in the mechanism for the hydrogenation of olefins by ruthenium(II) chloride. The mechanism for the hydrogenation of fumaric acid by this catalyst is shown in Fig. 1.8.

(2) Homolytic Fission

Homolytic fission is the splitting of the hydrogen molecule into two neutral atoms, which coordinate to different central metal atoms, as probably occurs in the presence of the pentacyanocobaltate ion (82).

$$2Co(II)(CN)_5^{3-} + H_2 \rightleftharpoons 2Co(III)H(CN)_5^{3-}$$

This catalyst, which is active in the homogeneous hydrogenation of conjugated olefins to mono-olefins gives an excellent example of the high stereoselectivity which

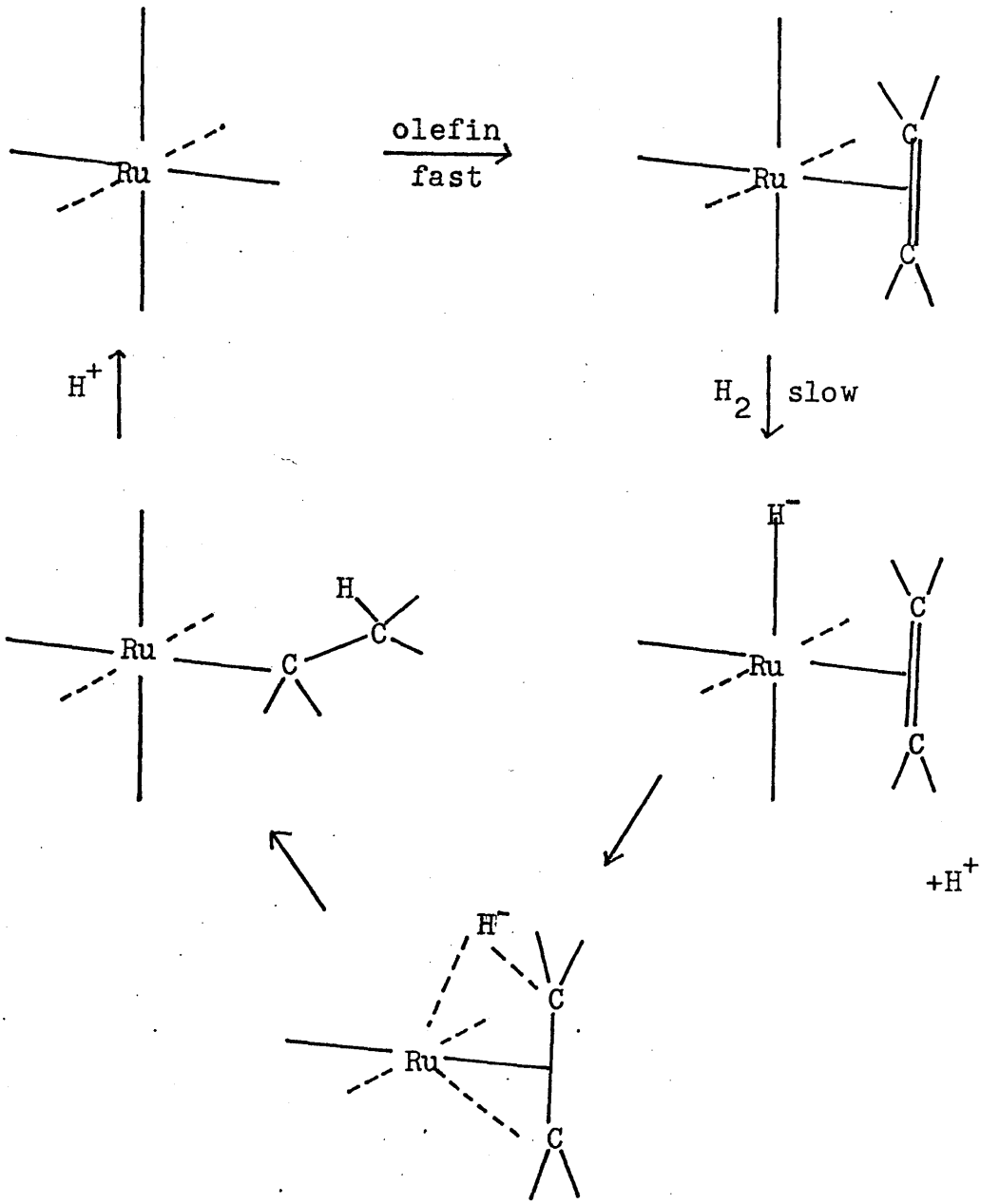

Fig. 1.8 Mechanism for the hydrogenation of olefins by $RuCl_4^{2-}$

may be shown in homogeneously catalysed reactions. It has been suggested (60) that the mechanism for the hydrogenation of buta-1,3-diene in the presence of this complex is as shown in Fig.1.9. At high concentrations of the cyanide ion, but-1-ene is formed preferentially, whereas at low concentrations trans but-2-ene is the predominant isomer produced. Thus, by careful control of the reaction conditions, a very high degree of selectivity may be obtained.

(3) Insertion

In this case, both hydrogen atoms coordinate to the same central metal atom. $IrCl(CO)(PPh_3)_2$, for example, acts in this way.

$$Ir(I)Cl(CO)(PPh_3)_2 + H_2 \rightleftharpoons Ir(III)H_2Cl(CO)(PPh_3)_2$$

The structure of this dihydrido complex has been formulated by Vaska (83) as:

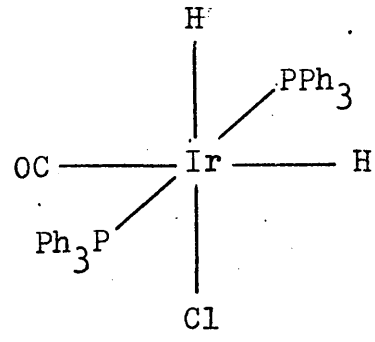

One of the most intensely studied reactions of this type is the hydrogenation of terminal olefins in the

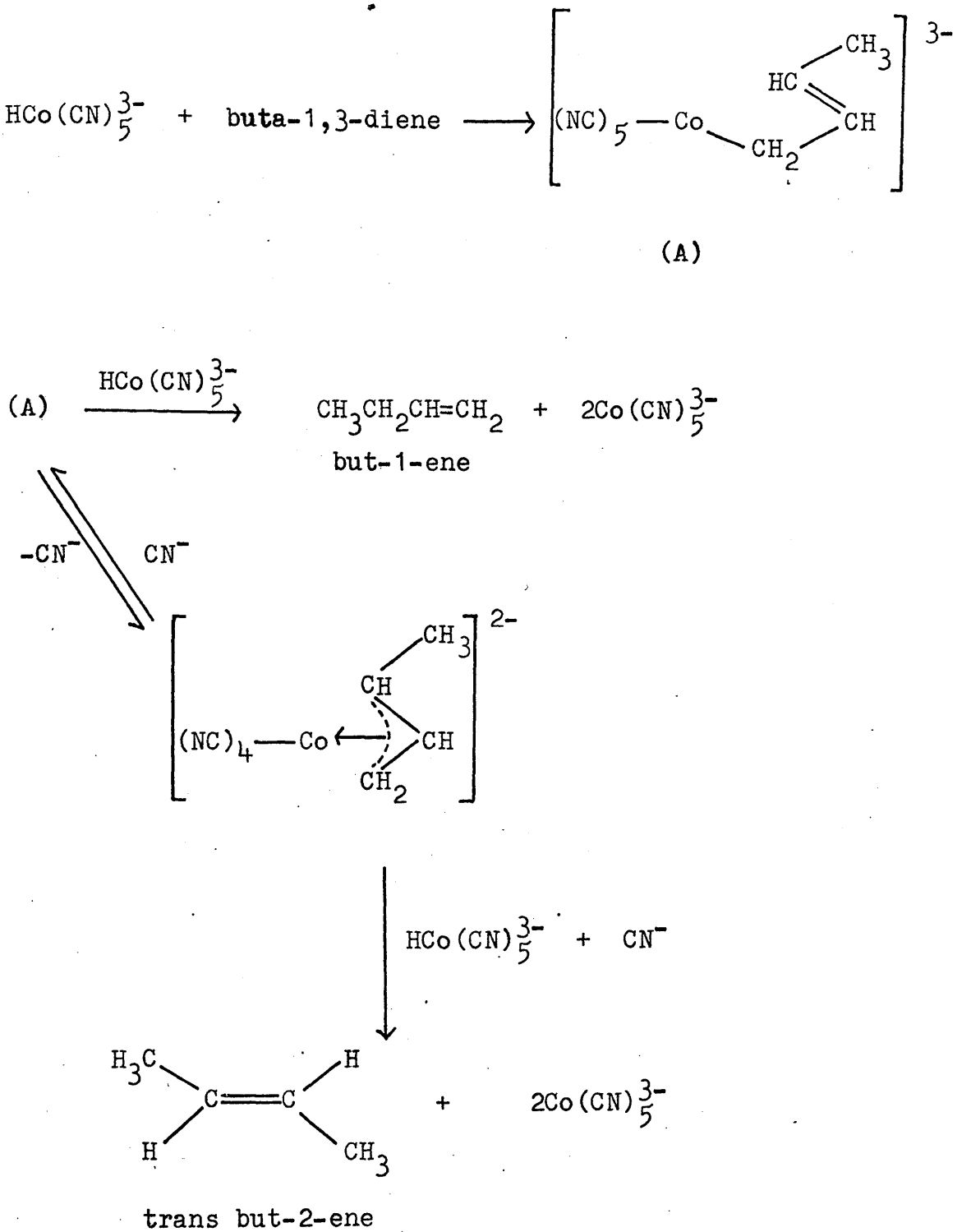

Fig. 1.9 Mechanism for the hydrogenation of buta-1,3-diene by $Co(CN)_5^{3-}$

presence of tristriphenylphosphine rhodium(I) chloride or Wilkinson's complex (59). From molecular weight measurements, it is thought likely that the following process occurs when the complex goes into solution:

$$\text{solvent} + (Ph_3P)_3Rh(1)Cl \rightleftharpoons (Ph_3P)_2Rh(1)Cl(\text{solvent})_x + Ph_3P$$

When the solution species in chloroform is exposed to molecular hydrogen, it reacts by an insertion mechanism to form a five coordinate dihydride species, $(Ph_3P)_2RhClH_2$ (A), which can be isolated. The benzene solutions also adsorb hydrogen rapidly and reversibly. When exposed to ethylene, the rust-coloured solvated complex turns yellow, producing the isolable olefin complex $(Ph_3P)_2RhCl(C_2H_4)$ (B). It is observed that higher olefins such as propene form no isolable complex and, whereas the ethylenic complex is formed in preference to the dihydride, when solutions of the rhodium complex are treated with hydrogen and propene the dihydride forms preferentially. The lower stability of the propene relative to the ethylene complex explains the ability of the system to proceed at a much higher rate in the hydrogenation of propene than in the hydrogenation of ethylene. Because of the high reactivity of the hydride intermediates, their formation is often the rate limiting step in the

overall reaction. The reaction sequences and the complex structures in the ethylene/hydrogen system are shown in Figs. 1.10(a) and (b).

Many other examples of homogeneous catalytic hydrogenation of unsaturated hydrocarbons have been reported, involving a number of catalysts, among which are $Fe(CO)_5$ and $Fe(CO)_3$(diene) (84,85,86), $HCo(CO)_4$ (87,88) and $IrI(CO)(PPh_3)_2$ (89).

1.6 Chemisorption and Coordination

With a view to obtaining a better understanding of the mechanisms of catalytic reactions, a number of workers have been interested in possible relationships between homogeneous and heterogeneous catalysis (18,55, 90,91,92,93). This approach, which allows the properties of the organic molecule chemisorbed on a metal atom or surface to be compared with the properties of the same molecule in an organometallic complex, has assisted in the consideration of the function of these as intermediates in catalytic reactions. If a relationship between these properties can be established, then the information obtained from the mechanistic studies of homogeneously catalysed reactions may lead to a greater understanding of the mechanisms in heterogeneous catalysis.

Apart from sharing the ability to catalyse a number

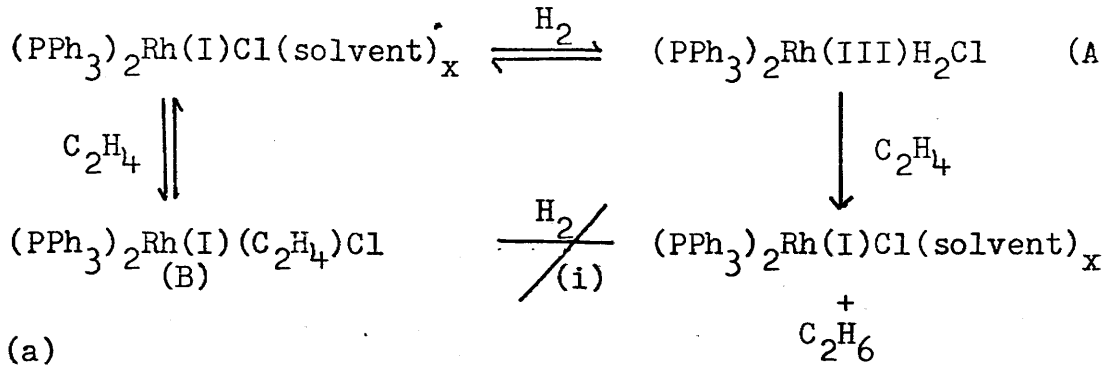

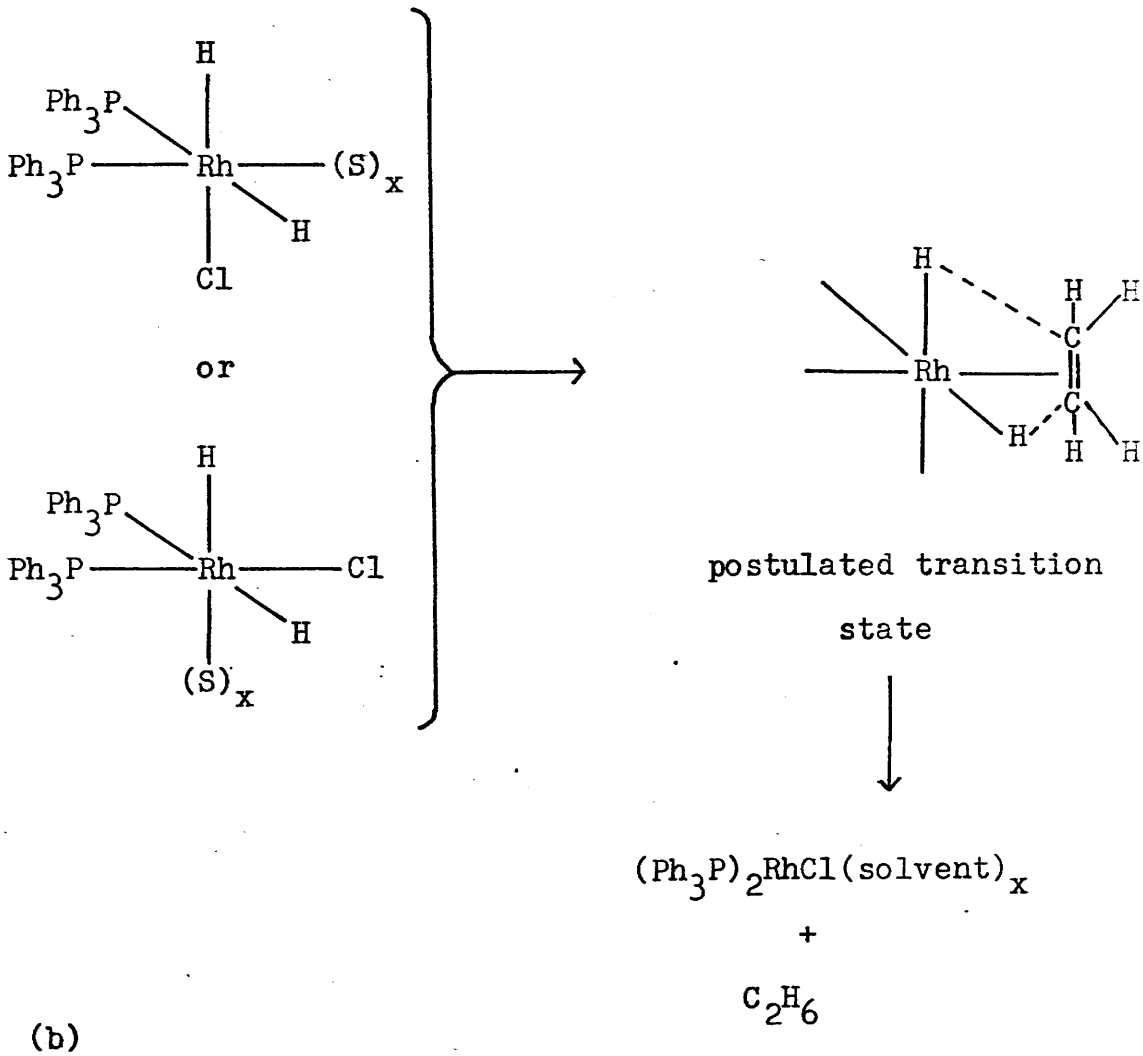

Figs. 1.10 Mechanism for the hydrogenation of olefins by tristriphenylphosphine rhodium(I)chloride.

of reactions such as the hydrogenation and the isomerisation of olefins, a number of similarities exist between homogeneous and heterogeneous catalysis. For example, the compounds most active in homogeneous catalysis are generally those containing elements of group (VIII), whose metals are also the most active in heterogeneous catalysis. Analogies have also been drawn between the stabilities of olefin complexes and the strengths of adsorption of the olefins on metals. Little is known about the bond strengths of the olefinic transition metal complexes, but it is found that the stability of the mono-olefin complexes of the d^8 metals decreases from Pt(II) to Pd(II) to Ni(II). Whereas no di-olefin complexes of Pd(II) of the form $(C_2H_4)_2MCl_2$ are known, the derivatives of Rh(I) and Ir(I) of the form $((C_2H_4)_2MCl)_2$ are quite stable. The difference in stability of complexes with doubly charged metal ions is due to the increasing ability for back donation of electrons with increasing atomic number, while the greater stability of the complexes of the singly charged metal ions is due to an increase in the ability for back donation with decrease in the formal charge on the central metal atom.

The sequence of chemisorption strengths of ethylene on various metals has been derived by Bond and co-workers from the analysis of deuterium-ethylene exchange(94).

They found this sequence to be

$$Pt \simeq Ir > Pd > Rh > Ru \simeq Os.$$

The positions of Fe, Co and Ni are uncertain but they probably lie around Pd and Rh. Analogous with coordination compounds, the strength of adsorption on the iso-electronic metals increases with atomic number, while, in the case of metals in the same row of the periodic table, strength of adsorption tends to increase with the number of d-electrons.

One further similarity between the two types of catalyst is that olefins and alkynes are chemisorbed more strongly than mono-olefins on to a metal surface and that the same effect is shown in the relative stabilities of complexes containing these molecules.

These comparisons have led to the consideration of further possible analogies: from his description of the molecular orbitals involved in chemisorption, Bond (18) has envisaged the electronic configuration for ethylene adsorbed on the (100) face of nickel (Fig. 1.11) to be analogous to that for the coordination of ethylene in a d^8 square-planar complex (80) shown in Figs. 1.5; considerations of the properties of supported metal crystallites, described in section 1.3, have shown the importance of the single surface metal atom as a site for adsorption (19,20); and the importance of the π-adsorbed species

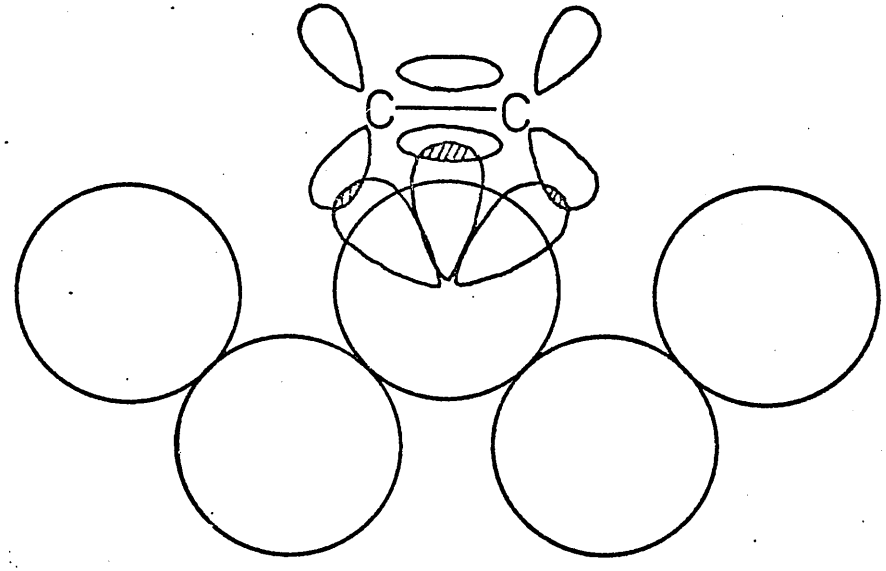

Fig. 1.11 Representation of π-adsorbed ethylene on the (100) face of a f.c.c. metal.

as an intermediate in heterogeneous catalysis, analogous to the π-coordinated complex in homogeneous catalysis, has been stressed by Rooney and Webb (43).

1.7 Reactions of Olefins on Supported Transition Metal Complexes

Some attempts to correlate the properties of homogeneous and heterogeneous catalysts have been made by supporting transition metal salts or complexes on an "inert" carrier and using these as heterogeneous catalysts. Acres and co-workers (95) attempted to combine the convenience of a solid catalyst with the superior selectivity and efficiency in use of metal atoms of a homogeneous catalyst by supporting a solution of rhodium trichloride in ethylene glycol on Silocel. Although the supported solution was active in the isomerisation of pent-1-ene to cis and trans pent-2-ene, the salt reduced to rhodium metal with use. Hayes (96) successfully supported ethylene platinous chloride $(C_2H_4.PtCl_2)_2$ on alumina and showed that the supported complex was active in the hydrogenation of ethylene to ethane. The complex did not reduce in the presence of the ethylene/hydrogen reaction mixture when the ratio $p_E:p_{H_2}$ was greater than unity but it reduced rapidly to platinum metal when exposed to hydrogen alone. He concluded that the π-bonded ethylene reacted with

hydrogen without the need for a σ-diadsorbed intermediate. More recently, Misono and co-workers (97) investigated a series of complexes of Pd(II), Pt(II), Ni(II) and Cu(II) with acetonylacetonate and dimethylglyoxime supported on silica gel and found these to be active in the isomerisation of but-1-ene. Their results showed that the activity of the catalyst was dependent upon the central metal atom, in that the activity increased in the sequence Cu(II) < Ni(II) < Pt(II) < Pd(II) and that this order was the same for both of the chelating ligands. They concluded that the isomerisation reaction over these metal chelates proceeded through some coordination complex.

The disproportionation of olefins over supported metal carbonyls has been one of the most intensively studied reactions over this type of catalyst (98,99,100, 101,102). Davie, Whan and Kemball(100), who studied the disproportionation of propylene to a mixture of butenes and ethylene on alumina supported molybdenum hexacarbonyl found that their catalyst, when activated by heating, differed in its infra-red spectrum from the unactivated catalyst and concluded that the species active in catalysis was of the form $Mo(CO)_x(propylene)_{6-x}$, where $x < 6$. From further investigation, however, Howe and co-workers (101) have concluded that the active species was, in fact, molybdenum in a higher oxidation state than zero.

CHAPTER 2

THE AIMS OF THE PRESENT WORK

An understanding of the factors which determine the activity of heterogeneous catalysts is important in the ability to design selective and stereospecific catalysts. In studies of the reactions of unsaturated hydrocarbons catalysed by metals, however, discussion of the mechanisms is severely restricted by a lack of knowledge of the nature of the catalytically active form of the adsorbed species and the nature of the active site on a catalyst surface. Many current ideas concerning these problems have been influenced by comparisons between heterogeneous systems and homogeneous systems involving organometallic complexes (18,42,43,52,53,55,90,91,92).

In an attempt to further the understanding of these factors, it was decided to investigate the catalytic properties of a number of supported metal salts and complexes using silica as the support material. The immediate aims of the work were as follows:

(1) to characterise the supported materials before, during and after reaction;

(2) to study the kinetic features of the hydrogenation and/or isomerisation reactions, as appropriate;

(3) to determine the distribution of the reaction products;

(4) to determine the distribution of deuterium in the

product hydrocarbons;

(5) to investigate the influence of the support on the supported compounds;

(6) to elucidate mechanisms for the reactions under investigation;

(7) to compare the properties of catalysts derived from supported compounds with the properties of known supported metal catalysts.

CHAPTER 3

E X P E R I M E N T A L

3.1 Materials

3.1.1 Catalyst Preparation

(i) Silica supported rhodium trichloride

13% w/w (5% with respect to Rh) rhodium trichloride supported on silica was prepared by suspending 20g. "Aerosil" silica (purity 99.9%)(Degussa, Ltd.) in a solution of 2.6g. hydrated rhodium trichloride (Johnson,Matthey & Co., Ltd.) in distilled water. The suspension was slowly evaporated, with constant stirring, to dryness and the residue ground to a fine powder.

(ii) Carbon-14 labelled triruthenium dodecacarbonyl

^{14}C labelled triruthenium dodecacarbonyl was prepared according to the method of Dawes and Holmes (103). A fast stream of ^{14}C labelled carbon monoxide, produced by the action of concentrated sulphuric acid on ^{14}C labelled formic acid (Radiochemical Centre, Amersham), was bubbled into a refluxing solution of 1g. of hydrated ruthenium trichloride (Johnson, Matthey & Co., Ltd.) in 100ml. of 2-ethoxy ethanol. On conversion of the ruthenium trichloride to the pale-yellow ruthenium carbonyl chloride species, the solution was cooled. In the second stage,

100 ml. ethanol and 1g. granulated zinc were added to the solution, which was vigorously agitated, refluxed and treated with a rapid stream of the labelled carbon monoxide. After completion of the reaction, $Ru_3(CO)_{12}$ was filtered from the cooled solution and purified by recrystallisation from toluene.

(iii) Silica supported triruthenium dodecacarbonyl and triosmium dodecacarbonyl

2% w/w triruthenium dodecacarbonyl on silica and 2% w/w triosmium dodecacarbonyl on silica were prepared in the following way. 1g. of "Aerosil" silica, which had been dried in vacuo at 500°C, was suspended in 20ml. of spectroscopic grade dichloromethane under a steady stream of dry nitrogen. 0.02g. of the triruthenium dodecacarbonyl (Alfa Inorganics) or of the triosmium dodecacarbonyl (Johnson, Matthey & Co., Ltd.) was dissolved in 10ml. of the solvent and the resulting solution added to the silica suspension, which was then stirred constantly and evaporated to dryness under the nitrogen stream. The residue, which was a fine, free-flowing powder, was stored under dry nitrogen.

10% w/w ^{14}C labelled triruthenium dodecacarbonyl on silica was prepared in a similar way to the above.

Attempts to support triiron dodecacarbonyl on silica resulted in the decomposition of the complex and the

formation of metallic iron.

3.1.2 Gases

(i) Hydrogen

Cylinder hydrogen (Air Products, Ltd.) was purified by diffusion through a heated palladium/silver alloy thimble at 200°C into a degassed storage vessel.

(ii) Deuterium

The deuterium (Norsk Hydro, Ltd.) was examined by mass spectrometry and found to be 99.9% isotopically pure. As the oxygen content was less than 10p.p.m., no further purification was carried out.

(iii) But-1-ene

Chemically pure grade but-1-ene (Matheson Co.,Inc.) was found to contain no impurities detectable by gas

chromatography and was merely degassed before use.

(iv) Helium

Cylinder helium (Air Products, Ltd.) was used as the carrier gas in the flow systems and in the chromatograph.

3.2 Apparatus

3.2.1 The Vacuum System

The apparatus used for storage and preparation of gases and for carrying out hydrogenation reactions is shown in Fig. 3.1. It was evacuated by a mercury diffusion pump(P_2), backed by an oil-filled rotary pump(P_1), producing a vacuum of better than 10^{-4}torr. All taps and joints were lubricated with "Apiezon N" high-vacuum grease.

3.2.2 The Pulse-Flow System

(i) The catalyst section

The work on rhodium trichloride/silica and test reactions on other supported complexes were carried out in a pulse-flow system, similar to that designed by Kokes and co-workers (104). It consisted of a microcatalytic reactor coupled to a gas chromatograph (Fig. 3.2).

The catalyst vessel (Fig. 3.3) was constructed of "Pyrex" glass in the shape of a pipette, with a copper

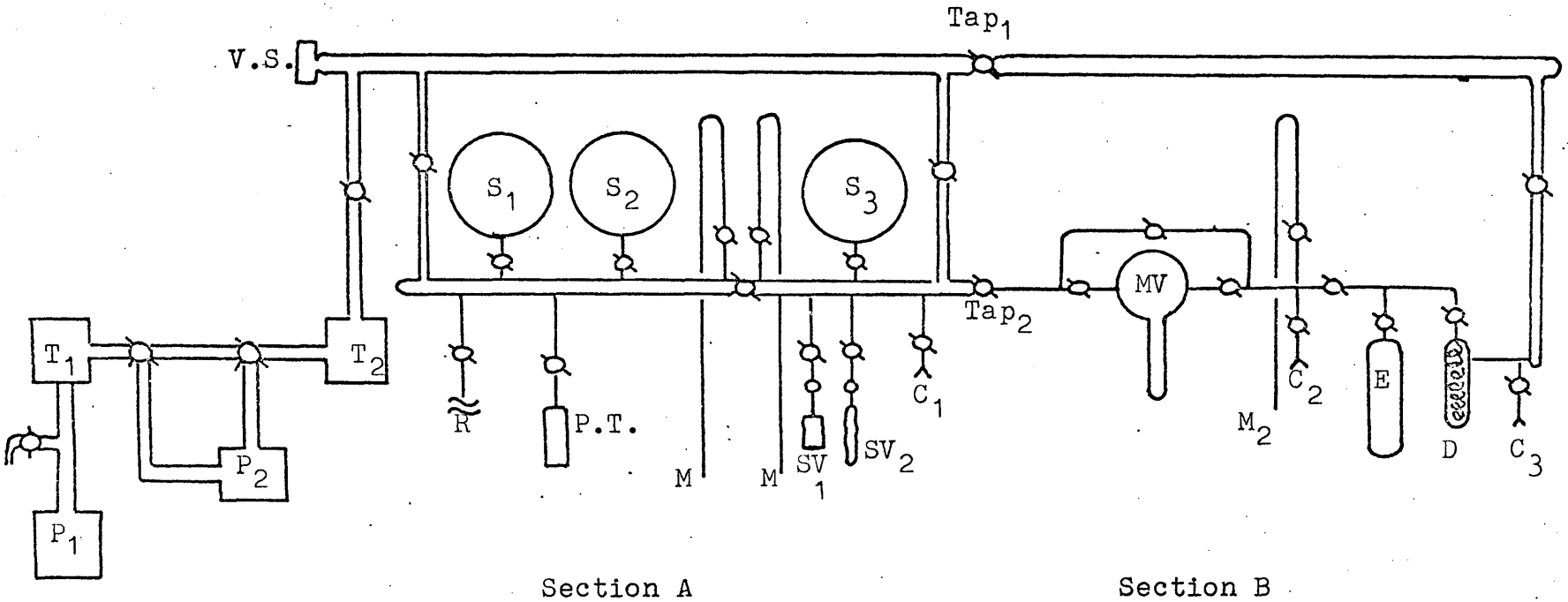

P_1 Rotary pump
P_2 Diffusion pump
V.S. Vacustat
M Manometer

P.T. Palladium thimble
R Lead to radio-counting flow system
S Storage vessel
T Cold trap
SV Sample vessel

Fig. 3.1 The vacuum system

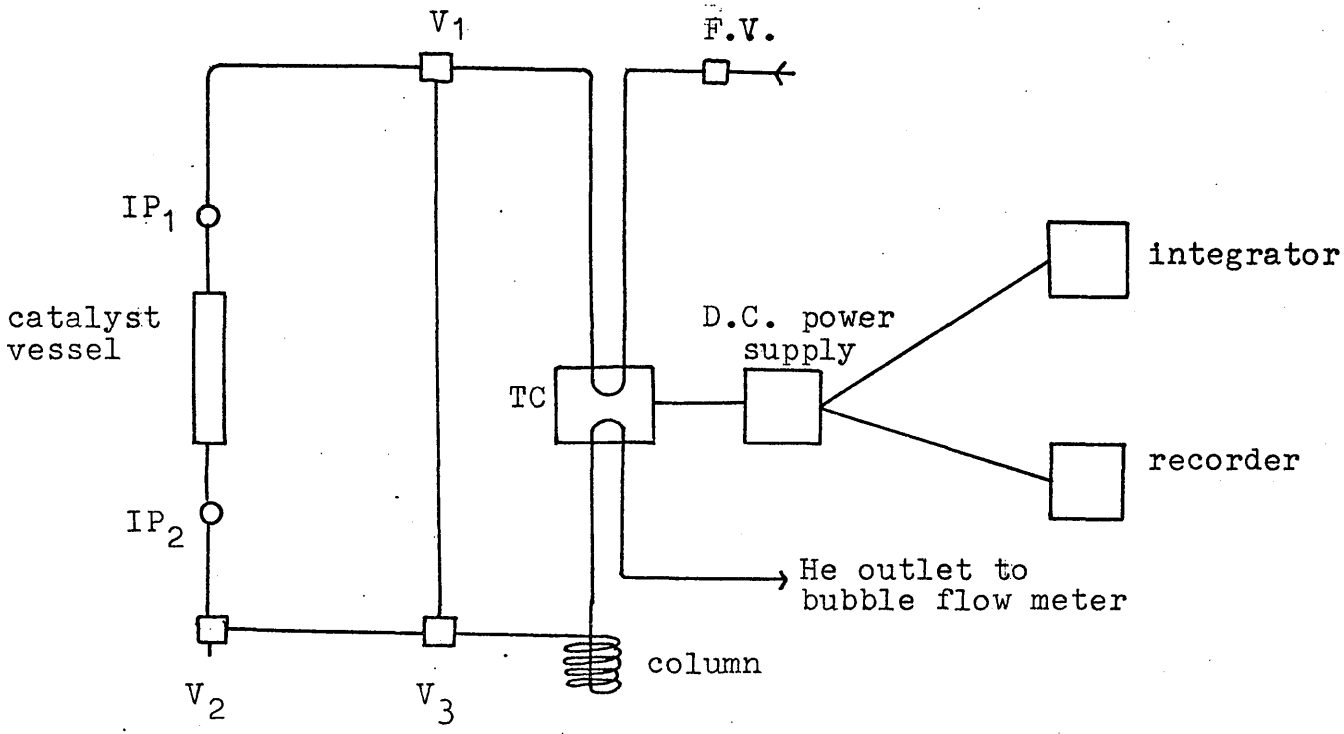

IP = injection port; V = switch valve; TC = katharometer; F.V. = fine control valve

Fig. 3.2 The flow system.

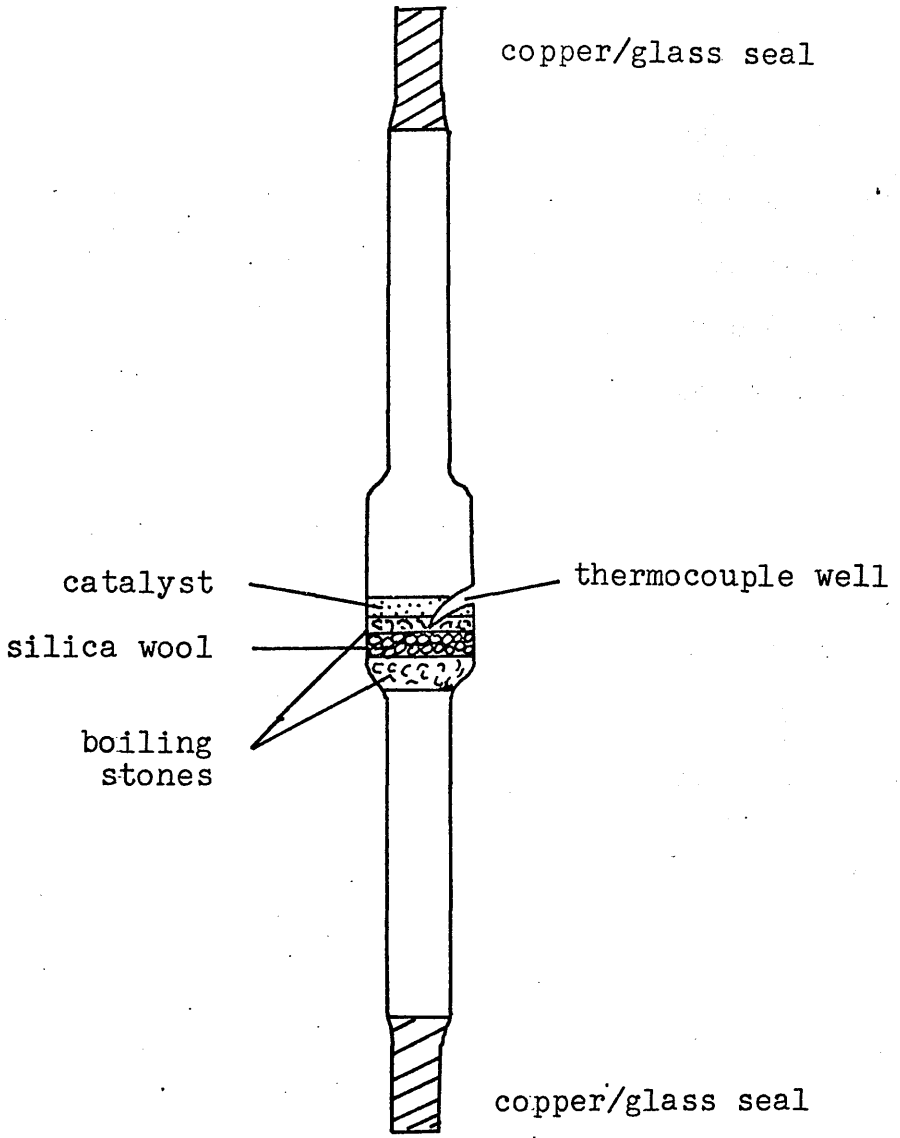

Fig. 3.3 The catalyst vessel

to glass seal at either end, which could be connected to the copper flow system with a "Swagelok" ¼" union (Crawford, Ltd.). Injection ports I_{P_1} and I_{P_2}, for reaction and calibration respectively, were situated above and below the catalyst bulb. Each port was constructed from a "Swagelok" ¼" T-piece union with a ¼" rubber seal (Hitachi, Ltd.) supported by two brass washers inserted into the leg of the "T". This system was found to give a good seal.

The temperature of the catalyst was controlled by an electric furnace surrounding the vessel and the current to the furnace could be varied by a "Variac" transformer. The temperature of the catalyst was measured to $\pm 1^{o}C$ by a "Comark" electronic thermometer fitted with a Cr/Al thermocouple.

Helium entered the system by way of a fine control valve, F.V. (Crawford, Ltd.), thence through the katharometer (Gow-Mac 10-952, Au-W) and into a switch valve V_1, from which it could be led either into the catalyst vessel through V_2 to V_3 or alternatively directly to V_3 via the by-pass. From V_3 it went through the chromatographic column and back into the katharometer. The rate of flow of carrier gas was measured by a bubble flow-meter attached to the gas outlet.

Gases for reaction were stored in the vacuum system

shown in Fig. 3.1, Section A. When required, they were transferred into one of the sample vessels, S.V., which were fitted with injection ports of diameter such that ¼" serum caps (Subaseal, Esco Rubber Co.) with both internal and external sealing edges could be used. Samples were removed from these vessels with a 1.0ml. Hamilton Gas-Tight Syringe fitted with a "Chaney Adaptor", which ensured that precise volumes of gases could be measured and then injected into the catalyst section of the flow system.

(ii) The chromatograph

A 30ft. ¼" O.D. copper column packed with 40% w/w acetonyl acetone on 60-80 mesh firebrick was found to be suitable for the separation of the reaction products. The corrected retention volumes for n-butane, but-1-ene, trans but-2-ene and cis but-2-ene were 680, 935, 1210, and 1420ml. respectively and after a decrease of 50% in these values, the column was repacked. A flow rate of 50ml.min.$^{-1}$ was found to give the optimum separation of the hydrocarbons. A typical trace is shown in Fig. 3.4.

TABLE 3.1

Operating Conditions for Acetonyl Acetone Column

Carrier gas	Helium
Input pressure	2.2 Atmos.
Flow rate	50±1.5ml.min.$^{-1}$
Temperature	0°C

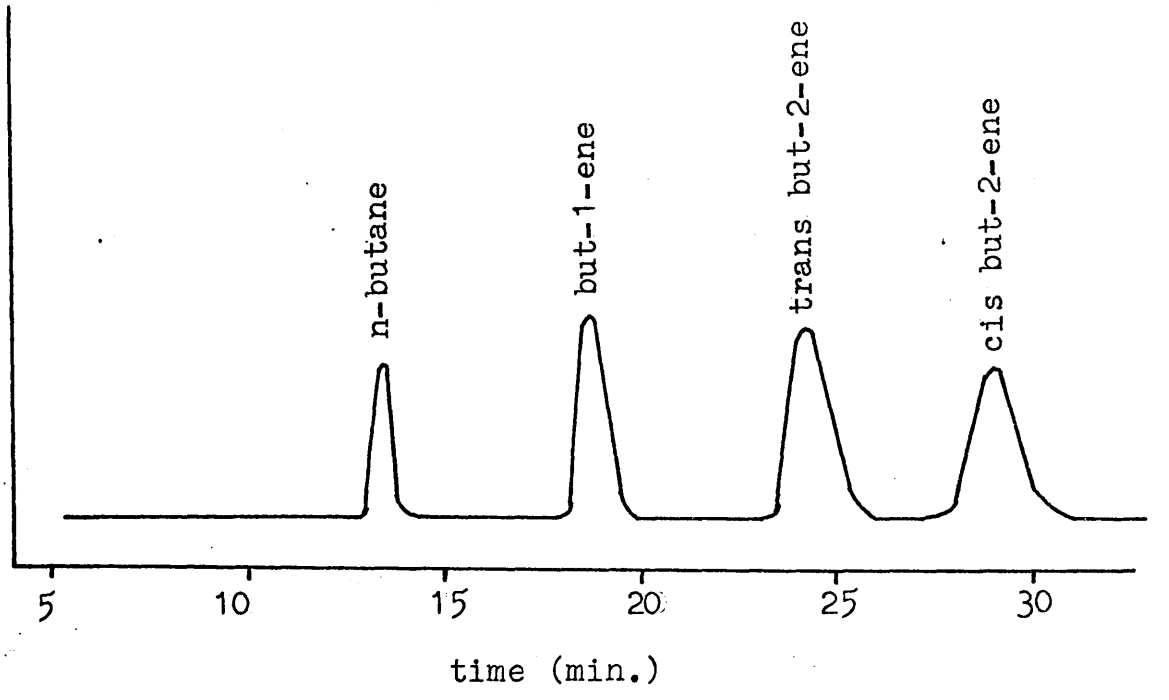

Fig. 3.4 Typical trace from acetonyl acetone column

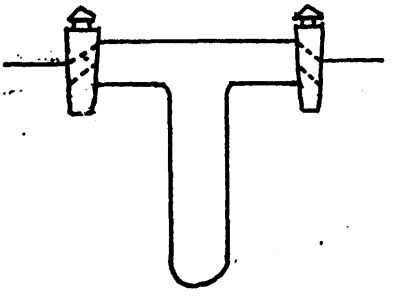

Fig. 3.5 A collector

The katharometer was used with a filament current of 300mA. supplied by a Gow-Mac D.C. Power Supply Control Unit. The output from the katharometer was fed back into the unit and then into an analogue to digital converter (105), the digital output from which was measured on an EKCO scalar. The signal from the unit was also led to a Servoscribe potentiometric chart recorder operated at 2mV. or 5mV. full-scale deflection. A plot of count rate against percentage deflection for the 5mV. range (105) shows a linear relationship above 100c.p.m. and the rate controlling potentiometer on the integrator was therefore adjusted so that 3% deflection on the recorder, normally used as the baseline, corresponded to a count rate of 100c.p.m.. By measuring the baseline count before and after the elution of each peak and by measuring the total counts for each peak and the time for which it was counted, the net counts could be obtained. This figure corresponded to the peak area in arbitrary units.

(iii) Experimental procedure

The procedure for the reactions over rhodium trichloride on silica was essentially the same as that for other test reactions. The switch valves V_1 and V_3 were turned so that the carrier gas flowed through the by-pass and the catalyst vessel was disconnected from the system. The vessel was then emptied, scrubbed clean, washed in

distilled water and dried. The silica wool plug and support of clean, dry boiling stones were inserted into the vessel and compacted to ensure a firm base. 0.2g. of the catalyst was placed in the vessel and compacted to a uniform thickness. The section was reconnected to the system and valves V_1 and V_3 were switched to allow helium to flow through the catalyst. By opening and closing valve V_2 several times, most of the air could be flushed out of this section into the atmosphere, thereby reducing the danger of oxidation of the filaments of the katharometer.

After the chromatographic trace on the recorder chart had returned to the baseline, indicating equilibration of the system and removal of the remaining air, the thermocouple was inserted into the well and the furnace slipped over the bulb. The temperature of the catalyst was then raised to activation temperature. After the required activation period, the temperature was lowered to reaction temperature.

The reactant gases were condensed or contracted (in the case of hydrogen) into a sample vessel (S.V.$_1$ or S.V.$_2$ in Fig. 3.1), to allow a pressure of slightly greater than one atmosphere to be attained so that, on sampling with the gas syringe, no air was admitted to the sample. At least two injections of a standard mixture of C_4

hydrocarbons were made into the calibration port before each run and injections were made occasionally during the series of reactions. This procedure ensured the reproducibility of the system when quantitative measurements were required. Samples for reaction were removed from the vessels and injected into the system at port P_1.

3.2.3 The Static Reaction System

In the experiments on hydrogenation reactions over silica supported triruthenium dodecacarbonyl and triosmium dodecacarbonyl, the whole of the vacuum system, except for $S.V._1$ and $S.V._2$, shown in Fig. 3.1 was used. The reaction vessels used in these experiments were all of the same design. Each consisted of a cylindrical "Pyrex" glass vessel attached via narrow bore tubing and a 2mm. tap to a "Quickfit" B10 cone. The capacity of the vessel was approximately 100ml. (or 200ml. when deuterium was used as reactant).

Gas mixtures were prepared by measuring the hydrocarbon from a storage vessel into the mixing vessel, M.V., which was then isolated from the rest of the system. After the gas had been condensed in the cold finger, the required pressure of hydrogen was admitted to the vessel, which was again isolated, and the gases allowed to warm up to ambient temperature. These were left to stand

for about 30 minutes to enable the gases to mix thoroughly.

Before each reaction series, the catalyst vessel was washed out with "aqua-regia", thoroughly rinsed with distilled water and dried in an oven. The catalyst was weighed into the vessel, which was then sealed, attached to the high vacuum line at socket C_2 and evacuated. After degassing for about 30 minutes, the temperature was raised to the activation temperature by means of a cylindrical electric furnace, the current to which was controlled by a Variac transformer. Temperatures were measured with a "Comark" thermocouple unit. After the required activation treatment and the catalyst was ready for use, the temperature was reduced to reaction temperature.

Reactions were carried out by admitting the required pressure of reactants into the reaction vessel and the pressure fall was measured on the mercury manometer M_2. At the desired pressure fall, the reaction was stopped by expanding the products into vessel E. These were then condensed into the spiral trap D and the unreacted hydrogen pumped away. After warming to ambient temperature, the hydrocarbon products were distilled into an evacuated sample vessel attached to the system at socket C_3. Between successive reactions, the catalyst vessel was evacuated for 20 minutes.

3.2.4 The Gas Chromatography System

This system is shown diagramatically in Fig. 3.6(a). The sample-handling system (Fig. 3.6(b)) could accept samples transferred from the static reaction system. It comprised a U-tube of ~14ml. capacity sealed at each end by three-way taps T_1 and T_2. Carrier gas could flow into the U-tube via T_1 and exit by T_2 or alternatively, by simultaneously turning T_1 and T_2, the gas could be diverted through the by-pass. When a sample was to be admitted to the chromatograph, the carrier gas was diverted through the by-pass while the U-tube and manometer M were evacuated. The sample vessel was inserted into socket C and the volume which had been open to the atmosphere evacuated. After isolating the section from the pumps, the required pressure of sample was admitted and taps T_1 and T_2 turned to allow the carrier gas to sweep the sample through the column.

To confirm the reproducibility of the system, two samples of a standard mixture of C_4 hydrocarbons were tested before each series of reaction products were analysed. The column consisted of 20' $\frac{1}{4}$" O.D. glass tubing packed with 40% w/w acetonyl acetone on 60-80 mesh firebrick. At an operating temperature of $20 \pm 3^{\circ}C$, the corrected retention volumes were 200, 385, 525, and 690ml. for n-butane, but-1-ene, trans but-2-ene and cis but-2-ene respectively, at a flow rate of 50ml.min.$^{-1}$

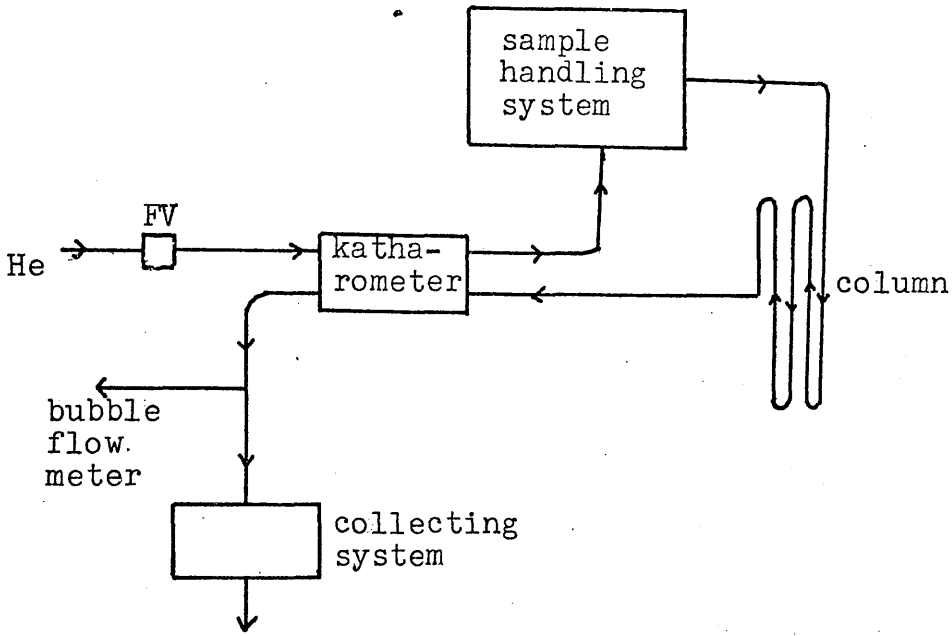

Fig. 3.6(a) Block diagram of chromatograph

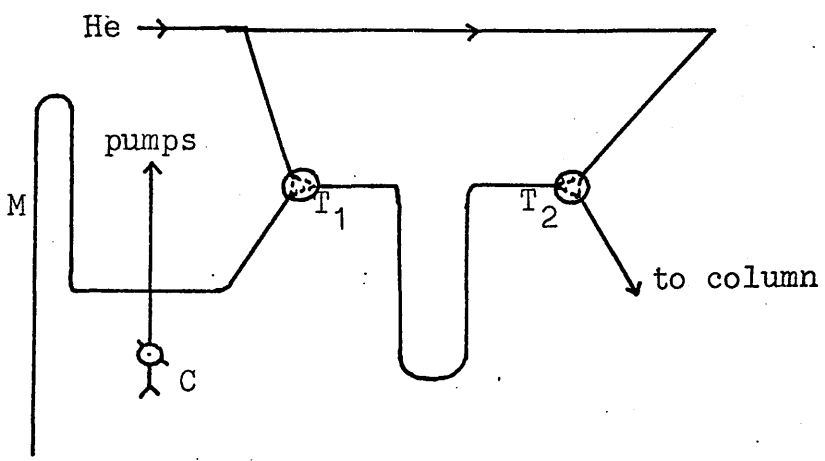

Fig. 3.6(b) The sampling system

The detector was a Gow-Mac hot-wire katharometer operated at a filament current of 250mA. supplied by a D.C. power unit (106). The output from the detector unit was fed into an integrator with automatic output and print-out (106). A continuous output was also taken from the integrating unit to a Servoscribe potentiometric recorder. Plots of total count against partial pressures of the eluant gases show a linear relationship over the range in which the instrument was used (Fig. 3.7).

3.2.5. Mass Spectrometry

Because the detection of gases by katharometer is non-destructive, it was possible to lead each fraction of the eluant gases into the collecting system (Fig. 3.6(a)), there to be collected and retained for analysis of the deuterium content by mass spectrometry.

The collecting system comprised a series of five traps, lightly packed with glass wool. Before each run on the chromatograph, the system was flushed out with helium and each U-tube surrounded by a Dewar flask containing liquid nitrogen. Thereafter, hydrocarbon samples could be condensed in turn out of the gas stream into each of the collectors by directing gas flow through the U-tube or the by-pass as appropriate.

After elution of the whole sample, the carrier gas

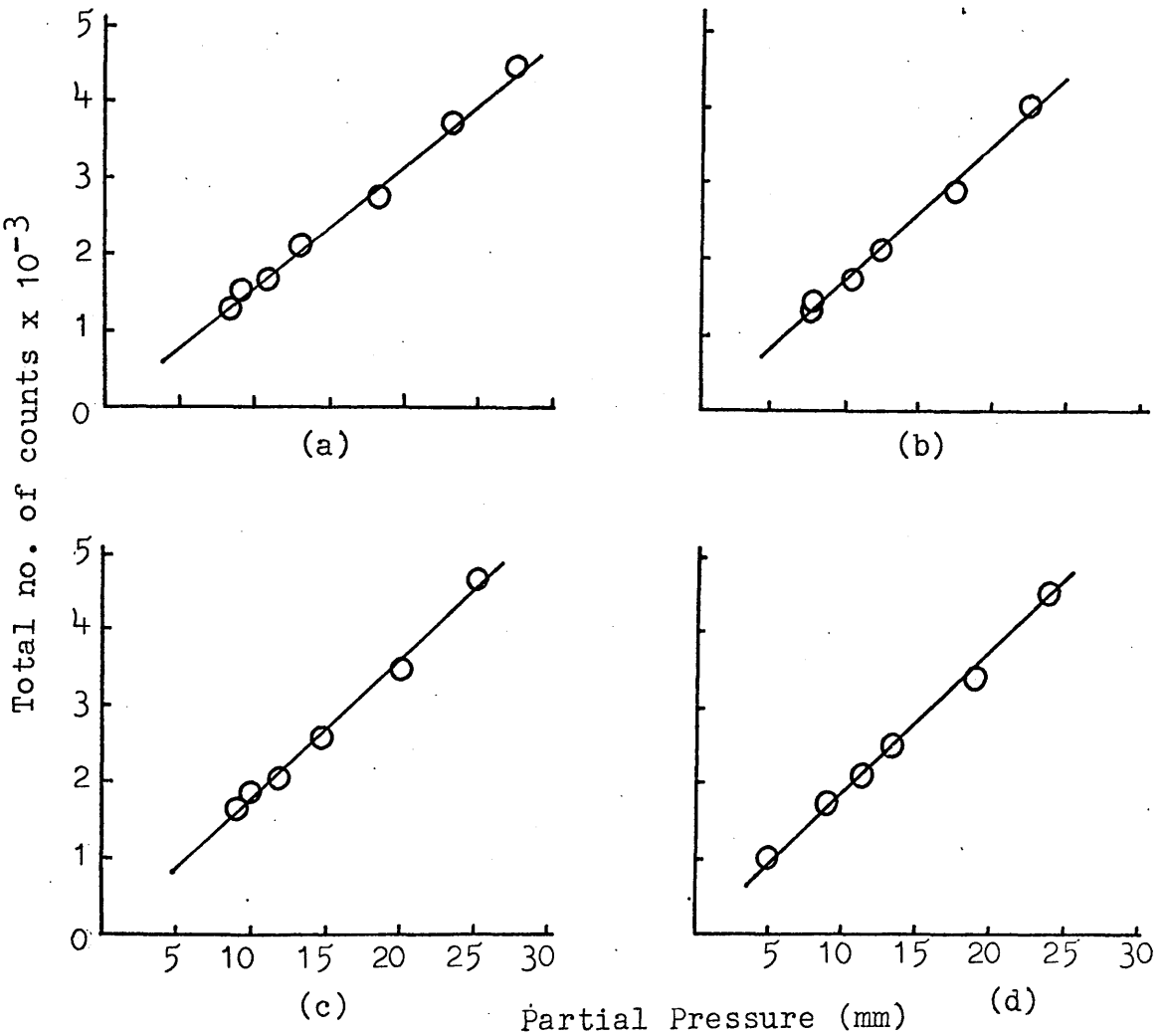

Figs. 3.7 Calibration plots for integrator with (a) but-1-ene, (b) cis but-2-ene, (c) trans but-2-ene and (d) n-butane.

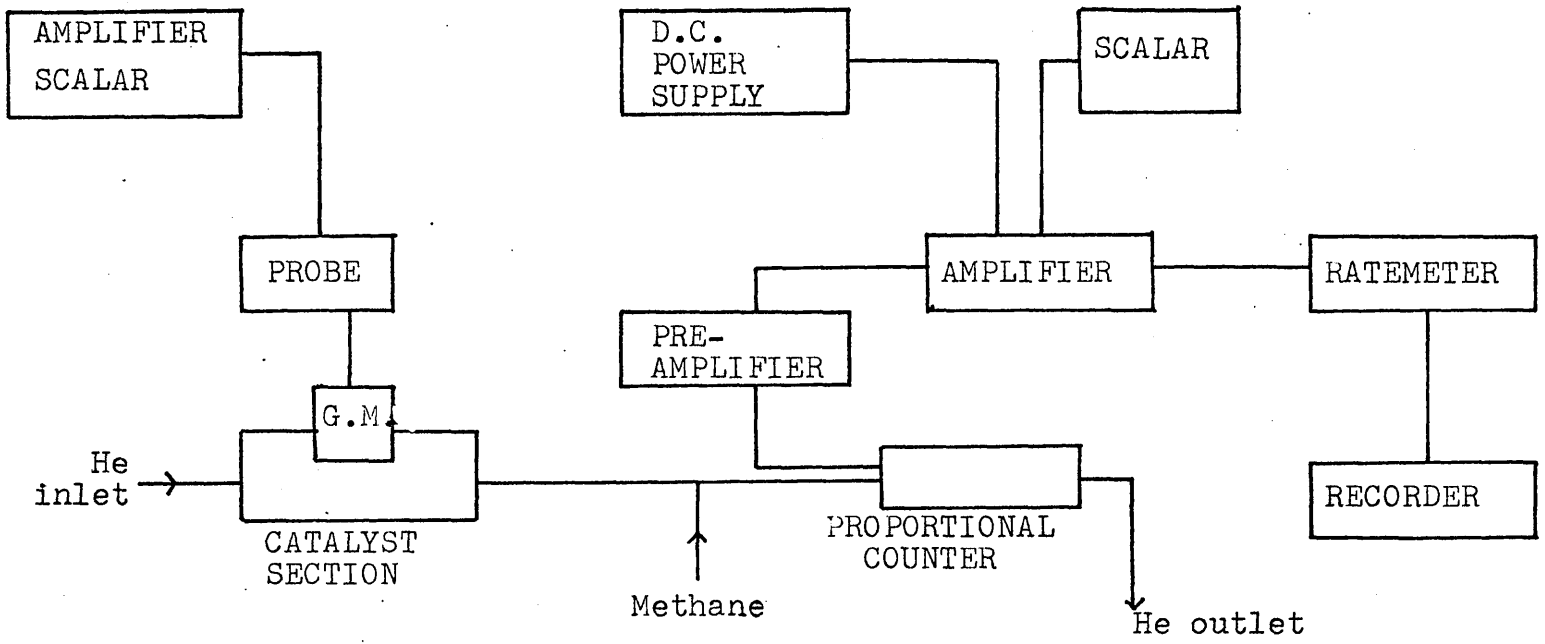

Fig. 3.8 Block diagram of the counting system.

stream was disconnected from the collecting system. One trap at a time was then evacuated and allowed to warm up to ambient temperature so that the hydrocarbon sample could be removed for analysis by condensing it into an evacuated sample vessel.

The analyses were carried out in an A.E.I. M.S.20 mass spectrometer, using the following operating conditions:

TABLE 3.2

Mass Spectrometer Operating Conditions

Magnet strength	4.5KG.
Electron energy	15eV.
Trap current	50 μV.
Ion repeller	-3.1V.

3.2.6. The Flow-Counting System

In the studies using carbon-14 labelled triruthenium dodecacarbonyl on silica, the ^{14}C counting system shown in Fig. 3.8 was used.

(i) The catalyst section

A diagram of the catalyst section is shown in Fig. 3.9. It comprised a "Pyrex" glass tube (35mm. O.D.) with a B34 Quickfit joint at one end. The side-arm J_2 was a B34 socket and the Geiger-Müller tube (Mullard, MX/168), which was suspended from a B34 cone, was inserted into this, so that the end window could look directly at the

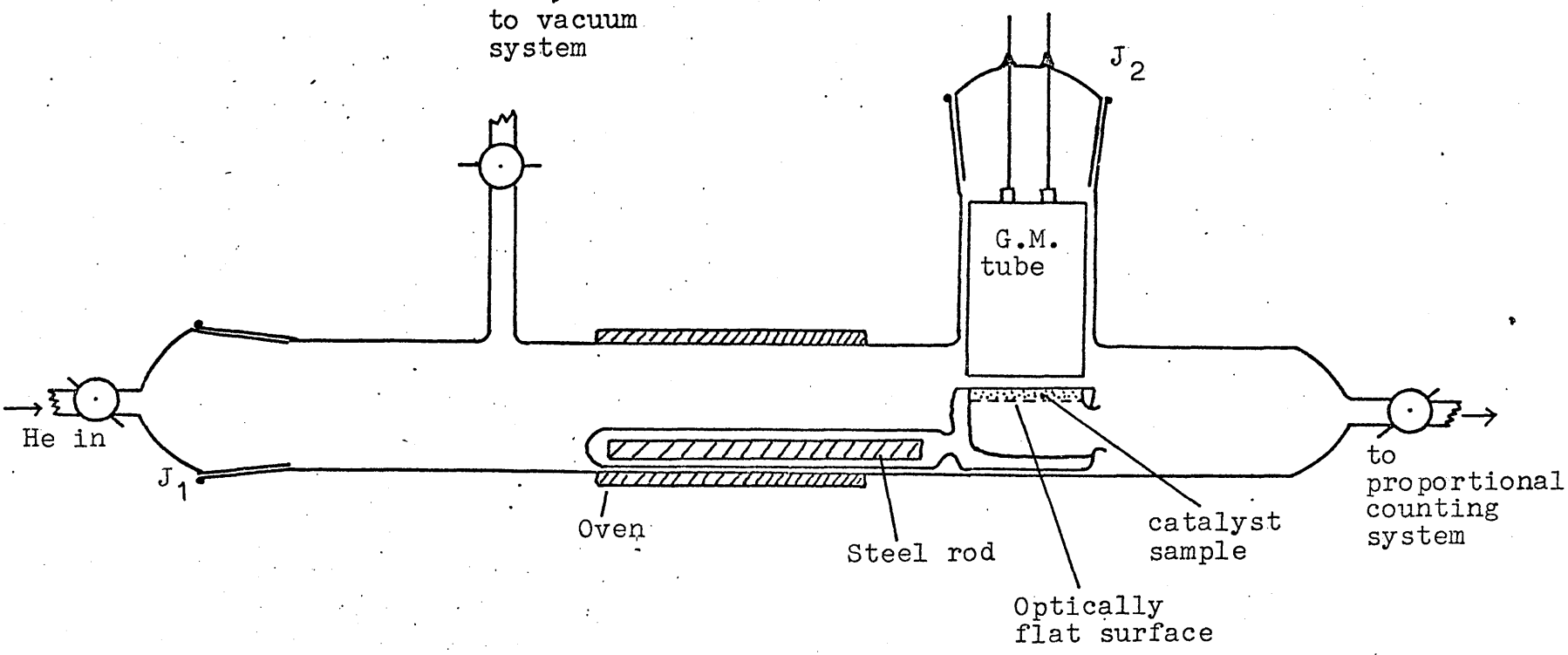

Fig. 3.9 The catalyst section

catalyst vessel. The catalyst vessel itself consisted of an optically flat glass surface set 2mm. below the rim of a "Pyrex" glass basin, which was attached to a glass rod containing a steel bar. This steel bar allowed the vessel to be manipulated with a horseshoe magnet from outside the catalyst section. So that the catalyst could be heated, an electric furnace was wound round the section and the temperature was controlled and measured by a "West" Thyristor Unit and thermocouple. Quickfit joints were sealed with "Apiezon W" black wax and the taps were lubricated with "Apiezon N" tap grease.

(ii) The counters

(a) The Geiger-Müller tube: A conventional end-window Geiger-Müller tube (Mullard MX/168) in conjunction with an EKCO Probe Unit was used to monitor the catalyst directly. Power was supplied from an EKCO scalar, the output from which was variable from 0-2000V. The determination of the plateau of the tube showed that the optimum operating voltage was 415 V.

(b) The proportional counter: Because of the practical problems involved in the continuous direct observation of the catalyst sample while it was being heated (maximum operating temperature of G.M. tube is $\sim 50^{\circ}C$) and because the efficiency of an end-window Geiger-Müller tube in counting carbon-14 β emissions is only $\sim 10\%$, a pro-

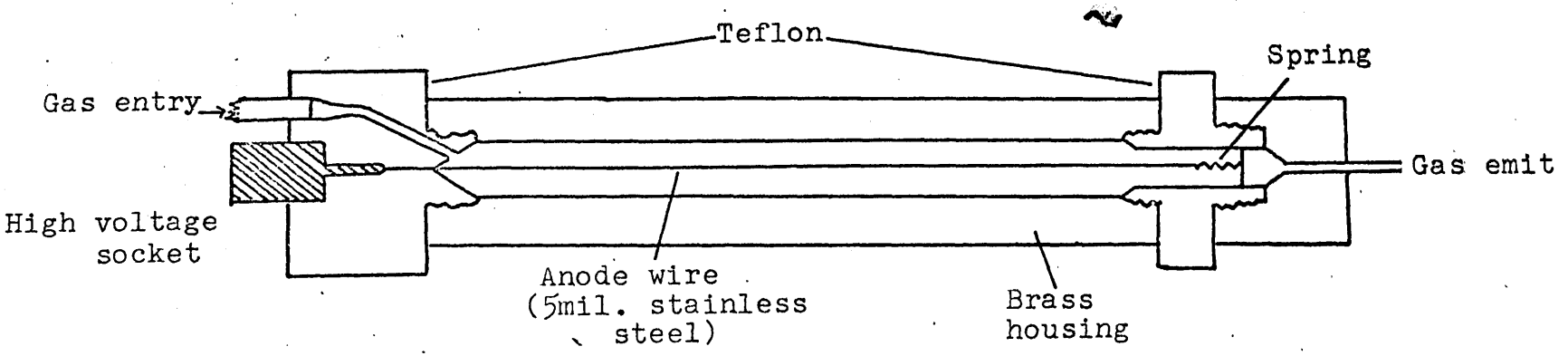

Fig. 3.10 The proportional counter

portional counter was incorporated into the flow system so that the carrier gas could be monitored continuously for carbon monoxide.

A proportional flow counter, similar in design to that of Schmidt-Bleek and Rowland (107), was modified to accommodate different connectors for the gas inlet and high voltage supply (Fig. 3.10).

The general block diagram in Fig. 3.8 shows the instrumentation used with the proportional counter. The power was supplied by a Dynatron N103 unit, the output from which was continuously variable from 300 to 3300 volts. The amplification was through a Dynatron 50D pulse amplifier, comprising a high gain preamplifier, connected to the counter with a short lead, and a main amplifier in which the gain could be altered in 2db steps within the range 0-40db. An EKCO 530D high speed scalar measured the amplifier output, which was also recorded by an EKCO N522C ratemeter, coupled to a Servoscribe potentiometric recorder. Discriminator units on the scalar and ratemeter allowed the optimum detection of certain pulses to be achieved.

In this work, a counting mixture of helium and methane was used and the ratio of helium to methane proved to be a critical factor in the determination of the plateau (108). By varying the flow rates of helium and methane, it was

found that at a helium flow of 36ml.min.$^{-1}$ and a discriminator bias setting of 15V., a ratio of 12:1 helium to methane gave the best plateau in terms of both length and slope (Fig. 3.11).

TABLE 3.3

Optimum Operating Conditions for Proportional Counter

Amplifier attenuation	32db
Time constant (differentiation)	3.2μsec.
Time constant (integration)	1.6μsec.
Helium flow rate	36ml.min.$^{-1}$
Methane flow rate	3ml.min.$^{-1}$
Applied voltage	2.4KV.
Discriminator bias	15V.

Because of the small amounts of tracer to be measured, a shield of lead bricks surrounded the counter, so that the background count rate could be kept at less than 3c.p.s.

(iii) Experimental procedure

Before each run, the catalyst vessel was thoroughly washed and dried. It was then inserted into the catalyst section of the system through J_1, which was then sealed. The rates of flow of helium and methane were adjusted to 36 and 3 ml.min.$^{-1}$ respectively and the vessel was positioned directly underneath the Geiger-Müller tube. After all the air had been swept out of the system, the

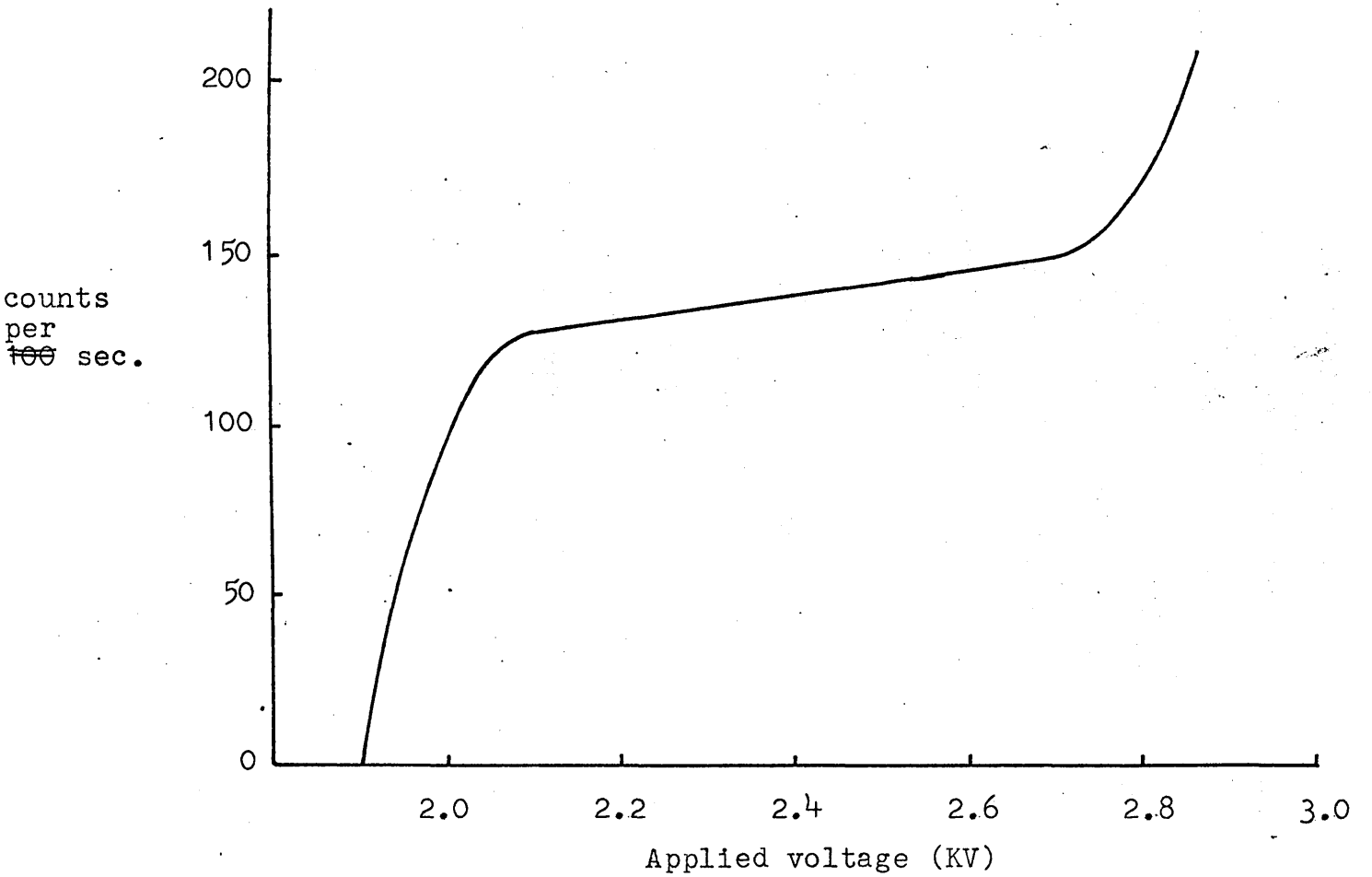

Fig. 3.11 Proportional counter plateau at 15V disc bias and 12:1 He:Me ratio.

instrumentation was switched on and the background count rate for each counter determined. With the power supply to the counters switched off, the vessel was removed and 0.5g. of catalyst placed on its flat surface and compacted. The vessel was then replaced under the Geiger-Müller tube, J_1 sealed and the gas and power supply restored.

After the determination of the count rate by the Geiger-Müller counter, the catalyst vessel was moved into the oven and the count rate on the proportional counter measured. The temperature of the oven was raised to the required level by altering the setting on the Thyristor unit and this level was attained within 30 seconds. The proportional count rate was measured at regular intervals, so that a trace of count rate against time at the given temperature could be obtained. After the count rate had stabilised, the power supply to the oven was disconnected and the catalyst allowed to cool. The cooled vessel was replaced under the Geiger-Müller tube and its activity remeasured. This procedure was repeated using progressively higher oven temperatures until the count rate, as measured by the Geiger-Müller counter, had diminished to background level.

CHAPTER 4

TREATMENT OF QUANTITATIVE DATA

4.1 The Hydrogenation Reaction

The pressure fall during the hydrogenation reaction was measured on the mercury manometer to an accuracy of within ± 0.5mm. The pressure fall was plotted against time and the gradient of the tangent to the curve at the origin or at the end of the induction period was taken as the initial rate of hydrogenation.

4.2 The Butene Distribution

4.2.1 Interpretation of the Gas Chromatography Traces

The area under a peak, as measured by the electronic integrator, was found to be proportional to the partial volume or partial pressure, as appropriate, of the corresponding eluant gas. The columns and katharometers were calibrated using samples of a standard mixture of all the gases to be encountered in the reaction analyses and the ratio of peak area to partial volume or to partial pressure for each gas, known as the sensitivity coefficient, was determined. This method allowed a high degree of reproducibility to be attained by the measurement of the mean sensitivity coefficient for each gas. To ensure

this reproducibility of the system, calibrations were carried out each morning before a series of reaction analyses and thereafter at frequent intervals throughout the day.

Partial volumes or partial pressures were calculated from the peak areas and from these figures, the percentage distribution of butenes and the required trans/cis ratios could be computed.

4.2.2 The Initial Rates of Isomerisation

The method first developed by Twigg (109) was used in the calculation of the initial rates of isomerisation of the but-1-ene. From this method, which is applicable only to double-bond migration reactions, the following equation (110) may be derived:

$$r_i = \left[\log_{10}(1-y_{eq}) - \log_{10}(y-y_{eq})\right] \times 2.303(1-y_{eq})\frac{(P_B)_o}{t_{ex}}$$

where, r_i = initial rate of isomerisation,

y = fraction of reactant butene remaining,

y_{eq} = thermodynamic equilibrium fraction of reactant butene,

$(P_B)_o$ = initial pressure of reactant butene,

t_{ex} = time from the start of reaction until sample was extracted from reaction vessel (the extraction time).

This model assumes that the adsorption coefficients of

but-1-ene, trans but-2-ene and cis but-2-ene are equal.

4.3 Determination of Reaction Kinetics

The dependence of the rates of reaction upon the initial partial pressures of the reactant gases in the hydrogenation and isomerisation reactions was determined on the assumption that the form of the rate expression is as follows:

$$\text{rate} = k p_{H_2}^{x} \cdot p_{C_4H_8}^{y} ,$$

where, k = rate constant,

p_{H_2} = initial pressure of hydrogen,

$p_{C_4H_8}$ = initial pressure of butene,

x and y = orders of the reaction with respect to hydrogen and butene.

By varying the initial pressure of hydrogen and keeping the initial pressure of butene constant, the rate expression reduces to an equation of the form

$$\text{rate} = K p_{H_2}^{x} .$$

When the order of the reaction was unity or zero with respect to hydrogen, this could be ascertained by inspection of the plot of rate versus p_{H_2}: a first order reaction gives a straight line passing through the origin, while a zero order reaction gives a straight line parallel to

the p_{H_2} axis. When the order of reaction was neither zero nor unity, then, by plotting log(rate) against log p_{H_2} the order of the reaction with respect to initial hydrogen pressure, which is equal to the slope of the resultant straight line, was determined. A similar series of reactions, where the initial pressure of butene was varied and that of hydrogen held constant, allowed the determination of the order of reaction with respect to initial butene pressure.

4.4 Determination of Activation Energies

The rate constant of a reaction is related to the temperature of reaction by the Arrhenius equation;

$$k = Ae^{-E_A/RT}.$$

When initial rates are considered, the term r_i may be substituted for the rate constant k, giving the expression

$$r_i = A^1 e^{-E_A/RT}$$

and hence, $\log_{10} r_i = \log_{10} A^1 - E_A/2.303RT$

where, E_A = activation energy in $cal.mol.^{-1}$,

R = gas constant ($1.986 cal.deg.^{-1} mol.^{-1}$),

T = temperature in degrees Kelvin,

A and A^1 = constants.

The initial rates were measured at a series of temperatures and plots of $\log_{10} r_i$ against the inverse of temperature were drawn. Since the gradients of these

lines are equal to $-E_A/2.303R$, the activation energies of the reactions could be calculated.

4.5 Analysis of Hydrocarbons by Mass Spectrometry

The hydrocarbon products of the reactions of but-1-ene with deuterium were analysed by mass spectrometry. At the operating electron beam energy of 15eV., each of the hydrocarbons underwent both ionisation and fragmentation. The intensity of the parent ion, which was always the most abundant, was taken as being equal to unity, while the intensities of the fragments were expressed in terms of f-values - the intensities of these fragments relative to the parent ion intensity of unity. The relevant species for butene, for example, are as follows:

$C_4H_8^+$	$C_4H_7^+$	$C_4H_6^+$
1	f_1	f_2

Such fragmentation must be taken into account when the distribution of deuterated butenes is to be calculated. On the assumption that the fragmentation pattern of a deuterated butene is the same as that for a light butene - and this has been shown to be justifiable (111) - a set of simultaneous equations may be compiled to permit the computation of the true intensities of the parent deuterated butenes. At a given mass to charge ratio (m/e), the observed ion current comprises two contributions:

(i) the parent ion of mass m; and

(ii) the fragments from species of higher mass.

The latter contribution is dependent on the f-values, which may be determined by experiment, and on a statistical factor to account for the probability of the formation of the given species from each ion of higher mass, assuming that there is no preferential splitting of the carbon-hydrogen or carbon-deuterium bonds. This scheme allows the calculation of the intensity of each parent ion after correction for fragmentation. Thus, the corrected intensities of the first and second fragments of the d_o- hydrocarbon should be zero. Experiments to determine these fragment intensities showed that they were generally less than 2% of the greatest intensity. This figure was acceptable within the experimental error of the system. The equations used in the analysis of each hydrocarbon are given in full in Appendix B.

Carbon-13 constitutes 1.1% of naturally occurring carbon. Accordingly, the parent ion intensities obtained from these simultaneous equations had to be corrected for the carbon-13 content of each C_4- hydrocarbon. This was done by subtracting 4.4% of the intensity of the ion current for the d_o-species from that of the d_1-species. 4.4% of the d_1-intensity, corrected for carbon-13, was then subtracted from the intensity for the d_2-species

and so on, until all the intensities had been corrected.

Deuterium distributions were calculated by expressing each of the final corrected intensities as a percentage of the total.

The deuterium number - the mean number of deuterium atoms contained in the molecule - was calculated from the expression,

$$D.N. = \sum_{i=1}^{n} id_i,$$

where d_i is the fractional abundance of the species containing i deuterium atoms.

CHAPTER 5

REACTIONS OVER SILICA SUPPORTED RHODIUM TRICHLORIDE

5.1 Preliminary Experiments

The investigation of the catalytic properties of supported rhodium trichloride was carried out using the pulse-flow reactor system. 0.2g. samples of catalyst were activated at 120°C for one hour in the helium stream. During activation, the dark pink colour of the unactivated catalyst deepened to brick red and this colour persisted indefinitely when the temperature was reduced to reaction temperature of 60 to 100°C. When the catalyst was cooled to room temperature in helium or in air, its colour lightened to the pink shade of the unactivated catalyst after several days.

The test gases were but-1-ene and a mixture of equal pressures of hydrogen and but-1-ene. Test reactions were carried out at temperatures between 60 and 100°C. When an injection of the gas mixture was made, it was found that the catalyst was active for the hydrogenation and isomerisation of but-1-ene but, by the third injection, the colour of the catalyst had turned black. Injections of the gas mixture and of hydrogen over fresh samples showed that the supported complex was extremely sensitive to molecular hydrogen and that it reduced rapidly in

the presence of that gas even at 60°C. Exposure of the supported complex to but-1-ene had no effect on its colour and it was found that the catalyst was active in the isomerisation of but-1-ene to cis and trans but-2-ene.

5.2 Isomerisation of But-1-ene over Silica Supported Rhodium Trichloride

The isomerisation reaction of but-1-ene on silica supported rhodium trichloride was carried out by injecting 0.25ml. samples of the gas over 0.2g. of the catalyst, which had been activated at 120°C to drive off physically adsorbed water. Each series of injections was made over a fresh sample of catalyst, which was activated in the helium stream and then cooled to the required temperature.

These experiments showed that no reaction occurred at temperatures below 60°C but that the conversion to cis and trans but-2-ene increased markedly as the temperature was increased to 70°C. Series of injections were carried out at temperatures of 70, 90 and 100°C. The analysis figures, together with the trans/cis ratios and percentage conversions are shown in table 5.1, where the butene yields are given as a percentage of the total hydrocarbon eluant. The terms but-1-ene, trans but-2-ene and cis but-2-ene have been abbreviated to B-1, t-B-2 and c-B-2 respectively for use in all tables. The results

TABLE 5.1

Isomerisation of But-1-ene over Silica Supported Rhodium Trichloride.

% butene distribution

Run No.	Temp.	B-1	t-B-2	c-B-2	Conversion %	t/c
A/1	90°C	24.8	46.4	28.8	73.2	1.61
A/2	"	33.1	38.9	28.0	66.9	1.39
A/3	"	44.9	30.6	24.5	55.1	1.25
A/4	"	48.0	29.3	22.7	52.0	1.28
A/5	"	52.8	24.7	22.5	47.2	1.10
B/1	70°C	27.9	42.9	29.3	72.1	1.47
B/2	"	53.7	24.7	21.7	46.3	1.14
B/3	"	57.5	21.3	21.3	42.5	1.00
B/4	"	61.1	18.3	20.6	38.9	0.89
B/5	"	65.4	16.5	18.1	34.6	0.91
C/1	100°C	15.9	53.3	30.8	84.1	1.73
C/2	"	23.3	48.1	28.6	76.7	1.68
C/3	"	34.7	40.2	25.2	65.3	1.60
C/4	"	45.5	32.4	22.1	54.5	1.47
C/6	"	63.5	21.0	15.5	36.5	1.35
C/5	"	55.8	25.4	18.8	44.2	1.35

are illustrated graphically in ~~tables~~ Figs. 5.1, 5.2, and 5.3.

The dominant feature to emerge from these results is the marked decrease in conversion with increasing injection number. This decrease is paralleled by a decrease in the trans/cis ratio of the product hydrocarbons, so that at 70°C the ratio falls eventually below unity.

At 70°C, the decrease in conversion is greatest between the first and second injections and it appears to start to level off thereafter. At 100°C, however, the difference in conversion between each injection appears constant throughout. The initial decrease at 90°C is less marked than at 70°C and the levelling off does not start until the third or fourth injection. A similar trend is shown in the variation of the trans/cis ratio with increasing injection number.

5.3 The Support Effect

The possibility that the support material itself might catalyse the reaction was investigated by a series of injections of but-1-ene over pure silica. 0.2g. of of the silica was heated at 120°C in the carrier gas stream for one hour, thereby reproducing exactly the conditions used for the activation of the silica supported rhodium trichloride catalyst. Injections of 0.25ml. but-1-ene were made into the gas stream and it was found

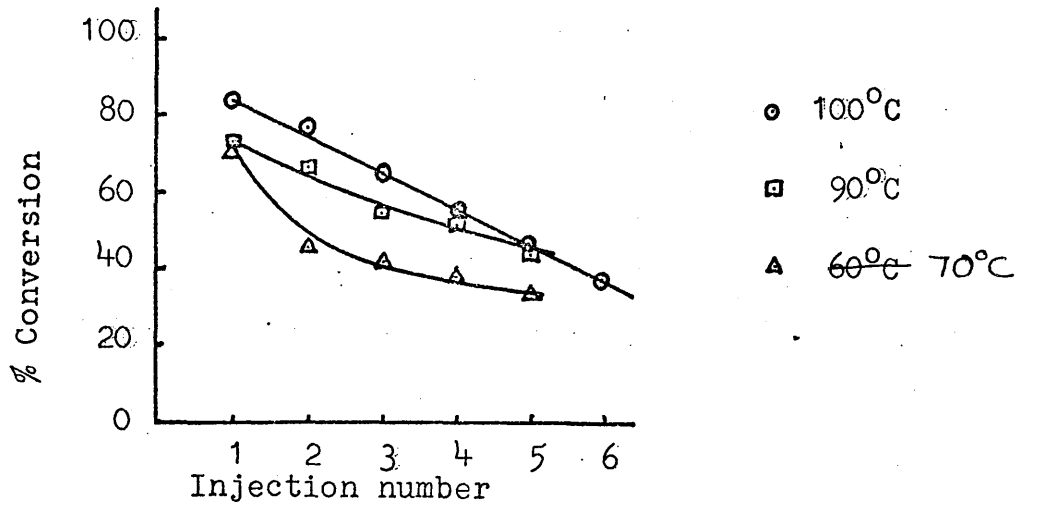

Fig. 5.1 Variation in % conversion with increasing injection number.

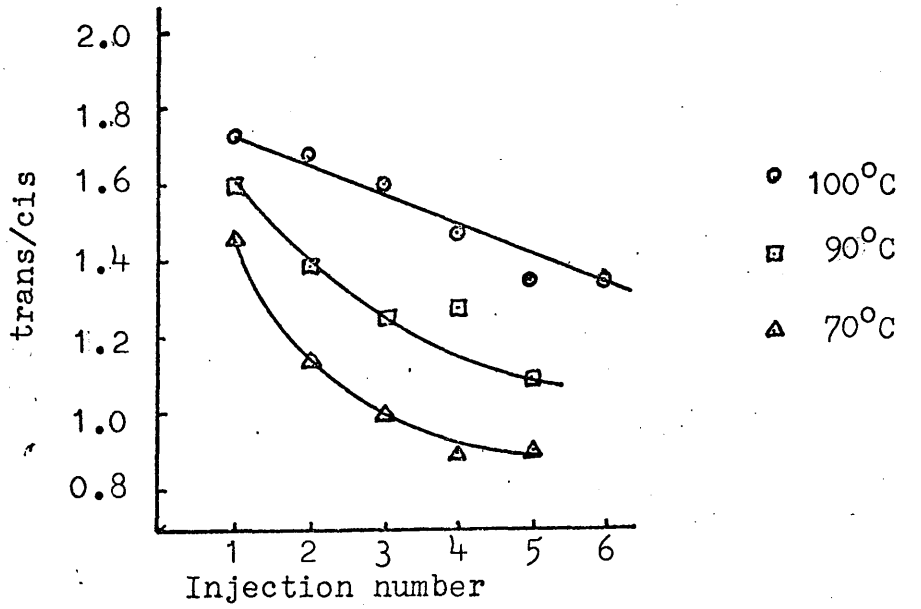

Fig. 5.2 Variation in product trans/cis ratio with increasing injection number

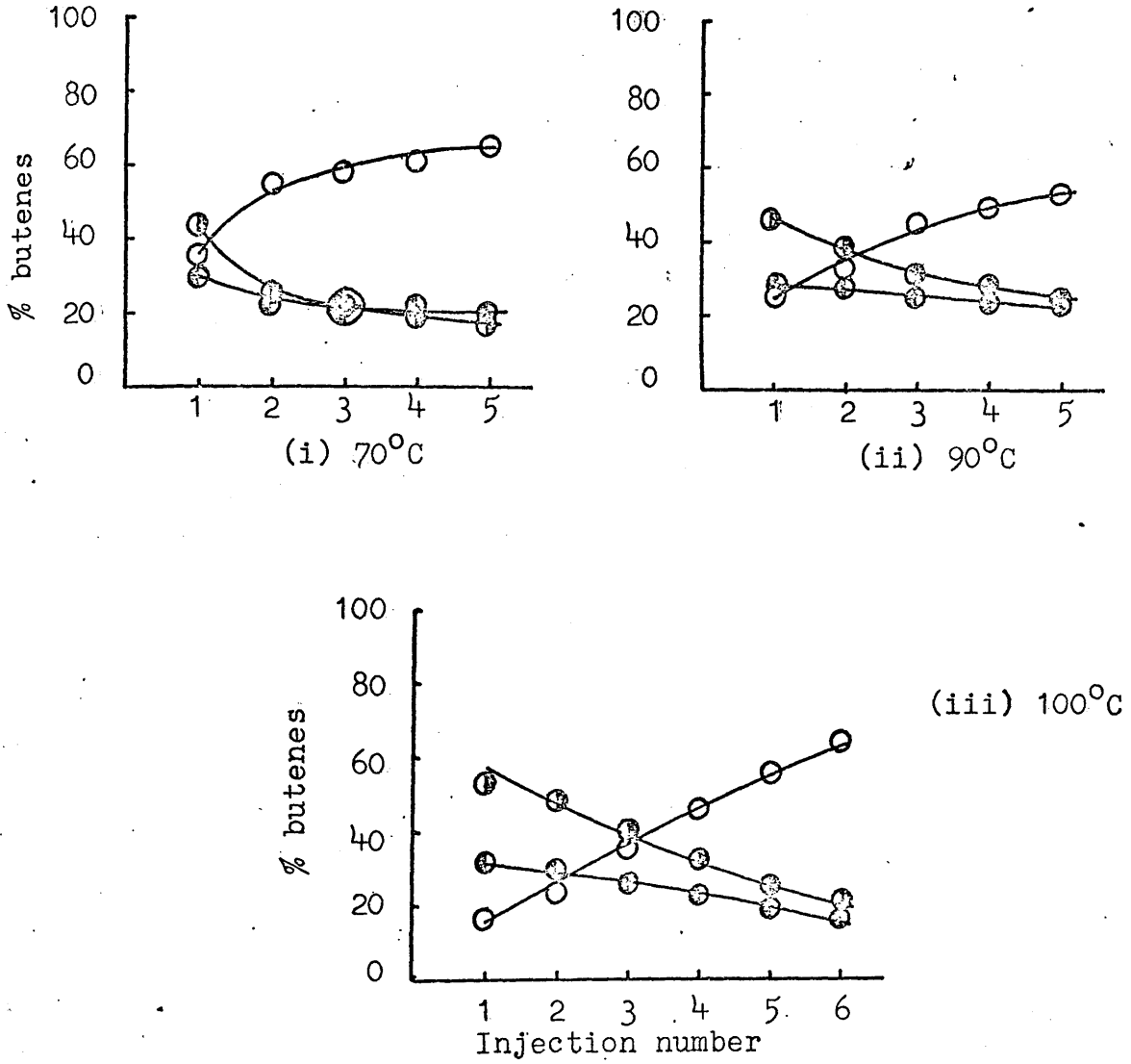

Figs. 5.3 Variation in % distribution of butenes with increasing injection number at various temperatures.

○=but-1-ene, ◑=trans but-2-ene, ◐=cis but-2-ene

that no products of isomerisation could be detected on the chromatograph. It is therefore apparent that silica itself is inactive for the isomerisation of but-1-ene under the conditions of these experiments.

CHAPTER 6

THE NATURE OF THE SILICA SUPPORTED TRIRUTHENIUM DODECACARBONYL

6.1 Preliminary Experiments.

The experiments to test for catalytic activity of the triruthenium dodecacarbonyl on silica were carried out using 0.4g. samples of the catalyst in the pulse-flow reaction system. As this system was not convenient for the collection of quantitative data, it was used only in the observation of physical changes undergone by the catalyst, when it was heated in the helium stream and/or when it was exposed to reactant gases. Gases used for test reactions were but-1-ene and 1:1 mixture of but-1-ene and hydrogen.

At ambient temperature, the catalyst was a pale-yellow colour. This colour persisted as the temperature was slowly increased until approximately 80°C, when there was a fairly rapid transition from yellow to pink. When the temperature was reduced back to ambient temperature, this colour persisted indefinitely. At temperatures greater than 200°C, the pink colour faded slowly to white and eventually darkened to pale grey. If the cooled pink form was exposed to air, its colour rapidly faded and after several days exposure, it too turned grey. Prolonged exposure of the yellow form to air caused it to turn grey,

although it did not pass through the transient pink stage. These transitions are shown in Fig 6.1.

The activities of the various forms of catalyst were then examined by injecting samples of the test gases into the system. It was found that the yellow form was inactive for the isomerisation and hydrogenation of but-1-ene and that no other hydrocarbons were detected by the chromatograph. After heating at 80°C for 30 minutes, however, the pink form showed a low activity for the hydrogenation and isomerisation of but-1-ene in the presence of hydrogen, producing n-butane and cis and trans but-2-ene. The pink form was also active in the isomerisation of but-1-ene with no hydrogen present. It was also found that the activity of the catalyst tended to increase slightly with successive injections until it eventually reached a plateau where it stabilised. If the catalyst was heated at 130°C for 30 minutes and then treated with the gas samples, no increase occurred and its activity remained constant for a number of injections. When the white form produced by the exposure of the pink form to air was heated at 130°C, it was found to be inactive in the hydrogenation of butene to n-butane, but it retained its activity for the isomerisation of but-1-ene, whether mixed with hydrogen or not. The grey form produced in the reactor showed activity for hydrogenation and

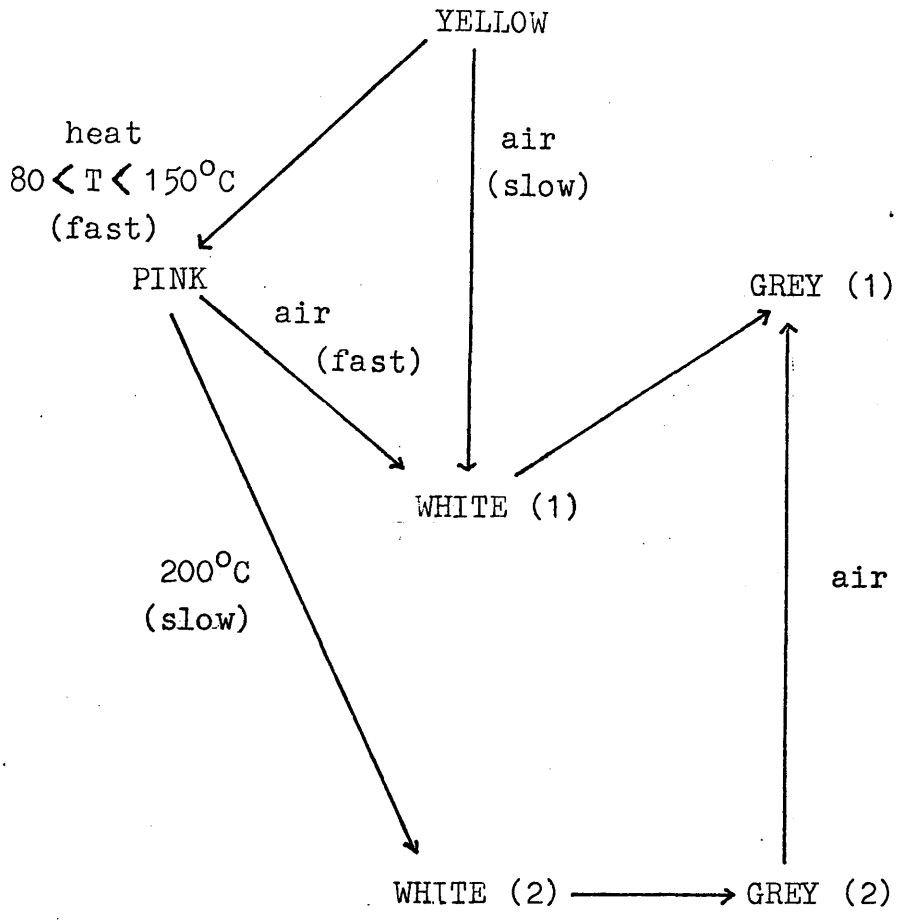

Fig. 6.1 Transitions undergone by supported complex under various conditions.

isomerisation of the but-1-ene in the mixture but did not catalyse the isomerisation of the butene on its own. The grey form which had been produced by the exposure of the yellow, pink or white form to air showed little or no such activity.

The qualitative results obtained from the test reactions are summarised below.

TABLE 6.1

Activities of the Various Forms of Catalyst

	Hydrogenation	Hydro-isomerisation	Isomerisation
Yellow	No	No	No
Pink	Yes	Yes	Yes
White	No	Yes	Yes
Grey (unexposed to air)	Yes	Yes	No
Grey (exposed to air)	No	No	No

6.2 Examination of the Catalyst by Infra-Red Spectroscopy.

Samples of silica supported triruthenium dodecacarbonyl were prepared for examination by Infra-Red Spectroscopy by pressing 0.1g. of the catalyst, supported by a paper disc, in a 16mm. stainless steel die at a pressure of 8 tons per sq. inch for five minutes. In the case of the pink form,

the sample was transferred from the catalyst vessel to the die in a nitrogen box. Immediately the die had been evacuated and pressed, the disc was transferred to the spectrometer and the spectrum of the required region taken on the Perkin Elmer P.E. 275 Spectrometer.

The spectra are shown in Figs. 6.2 and the relevant data summarised below:

TABLE 6.2

Observed Carbonyl Bands of Various Forms of the Complex

(i)	Solution of $Ru_3(CO)_{12}$ in methylene chloride	2060 cm^{-1} 2029 cm^{-1} 2007 cm^{-1}
(ii)	Yellow form (unactivated catalyst)	2065 cm^{-1} 2035 cm^{-1} 2010 cm^{-1}
(iii)	Pink form (activated catalyst)	2070 cm^{-1} 2050 cm^{-1} 2000 cm^{-1} 1970 cm^{-1}
(iv)	White form	2070 cm^{-1} 2000 cm^{-1}
(v)	Grey form (not exposed to air)	no carbonyl absorption
(vi)	Grey form (exposed to air)	

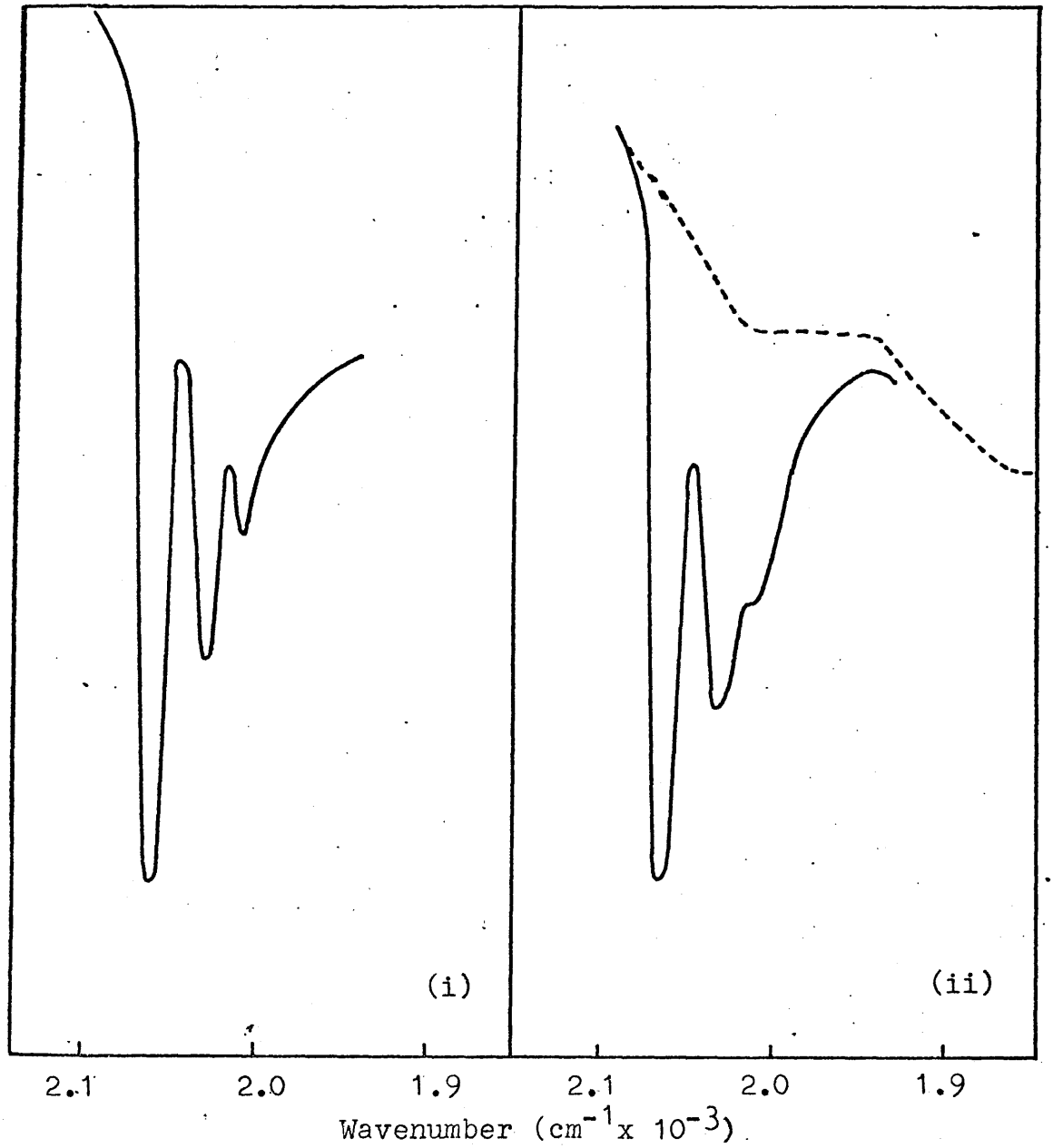

Fig. 6.2 Spectra of various forms of catalyst:
(i) Solution spectrum of $Ru_3(CO)_{12}$ in methylene chloride;
(ii) Freshly prepared supported complex (yellow form);

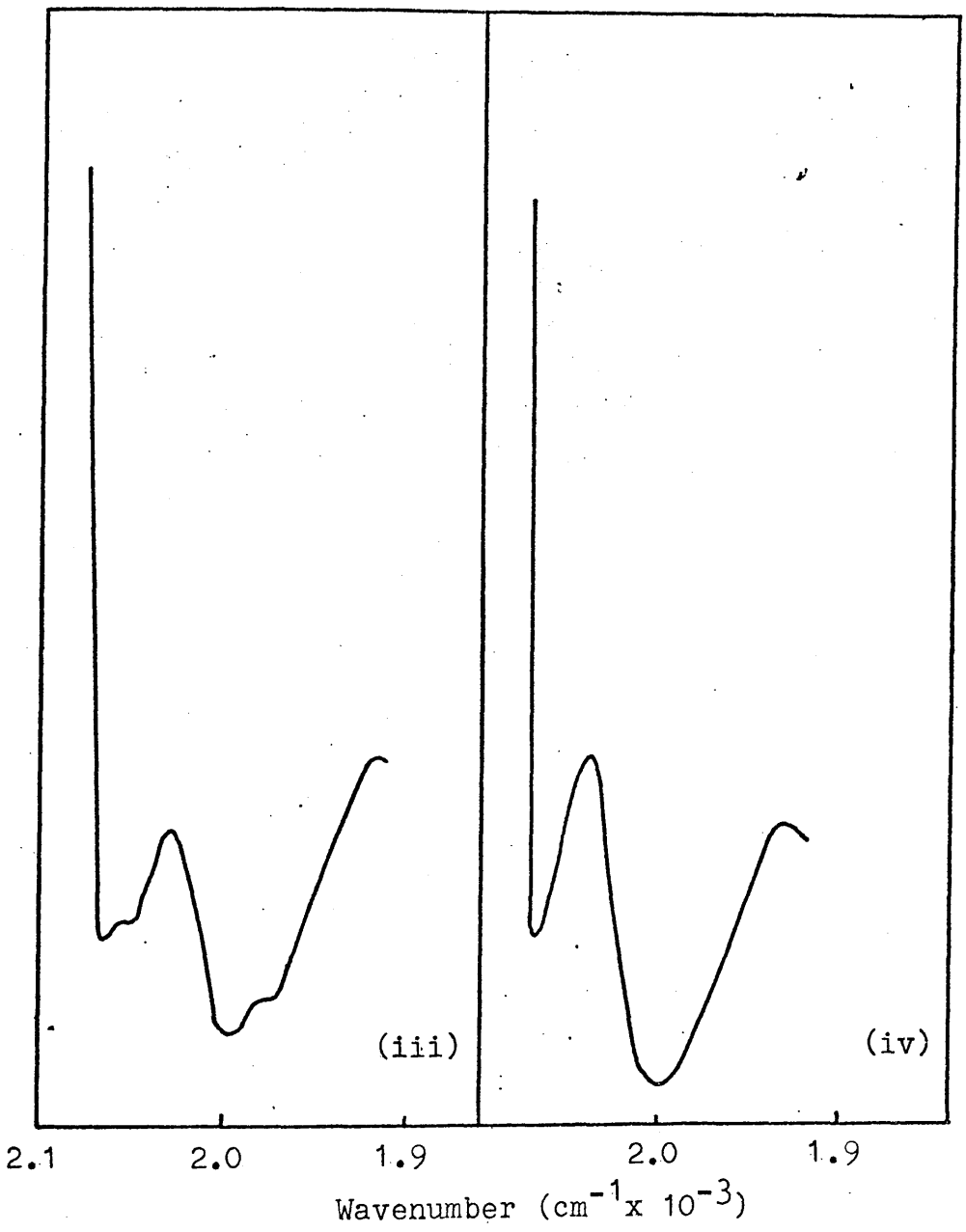

(iii) Activated catalyst (pink form);

(iv) White form.

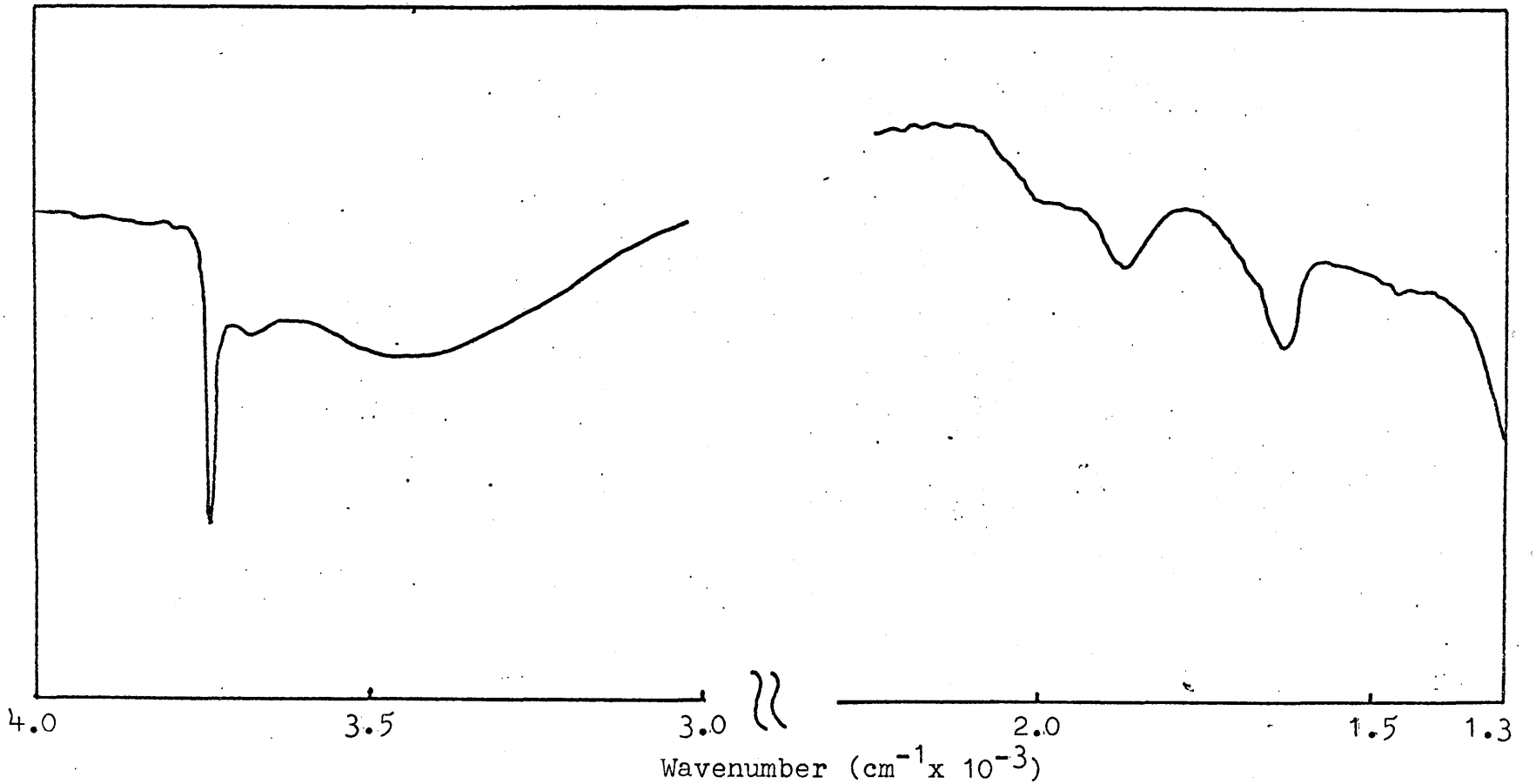

Fig. 6.3 Spectrum of dry "Aerosil" silica.

Fig 6.2(ii) shows a typical spectrum of the unactivated silica supported catalyst in the carbonyl region (2100 - 1850 cm^{-1}) and Fig. 6.2(i) shows the solution spectrum of triruthenium dodecacarbonyl in methylene chloride for comparison. Outside the carbonyl region, the catalyst showed an intense, sharp absorption at 3740 cm^{-1}, a broad absorption between 3700 and 3000 cm^{-1} and a further band of medium intensity at 1650 cm^{-1}. The spectrum of dry silica in Fig. 6.3 showed that these bands outside the carbonyl region were due to the silica support. The two absorption bands observed within this region at 2000 and 1860 cm^{-1} are shown superimposed on the spectrum of the unactivated catalyst in Fig. 6.2(ii).

Activation of the catalyst at 130°C (Fig. 6.2(iii)) causes the disappearance of the peaks at 2035 and 2010 cm^{-1}, and the growth of a band at 2000 cm^{-1} and the appearance of peaks at 2050 and 1970 cm^{-1}. A catalyst sample which had been maintained at a temperature of 100°C for several days and which had been used to catalyse a number of reactions gave a spectrum with bands of the same intensities as this. Exposure of the active species to air caused the disappearance of the peaks at 2050 and 1970 cm^{-1} (Fig. 6.2(iii)).

The effect of exposure of the unactivated catalyst to air is shown in Fig. 6.4. These spectra were taken on a Perkin-Elmer P.E. 225 Grating Infra-Red Spectometer, which

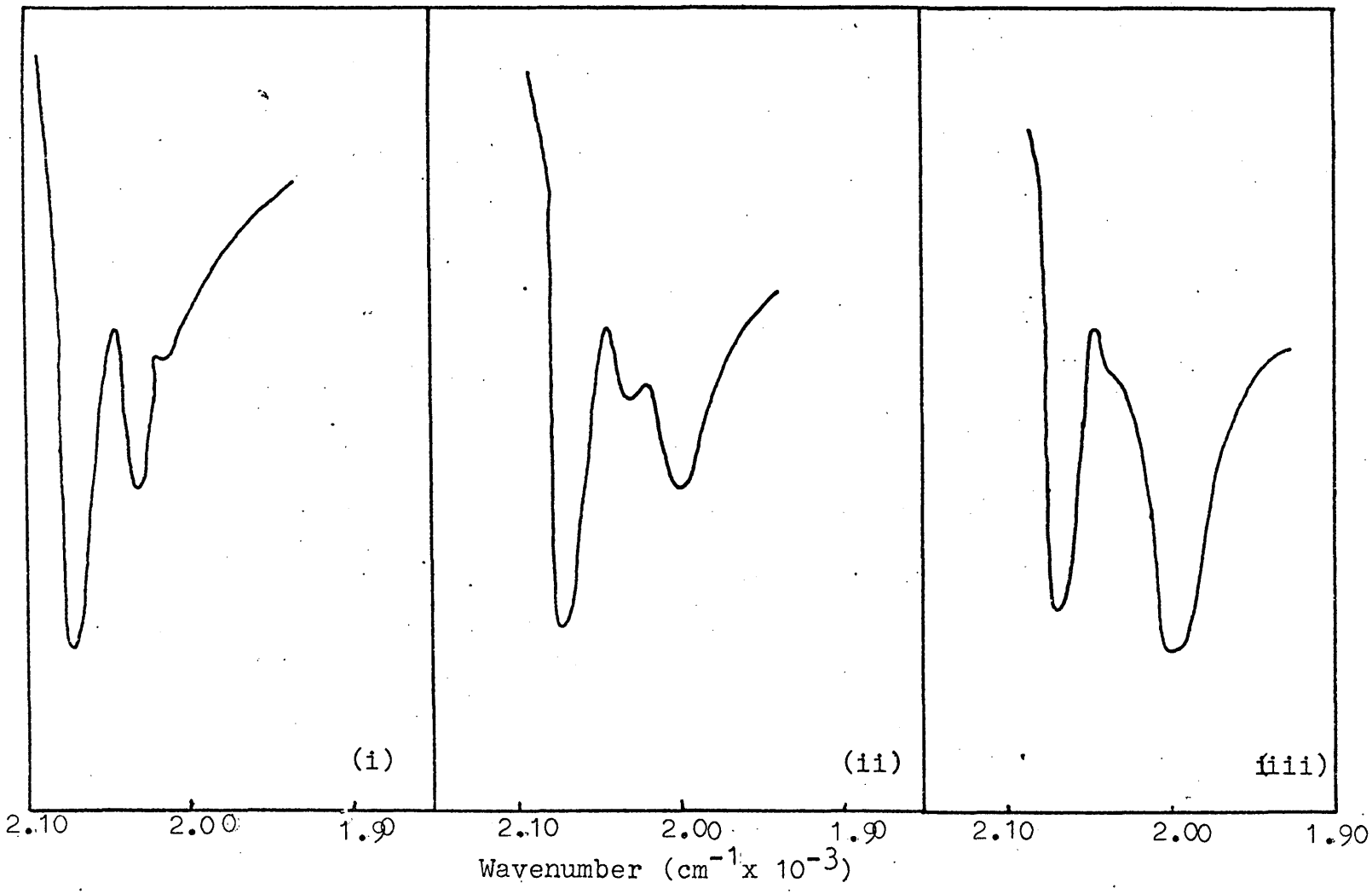

Fig.6.4 Changing spectrum of supported complex on heating in air:
(i) Freshly prepared; (ii) After 10 min.; (iii) After 20 min..

has a very hot source. Exposure of the catalyst sample to air while it sat in the proximity of the hot source caused the acceleration of the transition of the yellow form to white. Figs. 6.4(i), (ii) and (iii) are successive spectra of the same sample, with an interval of approximately ten minutes between each sprectrum. In this case, there is a growth of the peak at 2000 cm^{-1} and disappearance of the absorption band at 2030 cm^{-1}. There is no evidence of the peaks at 2050 or 1970 cm^{-1} which were present in the case of the activated pink form.

6.3 Radiochemical Examination of the Catalyst.

The catalyst used in these experiments was the 10% w/w carbon-14 labelled triruthenium dodecacarbonyl on silica. This catalyst, when unactivated, gave a count rate of approximately four times background as measured on the Geiger-Müller counter, providing much more reliable readings than the 2% catalyst, which could barely be detected by this method.

Background count rates were determined for periods of 7×10^4 seconds and were found to be 36 and 133 counts per 100 seconds for the Geiger-Müller and proportional counters respectively.

Traces obtained from the proportional counting system when the catalyst was heated at 70, 105 and 140°C in the

helium stream are shown in Figs. 6.5. At ambient temperature, the proportional count rate was taken when the catalyst was positioned inside the catalyst section and was found to be equal to the background level, indicating that little or no carbon monoxide was being given off. On heating to 70°C (Fig. 6.5(i)), however, there was an initial burst of carbon monoxide lasting between 60 and 100 seconds, after which the count rate dropped back to just above background. It then rose sharply to a maximum, when it began to tail off slowly until it finally stabilised just above background. On cooling, the count rate returned to background level. An attempt to reproduce this trace with the same catalyst sample at the same temperature failed, and the count rate rose only a little above background.

When the temperature of the same sample was raised to 105°C, there was again an initial burst of carbon monoxide given off, and a curve of similar shape to that at 70°C was obtained (Fig. 6.5(ii)). The maximum in this case, however, was found to be about 80 counts per 100 seconds higher than in the previous run at 70°C. The characteristic burst of carbon monoxide and subsequent smooth curve was repeated in the run at 140°C (Fig. 6.5(iii)) and the maximum of the curve was found to be higher than in either of the previous runs.

The count rates, corrected for background, obtained

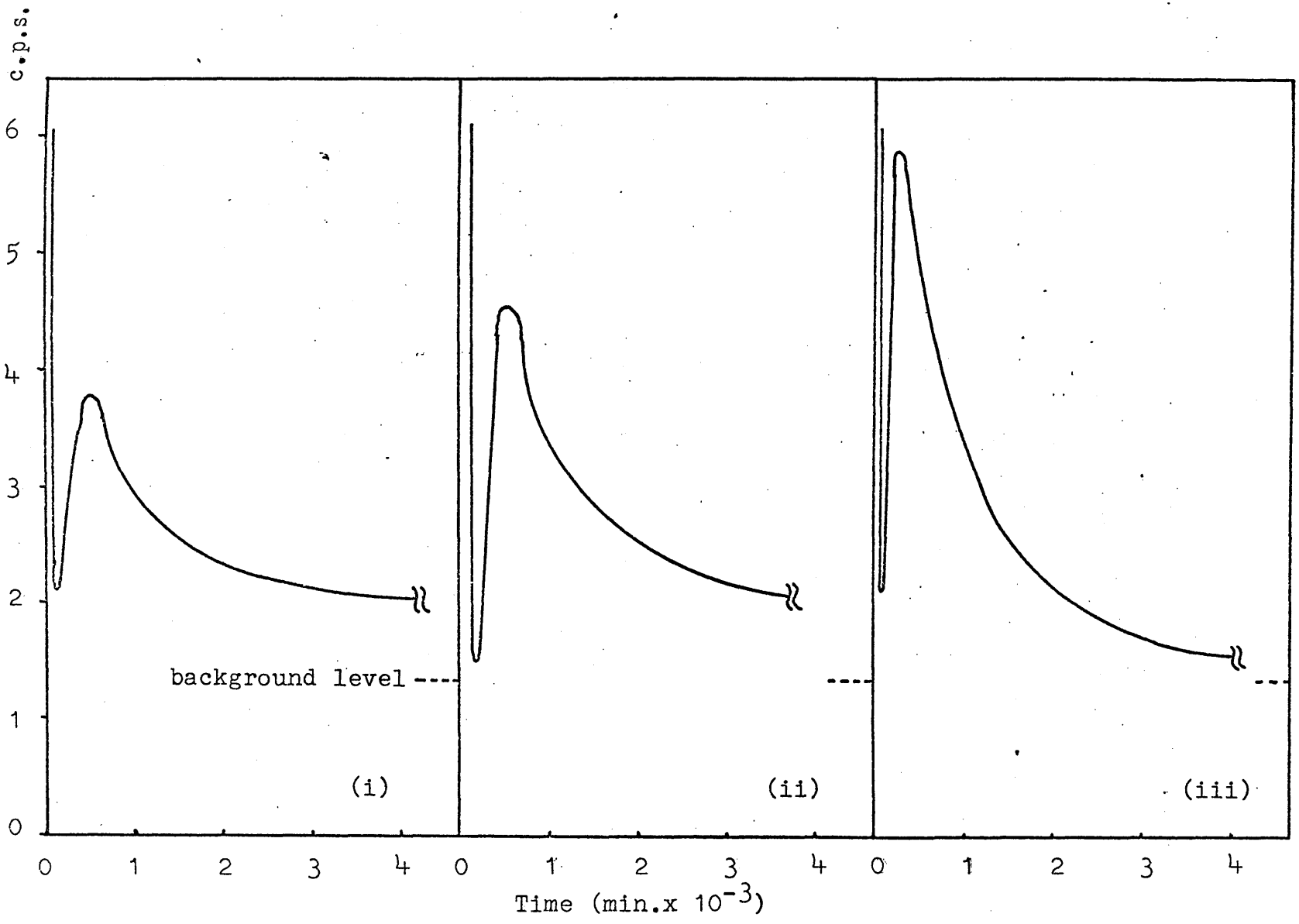

Fig. 6.5 Variation in count rate with time on heating the labelled catalyst at (i) 70°C, (ii) 105°C, (iii) 140°C.

from the Geiger-Müller counting system for the catalyst at various stages in the heat treatment are tabulated below:

TABLE 6.3

Count Rates for Catalyst during Heat Treatment

	Count Rate (counts/100 secs.)
Unactivated catalyst	152
After treatment at 70°C	168
After treatment at 105°C	104
After treatment at 140°C	16
After prolonged treatment at 140°C	14

The effect of temperature on the colour of the 10% catalyst was much more pronounced than on the 2% catalyst. Vivid yellow in colour at room temperature, it turned a pale shade of orange at 70°C and the intensity of this colour was greater at 105°C. At 140°C, however, the colour darkened rapidly and within a few minutes, it had turned jet black.

6.4 X-Ray Diffraction of the Catalyst.

X-Ray specimens were prepared for examination by mixing small samples of the catalyst with "Durofix" to make a thin "needle" of material. This was mounted in a "Philips" Derbye-Scharrer camera and exposed to copper K_α radiation of wavelength 1.5418Å. The exposure was through a nickel filter for 6 hours and the tube conditions were 35KV. and 15mA.

Photographs were taken of the unactivated catalyst, the white form and the grey form and of the dry silica. No diffractions were observable in any of these samples.

6.5. Electron Microscopy of the Catalyst.

To prepare the supported complex for examination, a small sample was mixed with a few drops of araldite resin and placed in the bottom of an embedding capsule. The sample was then centrifuged to compact it in the tip, topped up with resin and placed in an oven at 60 to 80°C for 12 hours. When the capsule was removed from the oven it was allowed to cool and then cut away, leaving the sample located in the tip. Thin sections of about 300Å were cut in an L.K.B. ultra-microtome using a glass-knife.

Catalyst samples were examined using a Siemens Elmiscope 1 Electron Microscope at 80KV. with double condenser illumination. The photograph showed only a few dark patches which might have been crystals, but selective diffraction photographs of these areas gave no diffraction pattern.

CHAPTER 7

REACTIONS OF BUTENES ON SILICA SUPPORTED TRIRUTHENIUM DODECACARBONYL

7.1 Reactions of Butenes with Hydrogen on $Ru_3(CO)_{12}/SiO_2$

The reaction of but-1-ene with hydrogen over $Ru_3(CO)_{12}/SiO_2$ was studied at temperatures between 80° and 150°C, using catalyst samples of 0.04g. Preliminary experiments were carried out using an initial pressure of 100mm. of a 1:1 mixture of hydrogen and but-1-ene.

It was found that the temperature and conditions of activation of the catalyst were critical in ensuring reproducibility of initial rates of isomerisation and hydrogenation. When the catalyst was activated at 110°C under vacuum and used in a series of reactions at 100°C, the initial rate of reaction tended to increase with run number until reaching a limiting value. This trend was repeated when activation was carried out at 120°C, although fewer runs had to be performed before the limit was reached. By carrying out experiments at a series of temperatures, it was found that the lowest temperature at which complete activation could be achieved was 140°C. For catalysts activated at this temperature, no dependence of rate upon run number was observed in subsequent series of reactions. A catalyst sample activated at 150°C showed no significant difference in activity

from that activated at 140°C. Thereafter, all activations were carried out at 145°C.

A typical pressure-fall against time curve is shown in Fig. 7.1, along with the plot to test for first order reaction. Since the latter plot is linear, the hydrogenation reaction has an order of unity. At reaction temperatures below 120°C, there was usually an induction period before hydrogenation began, although this did not necessarily appear in subsequent reactions. At 80°C, the induction period could be as long as 13 minutes for the first reaction and this value tended to fall slightly during subsequent reactions. At 115°C, the induction period was rarely greater than one minute. A pressure-fall against time curve showing this effect is given in Fig. 7.2.

The isomerisation of but-1-ene was studied by carrying out a series of reactions at varying conversions to n-butane at 130°C. At this temperature, there was no induction period. The analysis figures for the variation in butene distribution with conversion, together with the trans/cis ratio (t/c) and the time (t_{ex}) at which the products were extracted for analysis are given in table 7.1, in which the yield for each hydrocarbon is expressed as a percentage of the total hydrocarbon. The terms n-butane, but-1-ene, trans but-2-ene and cis but-2-ene are abbreviated to n-BUT, BUT-1, t-B-2 and c-B-2 for use in all tables. The variation in butene

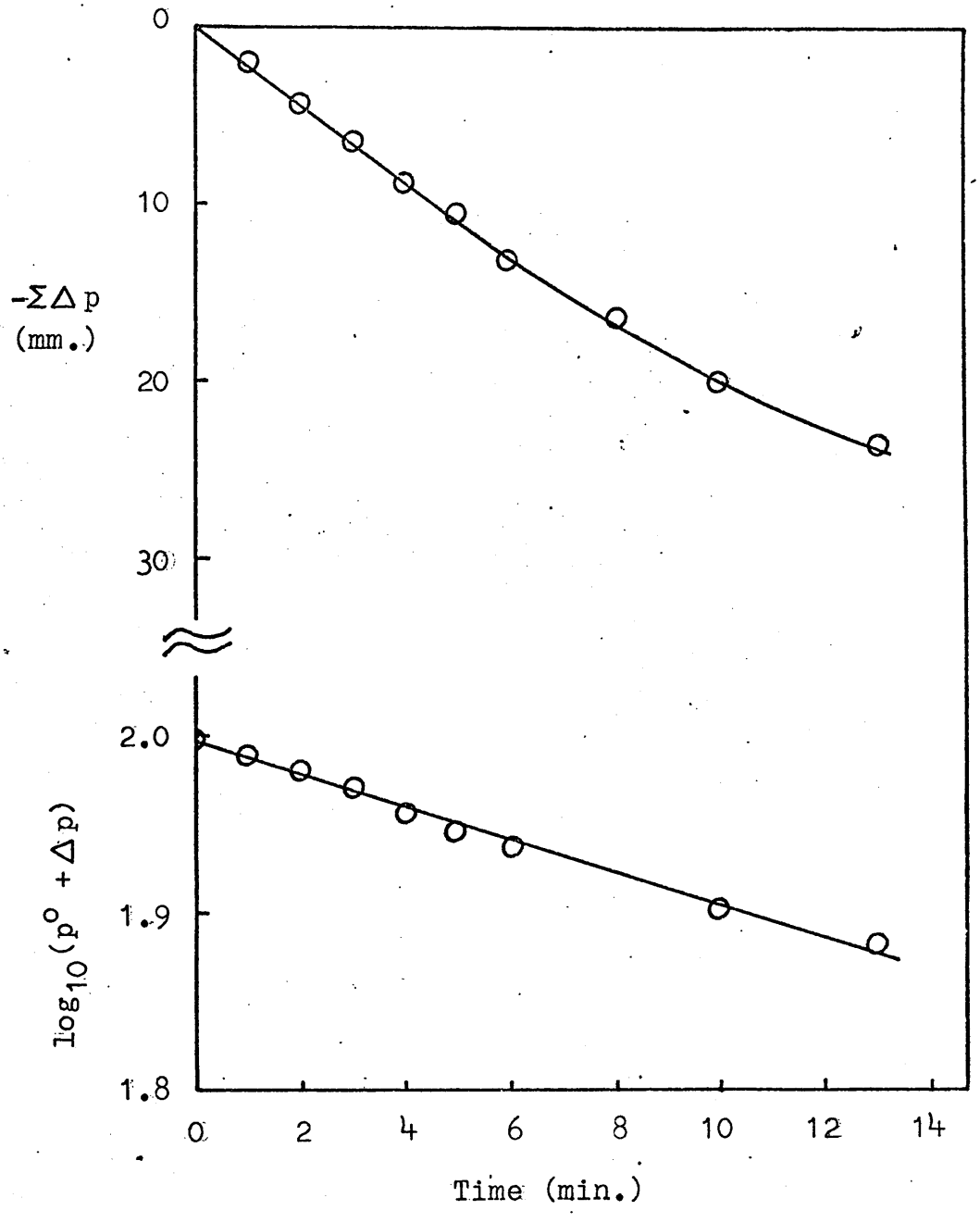

Fig. 7.1 Pressure fall against time curve for 50.0mm. but-1-ene and 50.0mm. hydrogen at 130°C. First order function plot is shown below.

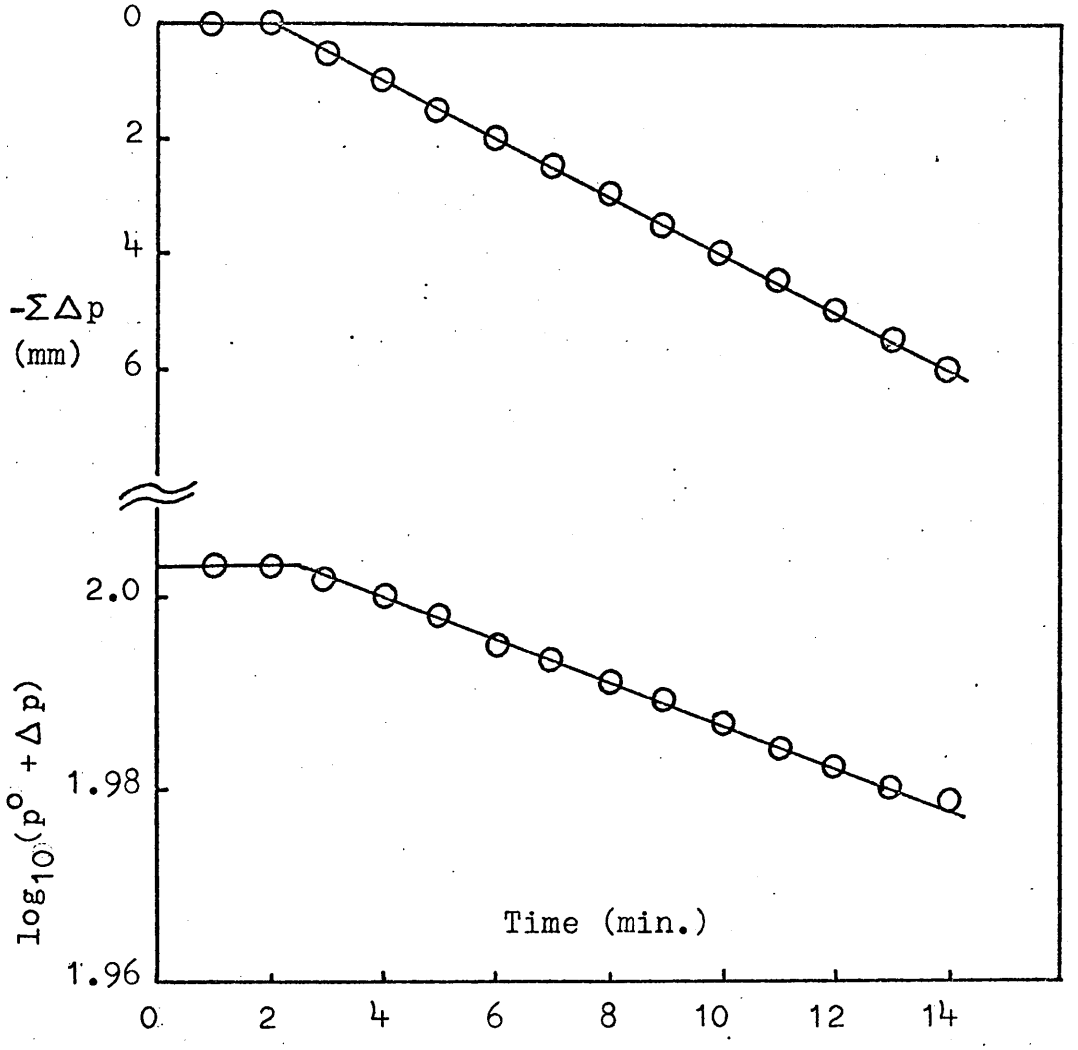

Fig. 7.2 Pressure fall against time curve for 50.5mm. but-1-ene and 50.5mm. hydrogen at 90°C. First order function plot is shown below.

TABLE 7.1

Variation of Hydrocarbon Distribution with Conversion at 130°C on $Ru_3(CO)_{12}/SiO_2$

Initial $p_{H_2} = p_{BUT-1} = 50 \pm 0.5$mm.

Catalyst Weight = 0.04g.

% hydrocarbon distribution

Reaction	n-BUT	BUT-1	t-B-2	c-B-2	t_{ex} (min.)	t/c
A/6	trace	85.8	8.8	5.2	0.5	1.69
A/5	3.7	54.3	24.8	17.1	2.0	1.45
A/7	6.4	37.4	35.2	21.0	3.5	1.68
A/4	9.3	29.7	37.5	23.7	4.5	1.65
A/3	10.7	28.5	39.6	21.2	4.0	1.87
A/2	14.4	28.6	36.3	20.7	10.0	1.75
A/1	16.8	26.4	36.7	20.1	11.0	1.82
A/10	36.9	21.4	26.2	15.5	19.5	1.69
A/9	38.7	23.1	25.1	13.1	20.0	1.93
A/8	99.0	0.1	0.6	0.3	∞	1.80
C/7	5.9	55.2	24.6	14.3	0.5	1.73
C/6	12.4	31.6	35.0	20.9	2.0	1.68
C/4	14.9	32.8	33.6	18.6	2.5	1.80
C/3	24.3	28.0	31.3	16.4	3.0	1.92
C/1	42.0	26.8	21.5	9.6	6.0	2.23
C/5	45.9	27.8	18.6	7.8	8.0	2.36
C/2	48.3	23.7	18.4	9.6	7.0	1.91
C/8	85.2	1.5	9.4	4.0	∞	2.35

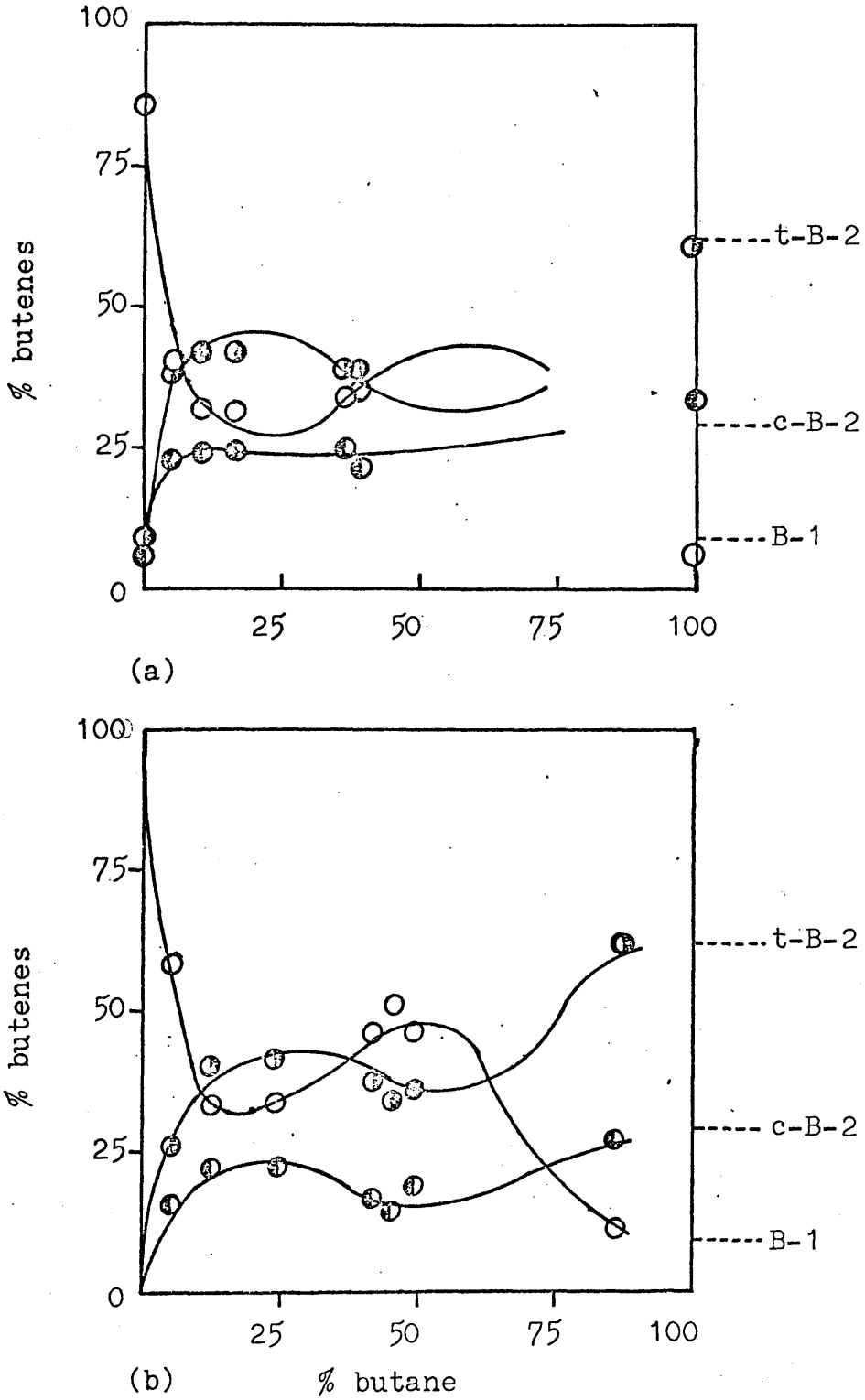

Fig. 7.3 Variation in butene distribution with conversion at 130°C. (a) Series A, (b) Series C.

distribution with percentage conversion is illustrated in Fig. 7.3 in which each butene is given as a percentage of the total butene yield. The equilibrium distributions of the butenes are shown on the right hand side of the plot.

It is interesting to note that, despite samples A and C being from the same batch of catalyst (stored under dry nitrogen), there is a large difference in the rates of the reactions. The reaction over sample A reaches 10% conversion and the minimum in the but-1-ene curve after 4 minutes, while the same stage is reached on sample C after 2 minutes. This difference in activity, however, did not seem to affect the overall shape of the distribution curve and that obtained over sample C is very similar to that on sample A.

The dominant feature to appear in series A was the minimum in the curve for but-1-ene and the corresponding maximum for trans but-2-ene. Although there was little apparent deactivation of the catalyst in successive runs for the hydrogenation reaction, as may be seen from the extraction times, it was thought that the shape of the curve may have been caused by a significant deactivation for isomerisation. Accordingly, series C was carried out using a fresh sample of catalyst and care was taken to ensure that the runs were carried out randomly to remove any possible run number effect.

Further experiments to test the dependence of product distribution on run number were conducted and the product distributions from a series of reactions taken to constant conversion were compared. These showed that, although there were differences in the product distributions and trans/cis ratios, no definite trend could be observed and that these differences generally fell within the experimental error for the chromatographic analyses of $\pm$ 2%, calculated from the variation in values obtained for each hydrocarbon in samples of the standard mixture.

The isomerisation reaction of cis but-2-ene was studied in a similar manner to that of but-1-ene and a series of reactions at varying conversions to n-butane were carried out at 130°C. The catalyst sample was the same as that used in series A. The data obtained from these experiments are given in table 7.2 and are shown graphically in Fig. 7.4. An interesting feature of this series was that the rate of the hydrogenation reaction for cis but-2-ene was approximately twice that for but-1-ene, despite both series being carried out over the same catalyst sample under comparable experimental conditions.

7.2 Kinetics and Activation Energies of the Hydrogenation and Isomerisation of But-1-ene

TABLE 7.2

Variation in Hydrocarbon Distribution with Conversion at 130°C on $Ru_3(CO)_{12}/SiO_2$

Initial $p_{H_2} = p_{c\text{-}B\text{-}2} = 50 \pm 0.5$mm.

Catalyst Weight = 0.04g.

% Hydrocarbon distribution

Reaction	n-BUT	BUT-1	t-B-2	c-B-2	t_{ex} (min)	t/c
B/5	0.0	1.0	3.4	95.6	0.5	0.04
B/6	8.0	3.3	31.6	57.0	2.0	0.56
B/3	13.1	3.3	32.8	50.8	3.5	0.64
B/4	13.7	2.7	31.9	51.7	3.0	0.62
B/2	23.4	3.1	29.6	43.9	4.0	0.67
B/1	26.4	2.8	27.6	43.5	5.0	0.64
B/7	32.1	2.2	25.7	40.0	10.0	0.64
B/8	48.6	1.2	17.7	32.5	25.0	0.55
B/9	64.5	1.5	12.0	22.0	60.0	0.55
B/10	79.6	2.2	11.5	6.7	∞	1.72

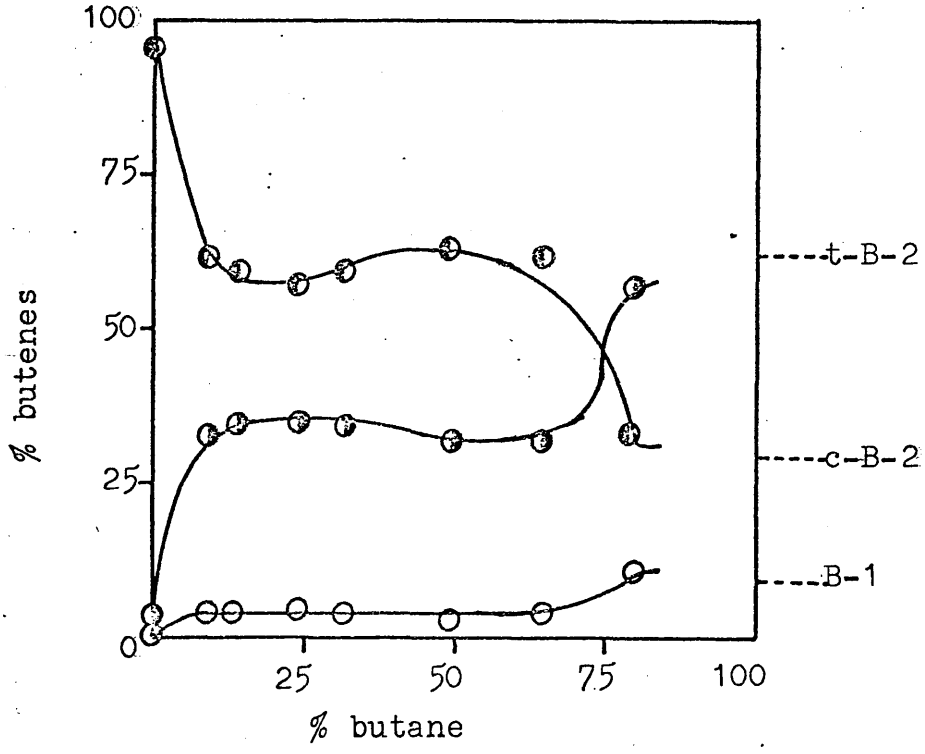

Fig. 7.4 Variation in butene distribution with conversion in reaction of cis-but-2-ene with hydrogen at 130°C. (Series B)

7.2.1 Kinetics of Reactions of But-1-ene with Hydrogen

The dependencies of the initial reaction rates and product distributions on initial hydrogen pressure were determined in a series of reactions at 128°C in which the initial pressure of but-1-ene was held constant at 50mm. and the initial hydrogen pressure was varied between 50 and 200mm. Similarily, the effect of varying the initial pressure of but-1-ene was determined in another series, also at 128°C, where the initial hydrogen pressure was held constant at 50 mm. and the initial pressure of but-1-ene varied between 36.0 and 201.0mm. In the first series, the products were extracted for analysis at constant conversion with respect to but-1-ene, while in the second series, they were extracted at constant hydrogen uptake. Because some of the reaction rates were very fast, particularly when the pressure of hydrogen was much higher than that of but-1-ene, three runs were usually made for each hydrogen/butene mixture: the first and third were to ensure reproducibility of rates of hydrogenation, while the products of reaction from the second run were extracted at the required conversion or hydrogen uptake for analysis.

To investigate the possibility of deactivation of the catalyst during the series, a "standard reaction" technique was used. The "standard reaction" was taken as that of 1:1 mixture of hydrogen and 1-butene. By carrying out such

reactions throughout the series, any change in activity of the catalyst towards hydrogenation or isomerisation could be observed.

The results of the series to determine the variation of rates of reaction with initial hydrogen pressure are shown in tables 7.3 and 7.4. All rates are quoted in units of mm. min^{-1}. The plot of r_h against p_{H_2}, shown in Fig. 7.5, gives a good straight line through the origin and so r_h is directly proportioned to p_{H_2}, indicating that the order of hydrogenation reaction with respect to initial hydrogen pressure is unity. The plot of r_i against p_{H_2} gives a fairly wide scatter of points (Fig. 7.5) as does the plot of log r_i against log p_{H_2} (Fig. 7.6) which does not give a good straight line. This scattering was probably due to the large error inherent in t_{ex}, caused by the difficulty in reading the time with precision when the rates of reaction were so high and the products had to be extracted at low conversion. However, a general trend of decreasing rate with increasing hydrogen pressure is apparent and a line of best fit may be drawn. From the gradient of this line, an order of approximately -0.15 ± 0.1 with respect to hydrogen may be derived for the isomerisation reaction.

Tables 7.5 and 7.6 show the dependence of the initial rates of reaction on the initial pressure of but-1-ene. Fig 7.7, in which r_h is plotted against p_{BUT-1} shows that

TABLE 7.3

Variation of Butene Distribution with Initial Hydrogen Pressure

Temperature = 128 ± 1°C Initial p_{BUT-1} = 50 ± 0.5mm.

Samples extracted after pressure fall of 5 ± 0.5mm.

Reaction	p_{H_2} (mm.)	% Butene distribution					
		%n-BUT	BUT-1	t-B-2	c-B-2	t_{ex} (min)	t/c
D/A1	50.0	11.5	41.5	42.4	16.1	4.0	2.63
D/A2	200.0	12.3	89.8	10.2	trace	0.6	v. high
D/A3	50.0	11.3	44.0	40.0	16.0	4.0	2.42
D/A4	154.0	8.8	78.8	15.6	5.5	1.25	2.84
D/A5	50.0	11.7	39.3	43.3	18.3	4.0	2.34
D/A6	100.0	9.5	63.0	26.4	10.6	2.0	2.49
D/A7	79	11.1	60.6	29.3	10.1	2.5	2.90

TABLE 7.4

Variation of Initial Reaction Rates with Initial Hydrogen Pressure at 128°C

Reaction	p_{H_2} (mm.)	r_h	r_i
D/A1	50.0	1.3	11.63
D/A2	200.0	5.4	9.05
D/A3	50.0	1.3	10.84
D/A4	154.0	4.2	9.96
D/A5	50.0	1.3	12.43
D/A6	100.0	2.5	12.01
D/A7	79.0	2.0	10.31

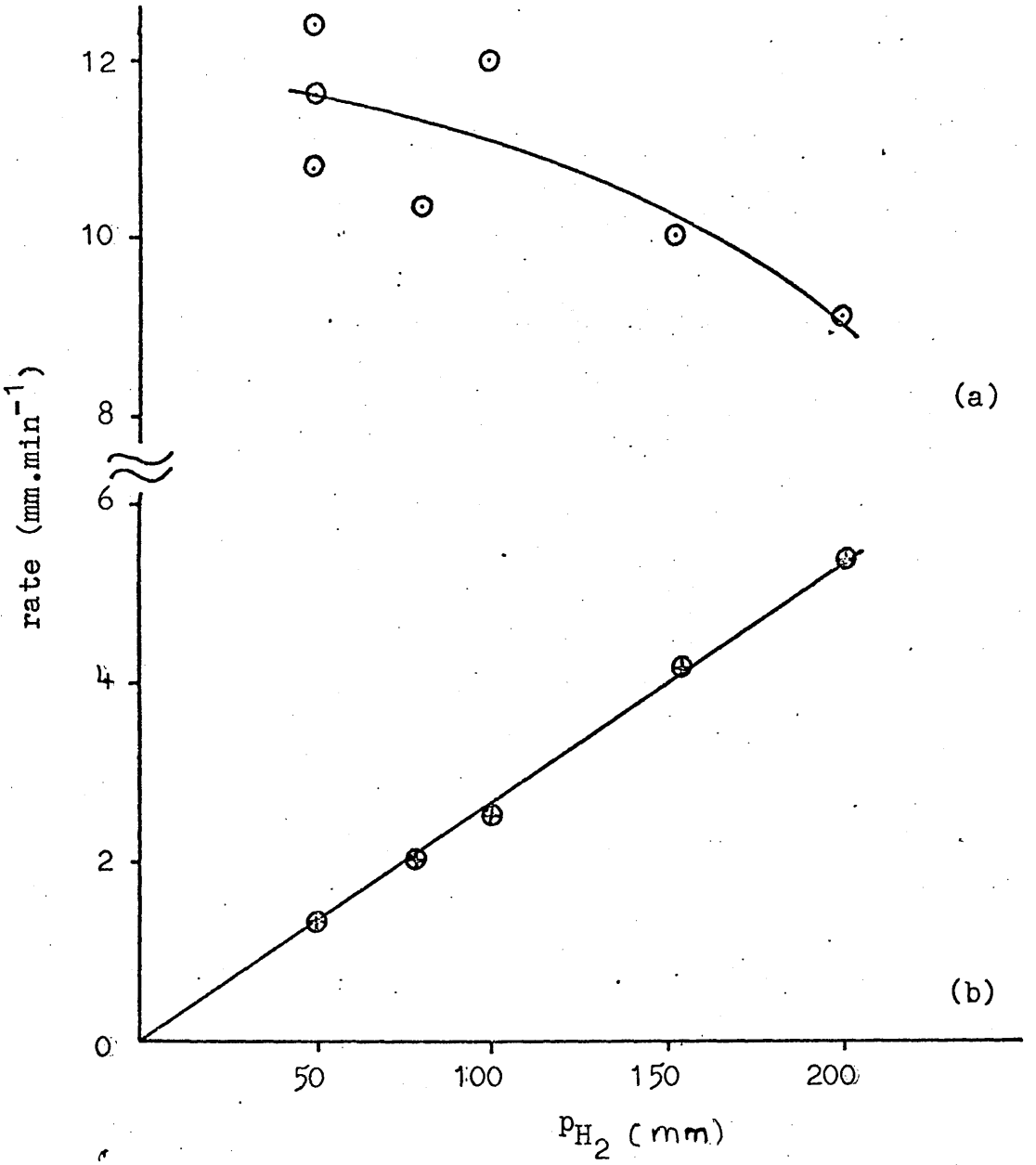

Fig. 7.5 Variation in rates of reaction with initial hydrogen pressure at 128°C.

(a) isomerisation

(b) hydrogenation

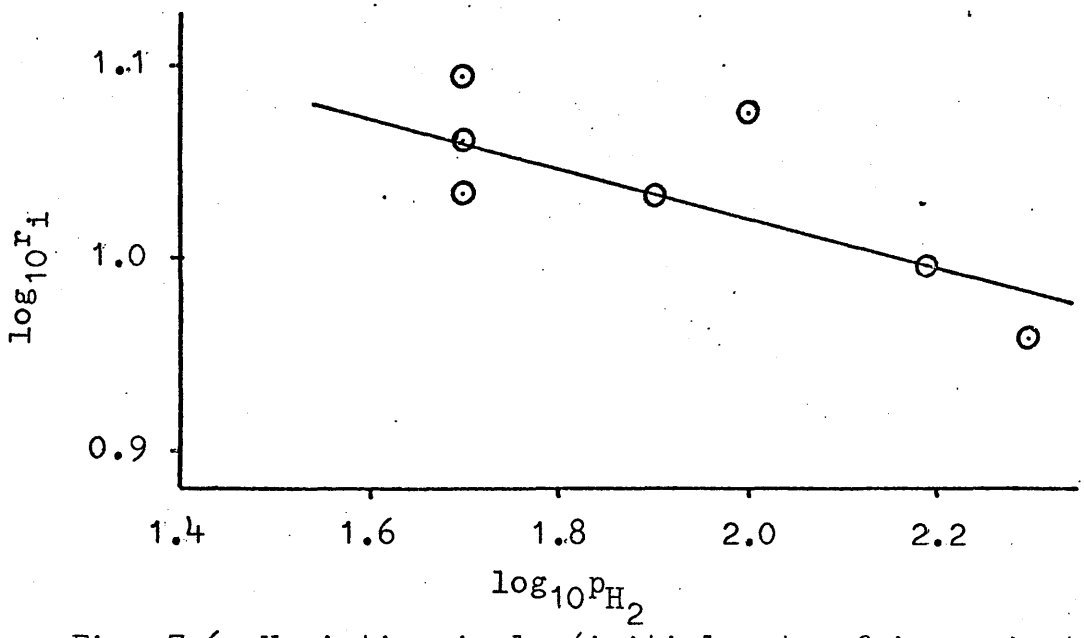

Fig. 7.6 Variation in log(initial rate of isomerisation) with log(initial hydrogen pressure) at 128°C.

TABLE 7.5

Variation of Butene Distribution with Initial Pressure of But-1-ene

Temperature = 128 ± 1°C Initial p_{H_2} = 50 ± 0.5mm

Samples extracted after pressure fall of 5.0 ± 0.5mm

Reaction	p_{BUT-1} mm.	%n-BUT	BUT-1	t-B-2	c-B-2	t_{ex} (min)	t/c
D/B1	50.5	8.6	36.0	43.1	21.0	4.0	2.05
D/B2	201.0	1.2	46.0	36.2	17.6	4.0	2.06
D/B3	153.0	2.3	43.2	37.4	19.4	4.0	1.93
D/B4	101.0	3.9	40.8	39.5	19.7	4.5	2.00
D/B5	51.0	8.5	36.2	43.2	20.2	4.0	2.14
D/B6	36.0	8.1	46.4	36.6	16.9	3.0	2.17
D/B7	74.0	6.0	46.3	34.4	19.3	4.5	1.78

TABLE 7.6

Variation of Initial Reaction Rates with Initial Pressure of But-1-ene at 128°C

Reaction	p_{BUT-1} mm.	r_h	r_i
D/B1	50.5	1.4	13.9
D/B2	201.0	1.3	41.0
D/B3	153.0	1.4	33.9
D/B4	101.0	1.3	21.3
D/B5	51.0	1.4	13.9
D/B6	36.0	1.3	9.7
D/B7	74.0	1.3	16.4

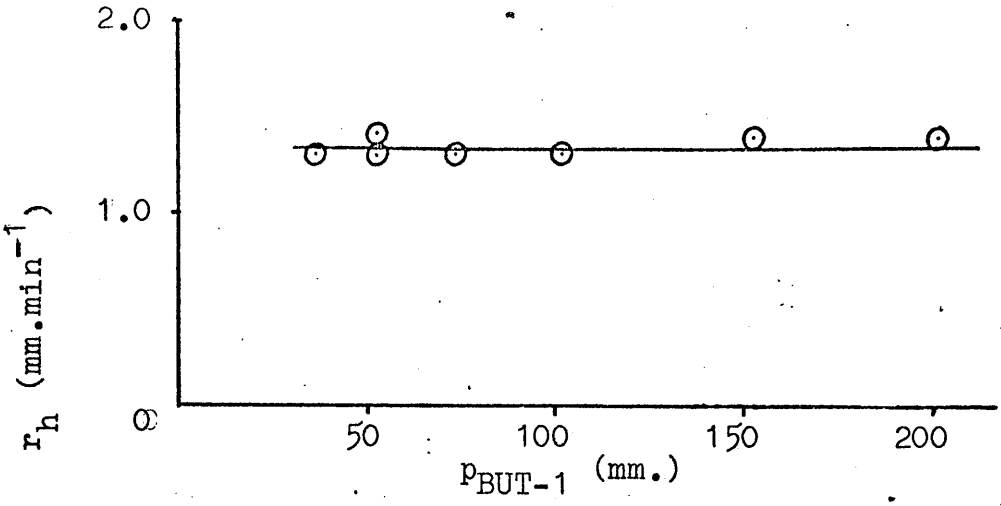

Fig. 7.7 Variation in rate of hydrogenation with pressure of but-1-ene at 128°C.

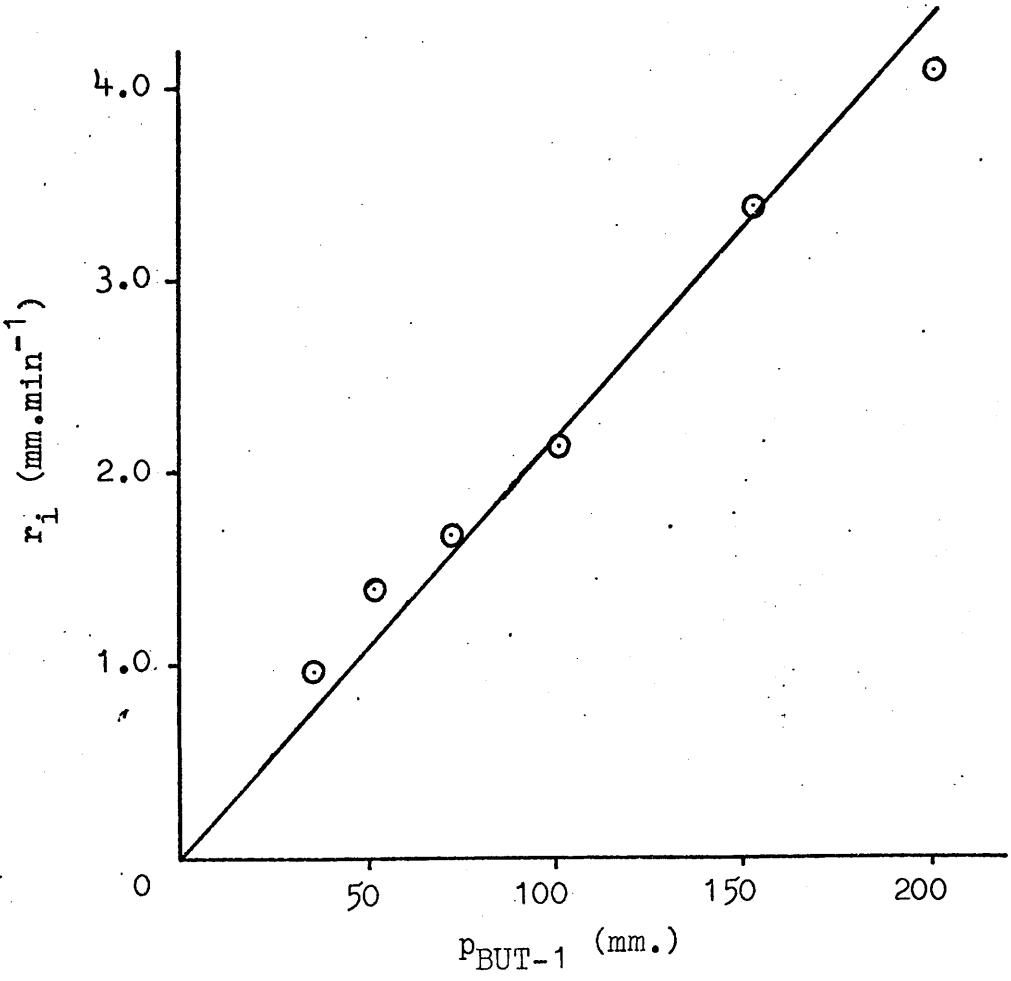

Fig. 7.8 Variation in rate of isomerisation with pressure of but-1-ene at 128°C.

the rate of the hydrogenation reaction is independent of the initial pressure of but-1-ene and that the order of the reaction with respect to but-1-ene is zero. The plot of r_i against p_{BUT-1} (Fig.7.8) is also reasonably good straight line passing through the origin, indicating an order of unity with respect to but-1-ene for the isomerisation reaction.

The values obtained for the orders of reactions are listed below.

TABLE 7.7

Kinetics of Reactions of But-1-ene.

Reaction	Order of Reaction	
	Hydrogen	But-1-ene
Hydrogenation	1.0 ± 0.05	0.0 ± 0.05
Isomerisation	-0.15 ± 0.1	1.0 ± 0.15

7.2.2 Determination of Activation Energies of Reactions on $Ru_3(CO)_{12}/SiO_2$

The dependence of rates of reaction and product distributions on temperature of reaction was studied at temperatures between 115 and 137°C (388 and 410°K). In this range, there was little or no induction period, so that there was only a minimal risk of isomerisation occurring without hydrogenation. Because there appeared to be no deactivation of the catalyst with run number, no "standard

reaction" was used. Reactions were carried out with equal initial pressures of hydrogen and but-1-ene of 50.0 ± 0.5mm. over 0.04g. of catalyst and the products were extracted at a pressure fall of 5 ± 0.5mm. (10% conversion).

The product distributions and initial rates of reaction are given in tables 7.8 and 7.9. Fig. 7.9 shows the Arrhenius plots of $\log_{10} r_h$ and $\log_{10} r_i$ against I/T. From the slopes of the lines, the activation energies for hydrogenation and isomerisation were calculated as 11.0 and 16.1 Kcal.mol.$^{-1}$ respectively.

7.3 Effects of Catalyst Aging.

As stated in Chapter 6, the supported complex tended to undergo some chemical changes when exposed to air for any length of time. In an attempt to determine the effects of such aging on the catalytic properties of the complex, three samples of catalyst were treated in different ways and were then used in the hydrogenation of but-1-ene. The catalyst histories and ages were as follows:

Sample 1 - kept in darkened bottle open to atmosphere (44 days old);

Sample 2 - kept in darkened bottle in dry atmosphere (50 days old);

Sample 3 - kept in light bottle in dry nitrogen (55 days old).

The colours of the samples 1, 2 and 3 were pale grey, white and pale lemon respectively.

TABLE 7.8

Variation of Butene Distribution with Temperature

$p_{H_2} = p_{BUT-1} = 50 \pm 0.5$mm.

Reaction	Temp. (°K)	% Butene distribution %n-BUT	BUT-1	t-B-2	c-B-2	t_{ex} (min)	t/c
D/1	410	11.9	36.5	40.6	22.9	2.5	1.77
D/2	409	11.2	38.9	41.5	19.7	2.5	2.11
D/3	400	10.6	37.9	43.6	18.6	3.5	2.34
D/4	400	10.5	41.1	42.3	16.6	3.5	2.55
D/5	388	9.9	39.5	44.0	16.5	5.5	2.67
D/6	397	10.5	39.1	44.4	16.5	4.5	2.69

TABLE 7.9

Variation of Initial Rates of Reaction with Temperature

Reaction	Temp. (°K)	r_h	r_i
D/1	410	2.20	21.88
D/2	409	2.20	20.75
D/3	400	1.55	14.89
D/4	400	1.55	13.38
D/5	388	1.0	7.66
D/6	397	1.30	11.26

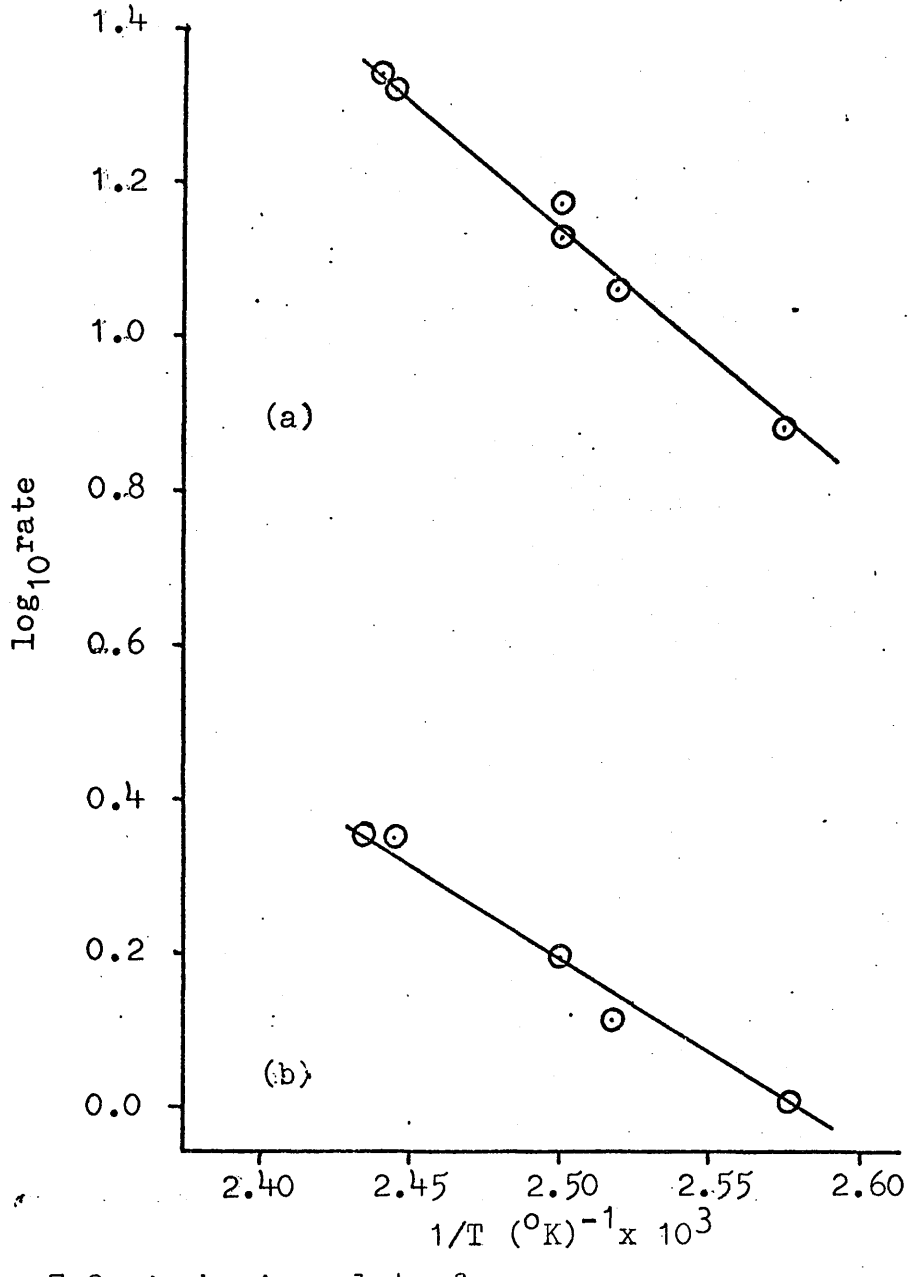

Fig. 7.9 Arrhenius plots for

(a) isomerisation and

(b) hydrogenation, over fresh catalyst.

Catalyst samples of 0.04g. were activated at 145°C using the same technique as for fresh samples. The dependence of rates of reaction and product distributions on temperature was investigated using temperatures between 105 and 142°C (378 and 415°K). Reactions were carried out using equal initial pressures of hydrogen and but-1-ene of 50.0 ± 0.5mm. and the products were extracted at a pressure fall of 5 ± 0.5mm. (10% conversion).

The product distribution and initial rates of reaction are given in tables 7.10 and 7.11. Figs 7.10, 7.11 and 7.12 are the Arrhenius plots of $\log_{10} r_h$ and $\log_{10} r_i$ against I/T for the reactions over samples 1, 2 and 3 respectively.

Although four of the plots give reasonably good straight lines, in each of two of them (Figs. 7.10 and 7.11), there is a point which occurs at a higher value of $\log_{10} r_i$ than expected. These points correspond to runs E/8 on sample 1 and F/6 on sample 2. In each of these runs, however, there was a short induction period before the hydrogenation reaction began. During this period, the isomerisation reaction alone would have been occurring and this effect may have produced the apparently high rate of the isomerisation reaction.

A summary of the activation energies of the hydrogenation and isomerisation reactions, as derived from

TABLE 7.10

Variation of Butene Distribution with Temperature over Aged Catalysts

$p_{H_2} = p_{BUT-1} = 50 \pm 0.5$mm

Reaction	Temp. (°K)	% Butene Distribution %n-BUT	BUT-1	t-B-2	c-B-2	t_{ex} (min)	t/c
Sample 1							
E/2	403	10.5	37.6	40.7	21.8	3.5	1.87
E/4	389	11.9	33.8	44.9	21.3	8.0	2.11
E/7	397	11.5	38.2	44.4	17.4	5.0	2.55
E/8	378	8.3	32.2	48.0	19.8	12.0	2.42
E/9	408	11.3	38.1	41.9	20.0	3.0	2.10
Sample 2							
F/4	403	10.2	40.0	42.9	17.1	6.5	2.51
F/5	390	9.6	35.8	43.9	20.3	9.0	2.16
F/6	384	7.5	38.2	44.0	17.8	9.0	2.47
F/7	413	8.5	40.5	41.8	17.7	5.0	2.36
F/8	397	10.7	43.3	40.4	16.3	7.0	2.45
Sample 3							
G/1	415	12.4	41.3	40.4	18.3	5.0	2.23
G/2	403	9.2	36.7	41.8	21.4	6.5	1.95
G/3	393	8.3	35.5	42.4	22.1	8.0	1.92
G/4	386	10.0	35.8	39.4	24.9	12.0	1.58
G/5	404	10.6	36.7	41.3	22.1	6.5	1.87

TABLE 7.11

Variation of Initial Rates of Reaction with Temperature over Aged Catalysts

Reaction	Temperature (^{o}K)	r_h	r_i
Sample 1			
E/2	403	1.5	15.1
E/4	389	0.75	7.2
E/7	397	1.0	10.5
E/8	378	0.5	5.4
E/9	408	1.75	17.2
Sample 2			
F/4	403	0.9	7.3
F/5	390	0.6	5.8
F/6	384	0.5	5.9
F/7	413	1.0	10.1
F/8	397	0.72	6.7
Sample 3			
G/1	415	1.0	10.3
G/2	403	0.8	8.4
G/3	393	0.65	7.0
G/4	386	0.5	4.5
G/5	404	0.8	8.2

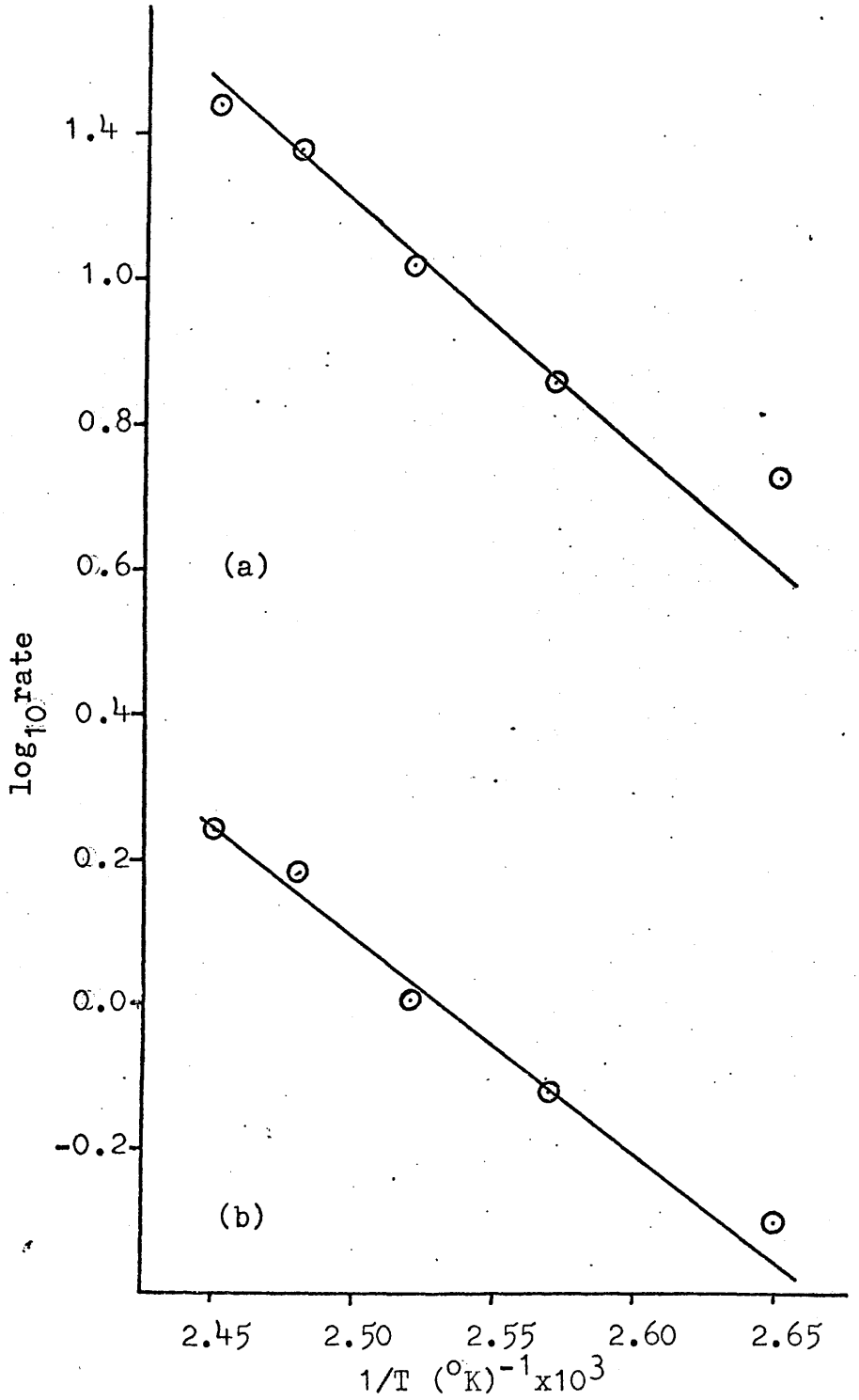

Fig. 7.10 Arrhenius plots for

(a) isomerisation and

(b) hydrogenation over catalyst sample 1.

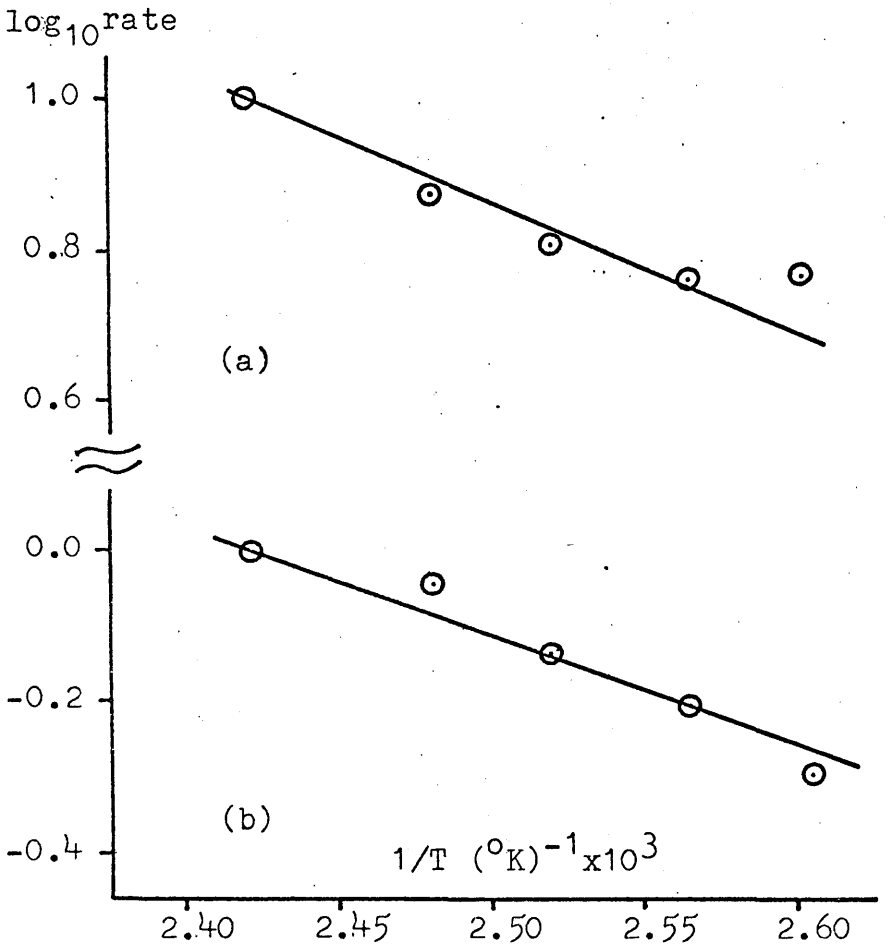

Fig. 7.11 Sample 2

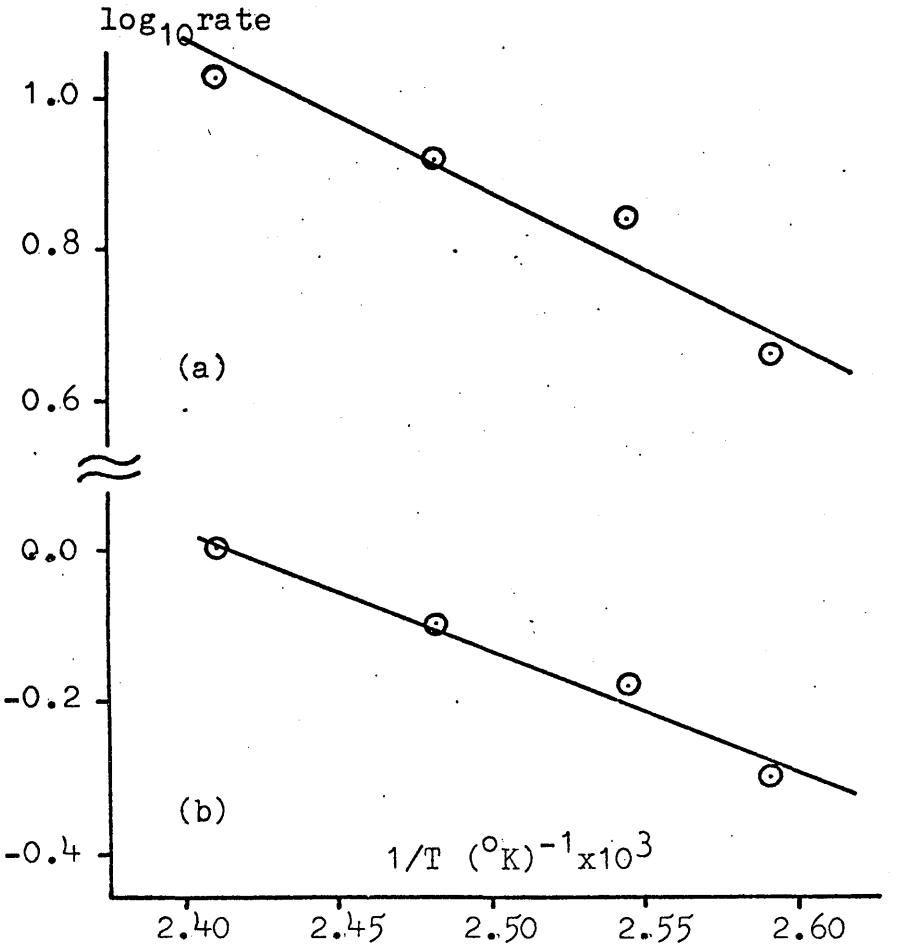

Fig. 7.12 Sample 3

Arrhenius plots for (a) isomerisation and (b) hydrogenation over different catalyst samples.

these plots, over the aged catalyst samples is shown in table 7.12 along with the values obtained from the series of reactions on the fresh catalyst. The activation energies for hydrogenation and isomerisation are denoted by E_h and E_i respectively.

TABLE 7.12

Summary of Activation Energies

Catalyst	E_h (Kcal.mol.$^{-1}$)	E_i (Kcal.mol.$^{-1}$)
Freshly prepared	11.0 ± 0.5	16.1 ± 1.0
Sample 1	13.3 ± 0.5	15.6 ± 1.0
Sample 2	9.0 ± 0.5	8.3 ± 1.0
Sample 3	8.4 ± 0.5	8.5 ± 1.0

7.4 Reactions of But-1-ene with Deuterium

The reactions of but-1-ene with deuterium on $Ru_3(CO)_{12}/SiO_2$ were carried out in essentially the same manner as those with hydrogen. However, to allow large samples of the product gases to be removed so that sufficient pressures of each constituent gas could be collected for analysis by mass spectrometry after elution from the gas chromatograph, a large reaction vessel (200ml. capacity) and a weight of catalyst of 0.04g. was used. The deuteration and isomerisation reactions were studied simultaneously using initial pressures of 50.0mm. each of deuterium and but-1-ene.

7.4.1 The Isomerisation of But-1-ene

The isomerisation of but-1-ene in the presence of deuterium was studied in a series of reactions at each of three temperatures - 130, 110 and 90°C. By extracting the reaction products at varying conversions to n-butane and determining the butene distribution at each conversion, the variation in butene distribution with percentage conversion was found for each temperature. The analysis figures are shown in table 7.13 and butene distribution curves are illustrated in Figs. 7.13 to 7.15.

As was the case in the reactions with hydrogen at 130°C, the butene did not reach equilibrium proportions even at very high conversions. Again, there is a maximum in the curve for trans but-2-ene and the minimum in that for but-1-ene.

Fig.7.15 is the distribution curve for the reaction at 90°C, in which there was an induction period of three minutes. The points at zero conversion are derived from reaction L/2, which was extracted after only two minutes and before the addition reaction had proceeded to a measurable extent.

TABLE 7.13

Variation of Butene Distribution with Conversion in the Reaction of But-1-ene with Deuterium

Initial $p_{D_2} = p_{BUT-1} = 50 \pm 0.5$mm

Catalyst weight = 0.08g.

% Hydrocarbon distribution

Reaction	Temp. (°K)	%n-BUT	BUT-1	t-B-2	c-B-2	t_{ex} (min)	t/c
K/4	403	8.9	19.3	44.6	27.1	1.5	1.64
K/2	"	22.3	17.0	39.8	20.7	5.0	1.90
K/1	"	49.7	14.3	22.3	13.7	18.0	1.62
K/5	"	71.8	11.2	12.1	4.9	25.0	2.47
0	391	14.7	19.3	38.3	27.7	2.5	1.38
M/3	383	4.8	17.5	51.3	26.4	6.0	1.94
M/5	"	10.9	16.0	49.4	23.7	7.0	2.08
M/4	"	25.0	19.2	38.8	17.1	15.0	2.27
M/2	"	43.5	17.5	29.3	9.7	35.0	3.02
M/1	"	74.9	6.7	13.8	4.6	60.0	3.00
L/2	363	0.0	45.3	41.2	13.5	2.0	3.05
L/5	"	8.0	18.7	48.8	24.6	8.0	1.99
L/4	"	17.0	17.8	45.2	19.9	16.0	2.27
L/3	"	63.2	10.2	18.3	8.3	75.0	2.21

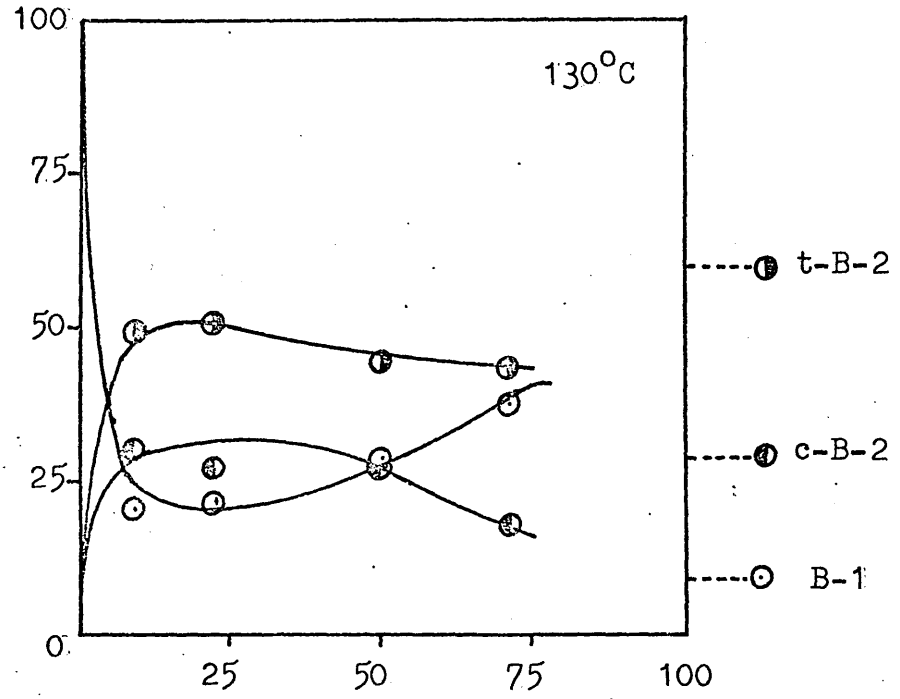

Fig. 7.13

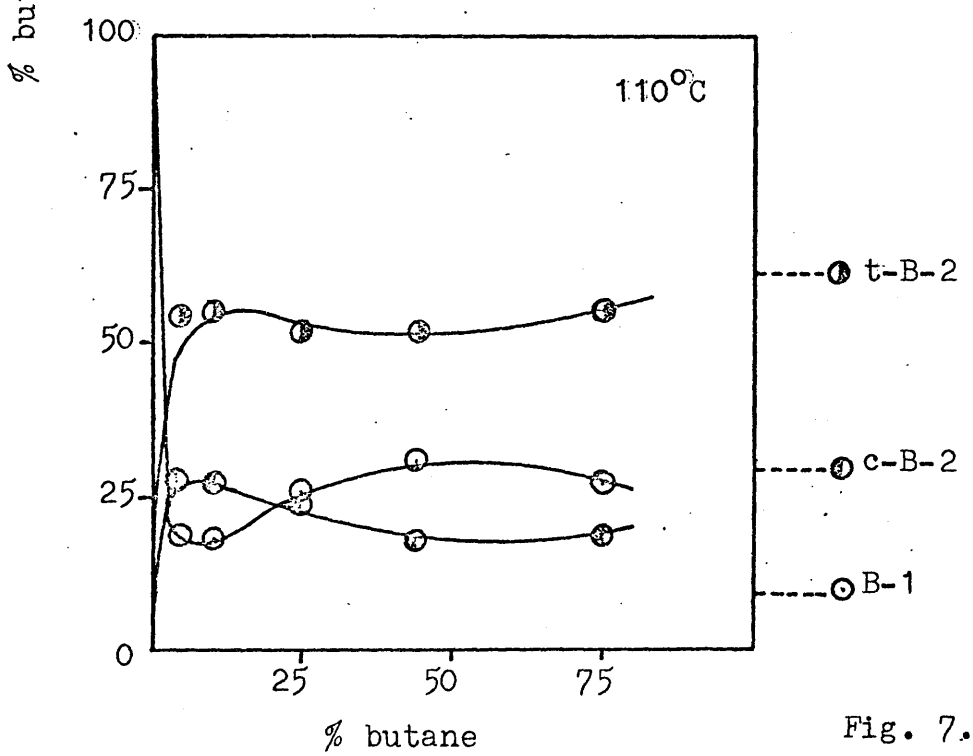

Fig. 7.14

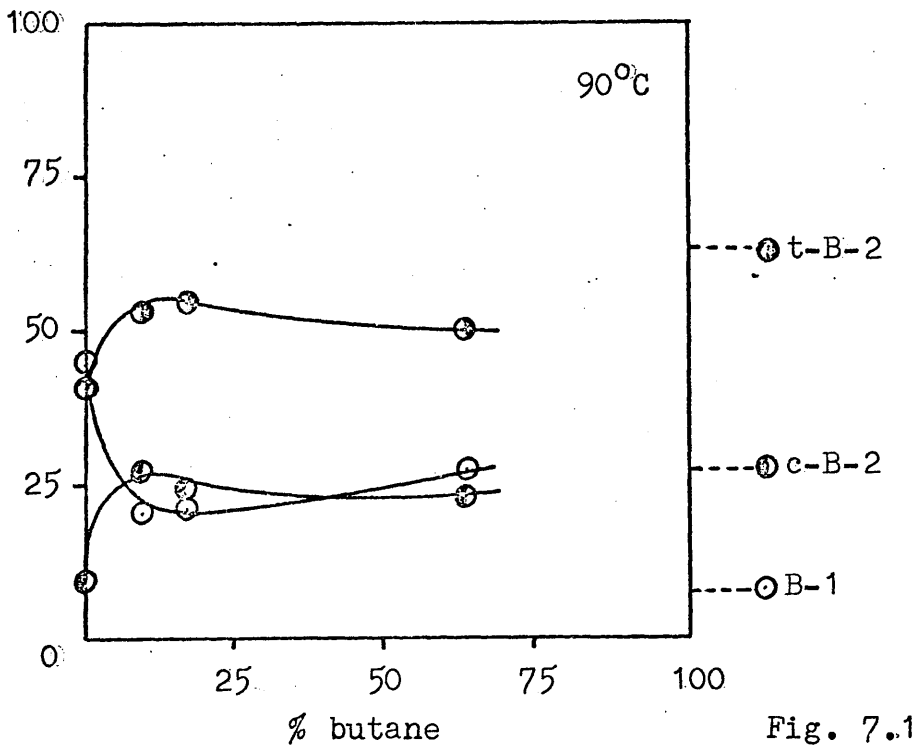

Fig. 7.15

Variation in butene distribution with conversion in the reaction of but-1-ene with deuterium at 130°, 110° and 90°C.

7.4.2 The Activation Energies of the Deuteration and Isomerisation Reactions

In all of the series, each at a different temperature, one sample was extracted for analysis at a pressure fall of 5.0 ± 0.5mm., as measured on the mercury manometer. Along with the results from run 0, the analysis figures were used in the computation of the rates of the deuteration and isomerisation reactions and the figures used for this purpose are shown in table 7.14. Table 7.15 shows the rates of deuteration (denoted by r_d) and isomerisation (r_i) at the different temperatures.

The Arrhenius plots showing the variation of $\log_{10} r_d$ and $\log_{10} r_i$ with the inverse of temperature (I/T) are illustrated in Fig. 7.16. As in the case of the addition and isomerisation reactions in the presence of hydrogen, the plots give reasonably good straight lines, except for the point derived from the temperature run (L/5). In the placing of the line of best fit, less weight has been given to the points derived from low temperature reactions than to the others, for which there was no induction period. From the slopes of these lines, activation energies for deuteration and isomerisation of 11.9 ± 0.5Kcal.mol.$^{-1}$ and 17.0 ± 1.0Kcal.mol.$^{-1}$, respectively, may be calculated. These values compare favourably with those obtained for the hydrogenation and isomerisation reactions in section 7.2.2.

TABLE 7.14

Variation of Butene Distribution with Temperature in Reaction of But-1-ene with Deuterium

Reaction	Temp. (°K)	% Butene distribution %n-BUT	BUT-1	t-B-2	c-B-2	t_{ex} (min)	t/c
K/4	403	8.9	21.2	49.0	29.8	1.5	1.64
L/5	363	8.0	20.3	53.0	26.7	8.0	1.99
M/5	383	10.9	18.0	55.4	26.6	7.0	2.08
O	391	14.7	22.6	44.9	32.5	2.5	1.38

TABLE 7.15

Variation in Rates of Hydrogenation and Isomerisation in Reaction of But-1-ene with Deuterium

Reaction	Temp. (°K)	r_d	r_i
K/4	403	1.63	61.6
L/5	363	0.43	11.1
M/5	383	0.63	16.9
O	391	1.0	33.4

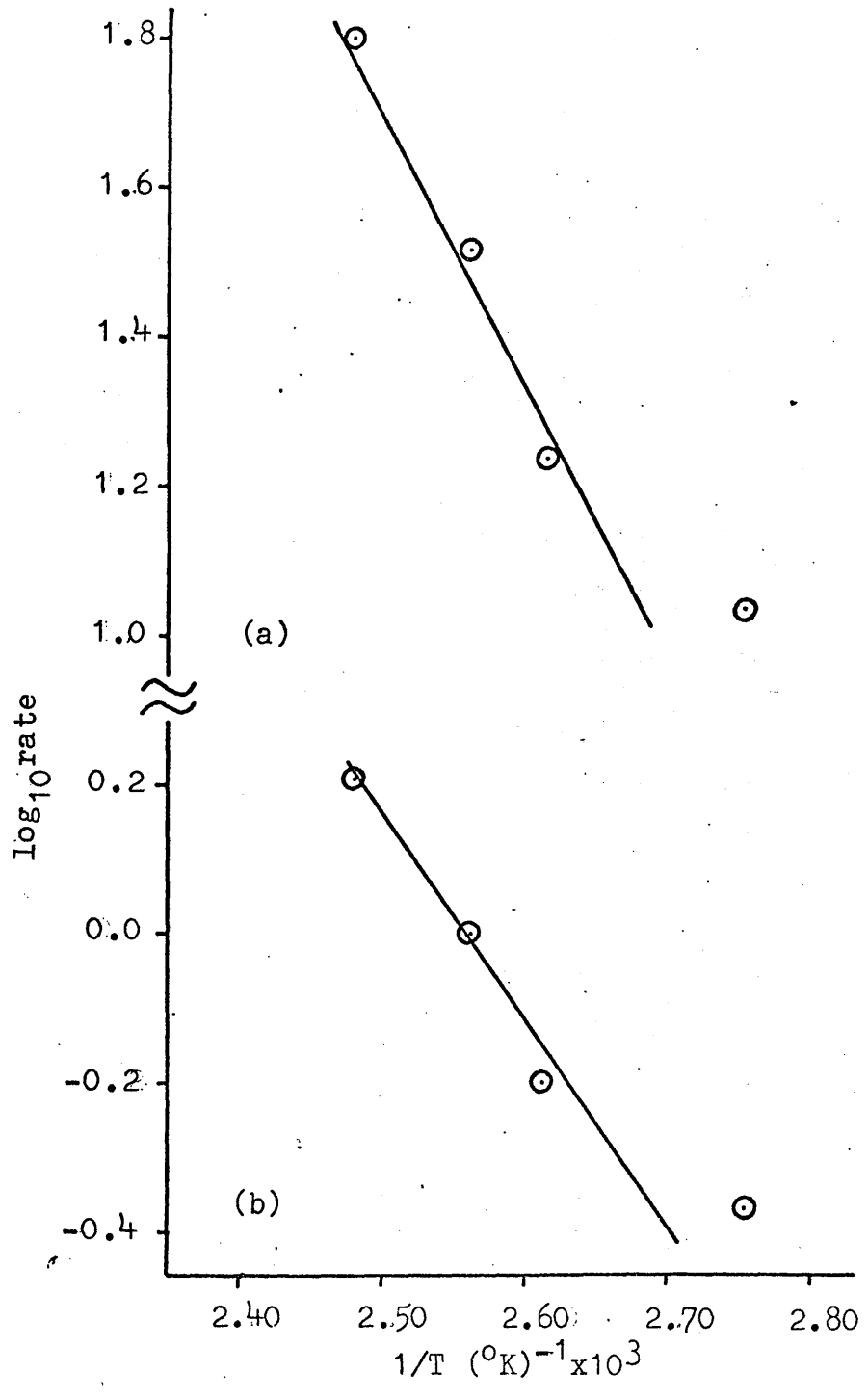

Fig. 7.16 Arrhenius plots for (a) isomerisation and (b) deuteration in reaction of but-1-ene with deuterium over fresh catalyst sample.

7.4.3 Deuterium Exchange Reactions of But-1-ene

To permit the study of the olefin exchange reaction with deuterium, the separated products of each reaction were collected for analysis by mass spectrometry. Sometimes, however, when the percentage conversion was low, only small samples could be collected and in such cases, the sensitivity of the spectrometer was often not high enough to allow a full spectrum to be obtained so that only the largest peaks were observed. The relative sensitivity of the instrument to n-butane was further caused by another effect: all the products for analysis underwent fragmentation at the filament of the spectrometer to C_3 hydrocarbons and this happened to a much greater extent with n-butane than with the butenes. Thus, when a low yield was obtained from the reaction, generally only the main peaks in the spectrum could be observed and sometimes, particularly in the analysis of n-butane, no spectrum could be observed at all.

For use in all tables, the corrected proportions of deuterated products are denoted by d_0, d_1 .....d_8, where the subscript indicates the number of deuterium atoms incorporated into each molecule. D.N. is the deuterium number for each product, i.e., the mean number of deuterium atoms per hydrocarbon molecule. The distributions of the deuterated products for the series at 90°, 110° and 130°C are shown respectively in tables 7.16, 7.17 and 7.18.

TABLE 7.16

Distribution of Deuterated Hydrocarbons with Conversion at 90°C

Reaction	d_0	d_1	d_2	d_3	d_4	d_5	d_6	d_7	d_8	D.N.
L/2	Conversion = 0.0%									
n-BUT	-	-	-	-	-	-	-	-	-	-
BUT-1	98.7	1.4	0.0	0.0	0.0	0.0	0.0	0.0	0.0	0.01
t-B-2	86.9	13.7	0.0	0.0	0.0	0.0	0.0	0.0	0.0	0.13
c-B-2	91.8	7.0	1.3	0.0	0.0	0.0	0.0	0.0	0.0	0.09
L/5	Conversion = 8.0%									
n-BUT	-	-	-	-	-	-	-	-	-	-
BUT-1	90.5	7.9	1.2	0.5	0.0	0.0	0.0	0.0	0.0	0.12
t-B-2	31.7	22.7	19.5	14.5	7.1	3.2	1.4	0.0	0.0	1.58
c-B-2	87.3	10.6	1.5	0.7	0.0	0.0	0.0	0.0	0.0	0.16
L/4	Conversion = 17.0%									
n-BUT	11.9	47.5	25.3	9.5	3.9	2.0	0.0	0.0	0.0	1.52
BUT-1	75.1	19.5	3.9	1.5	0.0	0.0	0.0	0.0	0.0	0.31
t-B-2	65.8	28.6	5.8	0.0	0.0	0.0	0.0	0.0	0.0	0.40
c-B-2	59.1	33.7	6.0	1.0	0.0	0.0	0.0	0.0	0.0	0.50

TABLE 7.16 (cont.)

Distribution of Deuterated Hydrocarbons with Conversion at 90°C

Reaction	d_0	d_1	d_2	d_3	d_4	d_5	d_6	d_7	d_8	D.N.
L/3	Conversion = 63.2%									
n-BUT	7.8	31.5	31.5	15.9	8.0	3.0	1.2	0.6	0.5	2.05
BUT-1	74.7	8.3	7.9	4.9	2.4	1.2	0.4	0.0	0.0	0.57
t-B-2	35.4	28.2	19.7	11.2	5.6	0.0	0.0	0.0	0.0	1.23
c-B-2	25.0	30.4	23.7	13.4	5.5	2.1	0.0	0.0	0.0	1.50

TABLE 7.17

Distribution of Deuterated hydrocarbons with Conversion at 110°C

Reaction	d_0	d_1	d_2	d_3	d_4	d_5	d_6	d_7	d_8	D.N.
M/3	Conversion = 4.8%									
n-BUT	22.2	38.1	28.1	8.1	3.5	0.0	0.0	0.0	0.0	1.32
BUT-1	90.9	7.3	1.2	0.7	0.0	0.0	0.0	0.0	0.0	0.12
t-B-2	82.3	14.6	1.8	0.8	0.5	0.0	0.0	0.0	0.0	0.23
c-B-2	83.8	12.6	2.5	1.2	0.0	0.0	0.0	0.0	0.0	0.21

TABLE 7.17 (cont)

Distribution of Deuterated Hydrocarbons with Conversion at 110°C

Reaction	d_0	d_1	d_2	d_3	d_4	d_5	d_6	d_7	d_8	D.N.
M/5	Conversion = 10.9%									
n-BUT	20.6	46.8	19.2	11.8	1.7	0.0	0.0	0.0	0.0	1.30
BUT-1	86.5	11.1	1.6	0.9	0.0	0.0	0.0	0.0	0.0	0.17
t-B-2	77.0	19.5	2.9	0.6	0.0	0.0	0.0	0.0	0.0	0.27
c-B-2	80.2	17.7	2.2	0.0	0.0	0.0	0.0	0.0	0.0	0.22
M/4	Conversion = 25.0%									
n-BUT	21.9	44.0	26.1	8.4	0.0	0.0	0.0	0.0	0.0	1.20
BUT-1	85.6	11.2	1.9	0.9	0.5	0.0	0.0	0.0	0.0	0.19
t-B-2	84.4	16.3	0.0	0.0	0.0	0.0	0.0	0.0	0.0	0.15
c-B-2	66.4	27.6	4.2	1.2	0.6	0.0	0.0	0.0	0.0	0.42
M/2	Conversion = 43.5%									
n-BUT	34.9	34.4	16.7	9.5	4.8	0.0	0.0	0.0	0.0	1.14
BUT-1	77.5	8.7	6.9	4.7	2.3	0.0	0.0	0.0	0.0	0.45
t-B-2	30.8	30.0	19.7	9.6	10.3	0.0	0.0	0.0	0.0	1.37
c-B-2	28.7	33.6	23.5	10.2	4.3	0.0	0.0	0.0	0.0	1.27

TABLE 7.17 (cont.)

Distribution of Deuterated Hydrocarbons with Conversion at 110°C

Reaction	d_0	d_1	d_2	d_3	d_4	d_5	d_6	d_7	d_8	D.N.
M/1	Conversion = 74.9%									
n-BUT	9.5	31.1	29.1	17.3	7.9	3.1	1.1	0.6	0.3	2.01
BUT-1	76.0	7.1	6.6	5.2	2.9	1.5	0.8	0.0	0.0	0.59
t-B-2	20.9	29.1	25.3	17.0	5.8	1.6	0.3	0.0	0.0	1.64
c-B-2	20.0	32.0	26.2	14.7	5.1	1.6	0.4	0.0	0.0	1.59

TABLE 7.18

Distribution of Deuterated Hydrocarbons with Conversion at 130°C

Reaction	d_0	d_1	d_2	d_3	d_4	d_5	d_6	d_7	d_8	D.N.
K/4	Conversion = 8.9%									
n-BUT	22.4	29.3	25.4	12.5	10.8	0.0	0.0	0.0	0.0	1.59
BUT-1	77.5	12.9	5.0	2.3	1.4	1.0	0.0	0.0	0.0	0.40
t-B-2	-	-	-	-	-	-	-	-	-	-
c-B-2	64.4	26.5	6.6	1.3	0.7	0.4	0.2	0.0	0.0	0.49

TABLE 7.18 (cont.)

Distribution of Deuterated Hydrocarbons with Conversion at 130°C

Reaction	d_0	d_1	d_2	d_3	d_4	d_5	d_6	d_7	d_8	D.N.
K/2	Conversion = 22.3%									
n-BUT	18.0	32.7	28.1	13.4	5.0	1.8	0.7	0.4	0.0	1.65
BUT-1	73.5	14.7	8.0	2.7	0.8	0.4	0.0	0.0	0.0	0.44
t-B-2	35.6	37.7	19.6	5.7	1.1	0.2	0.0	0.0	0.0	1.00
c-B-2	35.7	38.8	19.7	4.7	1.0	0.2	0.0	0.0	0.0	0.97
K/1	Conversion = 49.7%									
n-BUT	4.9	30.7	31.4	19.9	8.7	2.9	0.9	0.4	0.2	2.12
BUT-1	77.2	6.4	7.6	5.1	2.5	0.9	0.3	0.0	0.0	0.53
t-B-2	18.1	26.9	30.0	17.4	6.4	1.8	0.4	0.1	0.0	1.74
c-B-2	26.7	25.7	27.1	12.7	6.1	1.5	0.3	0.0	0.0	1.52
K/5	Conversion = 71.8%									
n-BUT	8.5	26.3	29.7	20.4	9.8	3.9	1.4	0.0	0.0	2.14
BUT-1	54.1	11.4	11.5	10.9	7.3	3.6	1.3	0.0	0.0	1.22
t-B-2	20.2	23.6	25.8	18.7	8.3	2.6	0.6	0.2	0.0	1.82
c-B-2	22.0	25.3	24.9	16.7	7.4	2.8	0.8	0.0	0.0	1.74

CHAPTER 8

REACTIONS OF BUT-1-ENE ON SILICA SUPPORTED TRIOSMIUM DODECACARBONYL

8.1 Preliminary Investigation

Preliminary experiments on $Os_3(CO)_{12}/SiO_2$ (2% w/w) were carried out in the pulse-flow reactor, using 0.2g. of the supported complex. The catalyst, which was pale lemon in colour at room temperature, was heated slowly in the reactor so that any colour change could be easily observed. The yellow colour of the catalyst persisted until the temperature was raised to 190°C, when it turned pale pink. When the temperature was reduced to ambient temperature, the pink colour did not fade, even after several days. Heating at 260°C did not cause any apparent further change in the catalyst, but at temperatures above 300°C, the pink colour gradually faded and the catalyst turned first to white and eventually to pale grey. When exposed to air, the colour of the yellow catalyst faded until, after several months, it turned white. The pink colour of the activated catalyst faded after several days' exposure to air.

The test gases used in this system were pure but-1-ene and a 1:1 mixture of hydrogen and but-1-ene. 0.25ml. samples of one of the test gases were injected over a fresh sample

of catalyst, which had previously been activated at 250°C, at a series of temperatures between 120° and 285°C. At temperatures lower than 120°C, no isomeration or hydrogenation was observed with either of the sample gases and the only hydrocarbon detected in the chromatograph was but-1-ene. At 160°C, significant amounts of cis and trans but-2-ene were detected after the injection of the but-1-ene/hydrogen mixture but there was no evidence of any n-butane. No such isomerisation occurred when the pure but-1-ene was injected into the system at the same temperature. At 185°C, there was still no evidence of the isomerisation of the pure but-1-ene in absence of H_2. However, when the but-1-ene/hydrogen mixture was introduced into the system at 185°C, traces of n-butane as well as large quantities of the isomerised products were detected. At the higher temperature of 228°C, the extents of hydrogenation and isomerisation were similar to those in the reaction at 185°C but traces of cis and trans but-2-ene were detected as products of isomerisation of the pure but-1-ene. These results are summarised in table 8.1.

Throughout its exposure to the but-1-ene and to the but-1-ene/hydrogen mixture at the temperatures of these tests, the catalyst maintained its pink colour.

Test reactions using the static system were carried out with either 0.04g. or 0.08g. of catalyst, which was activated in vacuo at 250°C for one hour. The catalyst temperature

TABLE 8.1

Distribution of Eluant Hydrocarbons from Test Reactions over $Os_3(CO)_{12}/SiO_2$

Temperature (°C)	% hydrocarbons			
	n-BUT	BUT-1	t-B-2	c-B-2
160	-	49.2	30.6	20.2
190	2.1	55.5	31.0	11.0
228	2.7	41.4	36.9	19.9
250	4.0	28.1	43.6	24.3
285	5.2	20.8	47.3	26.7

was reduced to the reaction temperature and a 1:1 mixture of but-1-ene and hydrogen was admitted to the reaction vessel ($p_{H_2} = p_{BUT-1} = 30.0 \pm 0.5$ml). The pressure fall was measured on the mercury manometer.

No hydrogenation was observed with the 0.04g. sample at temperatures lower than 200°C and the 0.08g. sample was used in all further reactions. At temperatures lower than 200°C, there was no pressure change, even after 30 minutes. At 220°C, however, the pressure fall was just detectable, although the rate of reaction was too slow to be measured. This was consistent with the very small extent of hydrogenation of each pulse of the but-1-ene/hydrogen mixture in the flow reactor.

8.2 Reactions of But-1-ene with Deuterium over $Os_3(CO)_{12}/SiO_2$

The reaction of but-1-ene with deuterium over $Os_3(CO)_{12}/SiO_2$ was studied using 0.08g. of the supported complex in the reaction vessel of 200ml. capacity. The catalyst was activated by heating it under vacuum for 14 hours at 250°C, after which the temperature was reduced to the reaction temperature of 220°C. The reaction mixture, composed of equal pressures of deuterium and but-1-ene, was admitted into the reaction vessel to a pressure of 60 ± 1mm. As the hydrogenation reaction was too slow to follow from the readings on the mercury manometer, the products of reaction

were extracted after a predetermined time interval. This method allowed the collection of products from reactions carried out to varying conversions.

After the reaction was stopped, the products were collected in a sampling vessel and transferred to the gas chromatograph for separation and analysis. The butene distributions at each conversion were calculated and these are shown in table 8.1 and are illustrated graphically in Fig. 8.1. Between each reaction, the vessel was evacuated for 30 minutes at reaction temperature.

8.3 The Exchange Reaction

The separated hydrocarbons were transferred to the mass spectrometer for analysis for deuterium content. The distributions of deutero-butane and the deutero-butenes at varying conversions to n-butane are shown in table 8.2.

The butane distribution showed a maximum of d_2 at all conversions. The proportion of the d_1 species in the butane distribution is, however, large. The deuterium number for the n-butane initially increases with conversion, reaching a constant value at about 9% conversion. In the case of the butenes, the proportions of exchanged products increase and their mass spectra broaden with increasing conversion. The exchange reaction of but-1-ene is important throughout the series and, except for the anomalous results from reaction J/4, the spectra of the three butenes are similar.

TABLE 8.1

Variation in Hydrocarbon Distribution with Conversion over $Os_3(CO)_{12}/SiO_2$ at 220°C

Catalyst weight = 0.08g. $p_{D_2} = p_{BUT-1} = 30 \pm 0.5$mm.

Reaction	% Hydrocarbon Distribution					
	n-BUT	BUT-1	t-B-2	c-B-2	t_{ex} (min)	t/c
J_2	2.6	60.6	20.7	16.1	15	1.29
J_7	6.0	32.8	33.9	27.3	120	1.24
J_6	9.2	19.9	46.7	26.3	240	1.78
J_4	31.9	16.0	32.4	19.7	300	1.65
J_3	33.4	11.6	32.4	22.6	840	1.43
J_5	71.3	4.2	15.3	9.2	2880	1.66

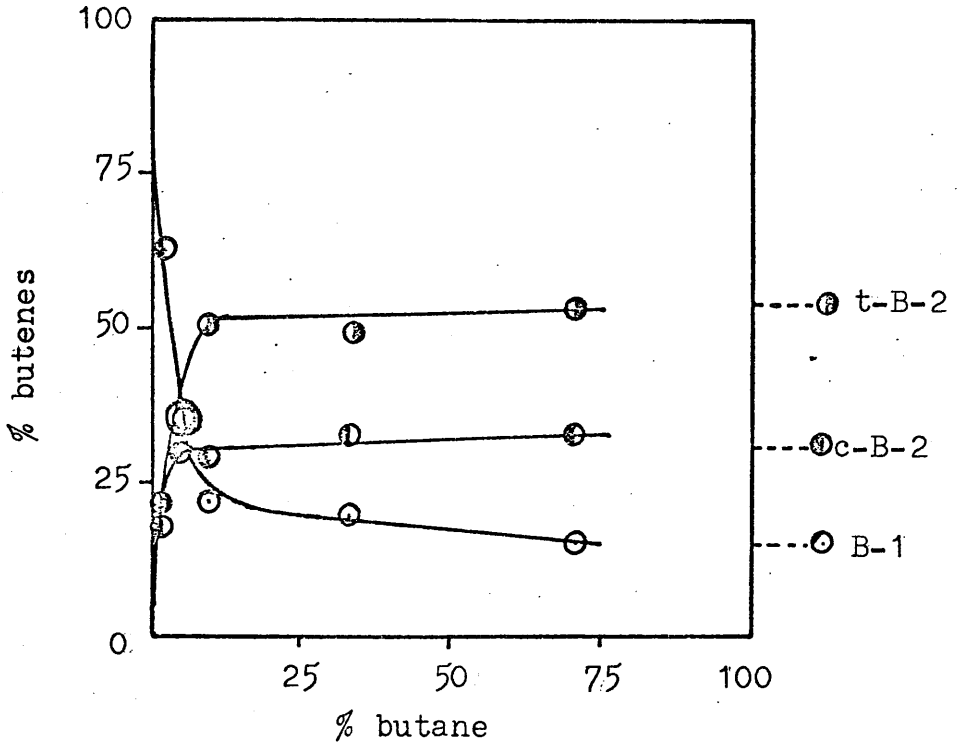

Fig. 8.1 Variation in butene distribution with conversion over freshly prepared sample at 220°C

TABLE 8.2

Distribution of Deuterated Hydrocarbons over $Os_3(CO)_{12}/SiO_2$ at 220°C

Reaction	d_0	d_1	d_2	d_3	d_4	d_5	d_6	d_7	d_8	D.N.
J/2	Conversion = 2.6%									
n-BUT	-	-	-	-	-	-	-	-	-	-
BUT-1	71.5	24.8	2.6	0.7	0.4	0.0	0.0	0.0	0.0	0.34
t-B-2	82.1	13.4	3.9	0.7	0.0	0.0	0.0	0.0	0.0	0.23
c-B-2	79.4	15.7	3.4	1.0	0.5	0.0	0.0	0.0	0.0	0.28
J/7	Conversion = 6.0%									
n-BUT	10.9	28.7	44.8	11.3	4.6	0.0	0.0	0.0	0.0	1.69
BUT-1	64.6	27.2	6.5	1.4	0.3	0.0	0.0	0.0	0.0	0.46
t-B-2	50.2	36.9	9.6	2.2	0.8	0.3	0.0	0.0	0.0	0.67
c-B-2	67.8	23.8	6.3	1.6	0.6	0.0	0.0	0.0	0.0	0.43
J/6	Conversion = 9.2%									
n-BUT	9.0	20.9	41.5	14.4	8.1	4.1	2.1	0.0	0.0	2.12
BUT-1	61.9	26.3	8.7	2.3	0.8	0.0	0.0	0.0	0.0	0.54
t-B-2	48.3	37.3	11.5	2.1	0.8	0.0	0.0	0.0	0.0	0.70
c-B-2	51.8	35.2	10.2	2.3	0.6	0.0	0.0	0.0	0.0	0.60

TABLE 8.2 (cont.)

Distribution of Deuterated Hydrocarbons over $Os_3(CO)_{12}/SiO_2$ at 220°C

Reaction	d_0	d_1	d_2	d_3	d_4	d_5	d_6	d_7	d_8	D.N.
J/4	Conversion = 31.9%									
n-BUT	9.5	25.9	31.5	17.7	8.2	3.5	2.5	1.2	0.0	2.15
BUT-1	56.4	19.7	14.0	7.2	2.1	0.5	0.0	0.0	0.0	0.81
t-B-2	25.9	32.6	25.4	11.6	3.4	0.9	0.2	0.0	0.0	1.37
c-B-2	23.9	34.3	25.3	11.9	3.5	0.8	0.3	0.0	0.0	1.40
J/3	Conversion = 33.4%									
n-BUT	8.2	28.1	32.8	18.9	8.0	4.2	0.2	0.0	0.0	2.02
BUT-1	18.4	31.1	28.9	15.5	5.0	1.2	0.0	0.0	0.0	1.61
t-B-2	18.1	29.8	28.6	16.4	5.8	1.2	0.2	0.0	0.0	1.66
c-B-2	17.1	32.9	28.9	15.2	4.5	1.1	0.3	0.0	0.0	1.61
J/5	Conversion = 71.3%									
n-BUT	8.8	25.7	32.1	19.0	9.7	3.4	1.0	0.3	0.0	2.11
BUT-1	14.4	27.3	27.7	17.1	8.5	3.4	1.7	0.0	0.0	1.95
t-B-2	-	-	-	-	-	-	-	-	-	-
c-B-1	16.5	30.0	29.1	16.8	5.7	1.5	0.4	0.0	0.0	1.71

CHAPTER 9

UNSUCCESSFUL ATTEMPTS TO FIND OTHER CATALYTICALLY ACTIVE SUPPORTED SYSTEMS

Experiments were carried out to investigate the possibility of supporting a number of different transition metal complexes and, when this was successful, to investigate the catalytic properties of the supported complex in reactions involving but-1-ene with and without hydrogen. The complexes investigated were chosen either (a) because they had been used successfully by other workers as catalysts in the homogeneous phase or (b) because they contained an olefinic or allylic ligand, which might participate in exchange with an olefinic molecule.

The general method of supporting the complexes was by impregnation of "Aerosil" silica or α-alumina with a solution of the complex in a suitable solvent under a stream of dry nitrogen. The complexes used were:

(i) tristriphenylphosphinerhodium(I) chloride, $(Ph_3P)_3RhCl$;

(ii) titanocene dichloride, $(C_5H_5)_2TiCl_2$;

(iii) potassium ethylene trichloro-platinate, $KPt(C_2H_4)Cl_3$;

(iv) ethylene palladous chloride, $\left[(C_2H_4)_2PdCl_2\right]_2$;

(v) triiron dodecacarbonyl, $Fe_3(CO)_9$.

The conditions under which each attempt at supporting a complex was made are shown in table 9.1.

TABLE 9.1.

Conditions for Supporting Various Complexes

	Complex	Support	Solvent
(i)	$(Ph_3P)_3RhCl$	(a) SiO_2 (sample A)	benzene
		(b) deuterated SiO_2 (sample B)	deutero-chloroform
(ii)	$(C_5H_5)_2TiCl_2$	SiO_2	methylene dichloride
(iii)	$KPt(C_2H_4)Cl_3$	(a) dry SiO_2	dry ethanol/ benzene
		(b) α-Al_2O_3	" "
(iv)	$(Pd(C_2H_4)Cl_2)_2$	dry SiO_2	benzene
(v)	$Fe_3(CO)_{12}$	dry SiO_2	methylene dichloride

The only complexes in this series which were successfully supported were tristriphenylphosphinerhodium(I) chloride and titanocene dichloride. In all of the other cases, the complexes had reduced to the metal before all of the solvent had been removed in the nitrogen stream.

Experiments to test the catalytic activity on the pink $(C_5H_5)_2TiCl_2/SiO_2$ and of the biege $(Ph_3P)_3RhCl/SiO_2$ were carried out in the pulse-flow reactor. But-1-ene and 1:1 mixture of but-1-ene and hydrogen were used as the test gases.

Attempts were made to activate the supported complexes at various temperatures, but no colour change was observed at temperatures below 200°C, and, on injection of the test gases at each of these temperatures, the only hydrocarbon detected by the chromatograph was but-1-ene.

The $(Ph_3P)_3RhCl/SiO_2$ system was studied by infra-red spectroscopy to attempt to find possible reasons for the inactivity of the supported complex. The spectrum of the dark red $(Ph_3P)_3RhCl$ in the form of a KBr disc is shown in Fig. 9.1. The main absorption bands in the region 1300 - 4000cm^{-1} lie at the frequencies 1430, 1480, 1570, 1580 and 3050cm^{-1}. The spectrum of untreated silica is shown in Fig. 9.2 and, in this case, there are broad absorption bands centred at 1300, 1630 and 1870cm^{-1}, a sharp peak at 3740cm^{-1} and a very broad absorption band between 2800 - 3700cm^{-1}. The spectrum of $(Ph_3P)_3RhCl$ supported on SiO_2 by impregnation from spectroscopic grade benzene (Sample A) is shown in Fig. 9.3, in which all the bands appearing in the spectrum of the complex on its own may be seen to be superimposed upon the spectrum of silica. However, two bands, which appeared in neither the spectrum of the complex on its own nor that of silica may be seen in the spectrum of the supported complex: a weak band at 1460cm^{-1} and a strong absorption centred at 1990cm^{-1}. A summary of the absorptions in each of the three spectra is shown in table 9.2. In this

TABLE 9.2

Summary of Infra-Red Data

Spectrum	Frequency of Absorption (cm^{-1})
$(Ph_3P)_3RhCl$ in KBr disc	1430 (s)
	1480 (s)
	1570 (w)
	1580 (w)
	3050 (m)
Untreated SiO_2	1300 (s)
	1630 (m)
	1870 (m)
	3000 - 3700 (s)
	3740 (s)
$Ph_3P)_3RhCl/SiO_2$ (Sample A)	1300 (s)
	1440 (s)
	1460 (w)
	1485 (s)
	1590 (m)
	1640 (m)
	1820 - 1900 (m)
	1990 (s)
	2700 - 3700 (s)

table, the intensity of each band is indicated by s, m or w, corresponding to a strong, medium or weak absorption.

In an attempt to elucidate the nature of the chemical group producing the new absorption bands and to ensure that these were not caused by residual impurities from the benzene, a completely different method was used in supporting the complex. The silica was first heated at 480°C in vacuo, with the constant pumping, for five hours and then exposed to 200mm. of deuterium for 24 hours. After cooling, the deuterium was pumped off and the spectrum of the dry silica showed partial exchange of the surface hydroxyl groups, by the reduction in intensity of the band at 3740cm^{-1} and the appearance of a new band of weak intensity at 2760cm^{-1}. The silica was then treated with heavy water (D_2O) for some hours and dried in vacuo at 100°C.

The pretreated silica was impregnated with $(Ph_3P)_3RhCl$ from a solution of the complex in spectroscopic grade deuterochloroform and was dried under a stream of nitrogen. The resulting free-flowing powder (Sample B) had the same beige colour as sample A. The spectrum of the resulting supported complex is shown in Fig. 9.4. Apart from the difference in the relative intensity of the band at 1990cm^{-1}, which is slightly smaller in the spectrum of sample B, the spectra of samples A and B are very similar. No new band appears in the spectrum of sample B to

compensate for the lowering in intensity of the peak at $1990cm^{-1}$ and this difference may be due solely to a difference in surface concentration of the supported complex.

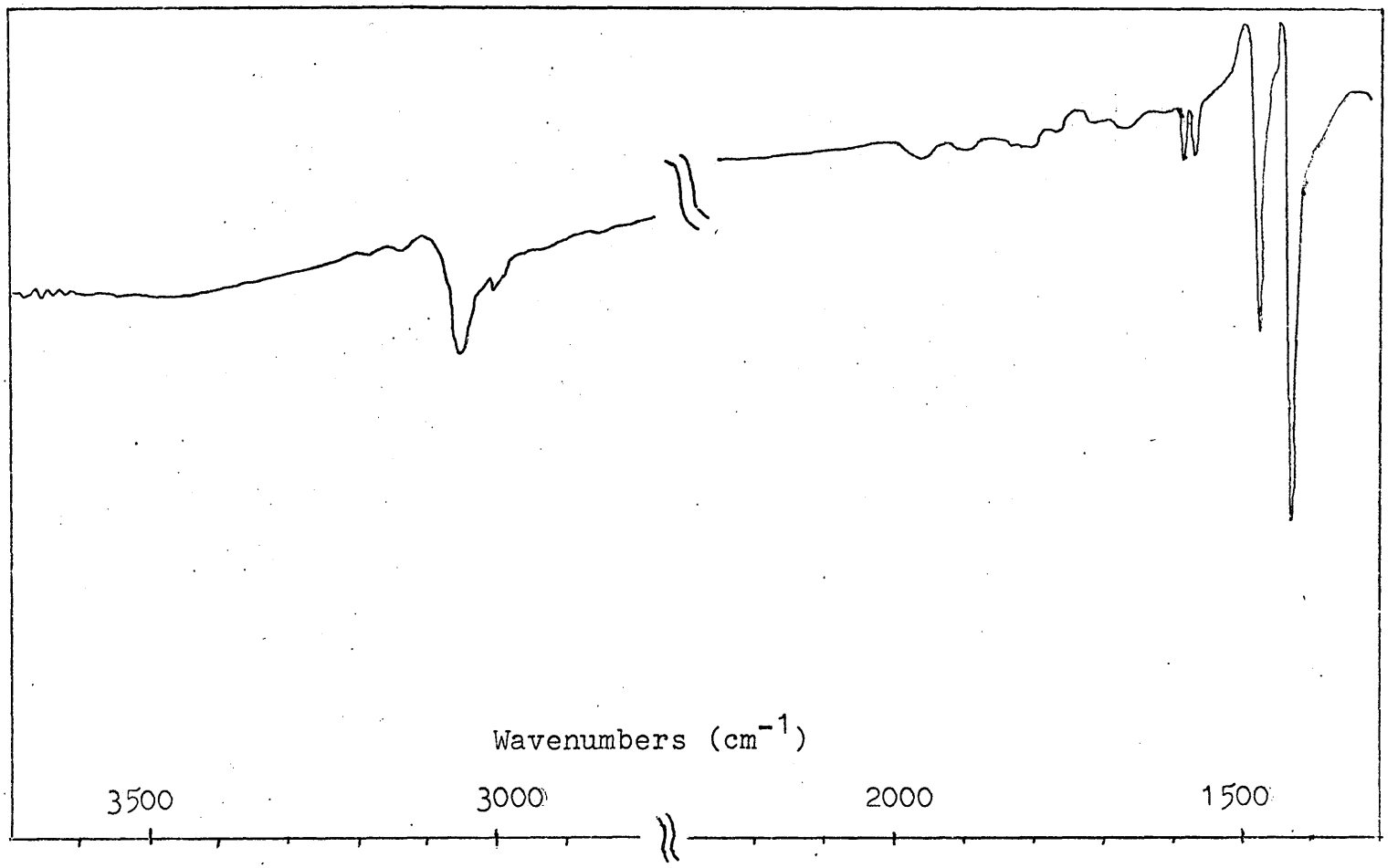

Fig. 9.1 Spectrum of tristriphenylphosphinerhodium chloride in KBr disc.

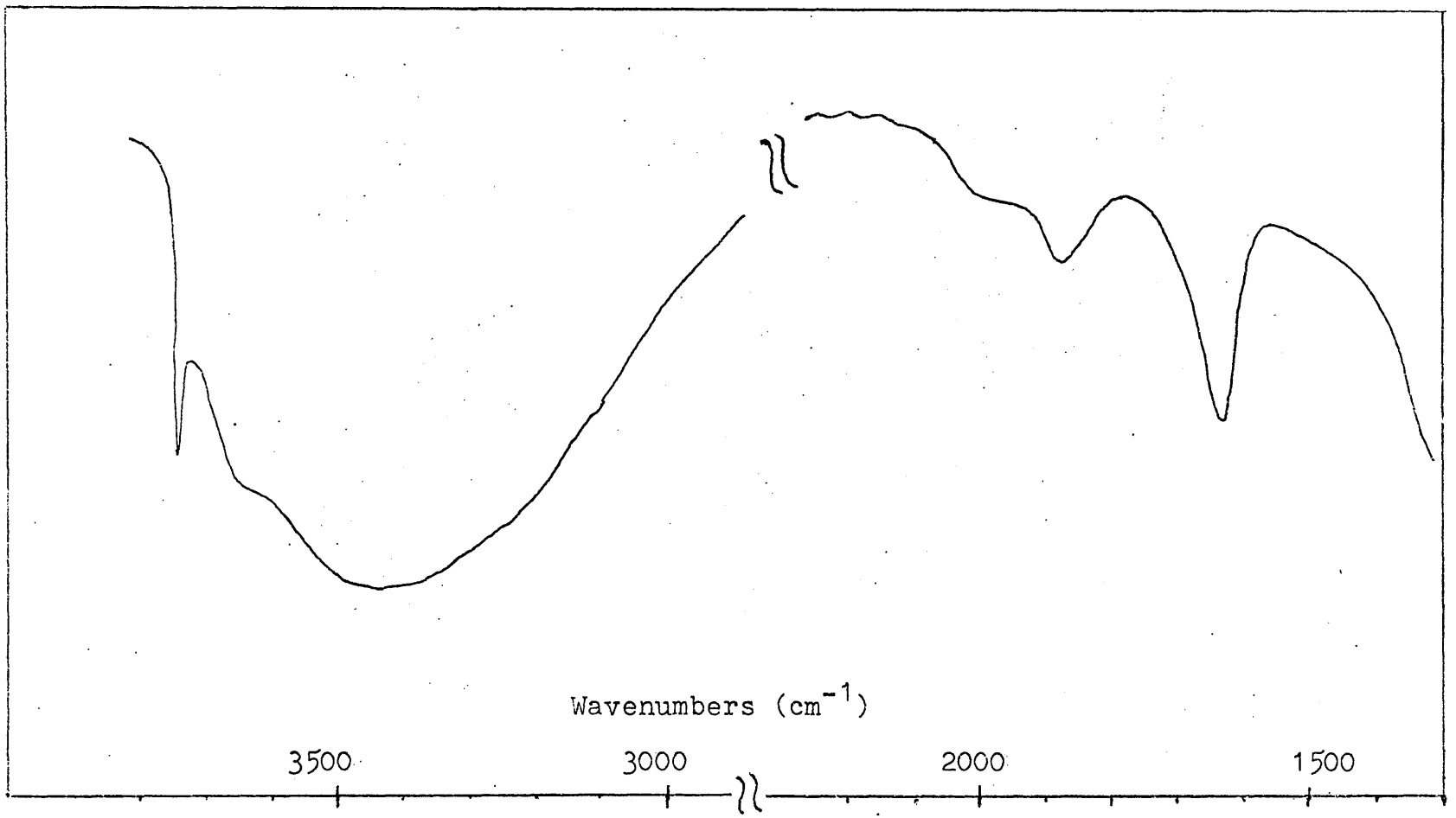

Fig. 9. 2 Spectrum of Untreated 'Aerosil' Silica.

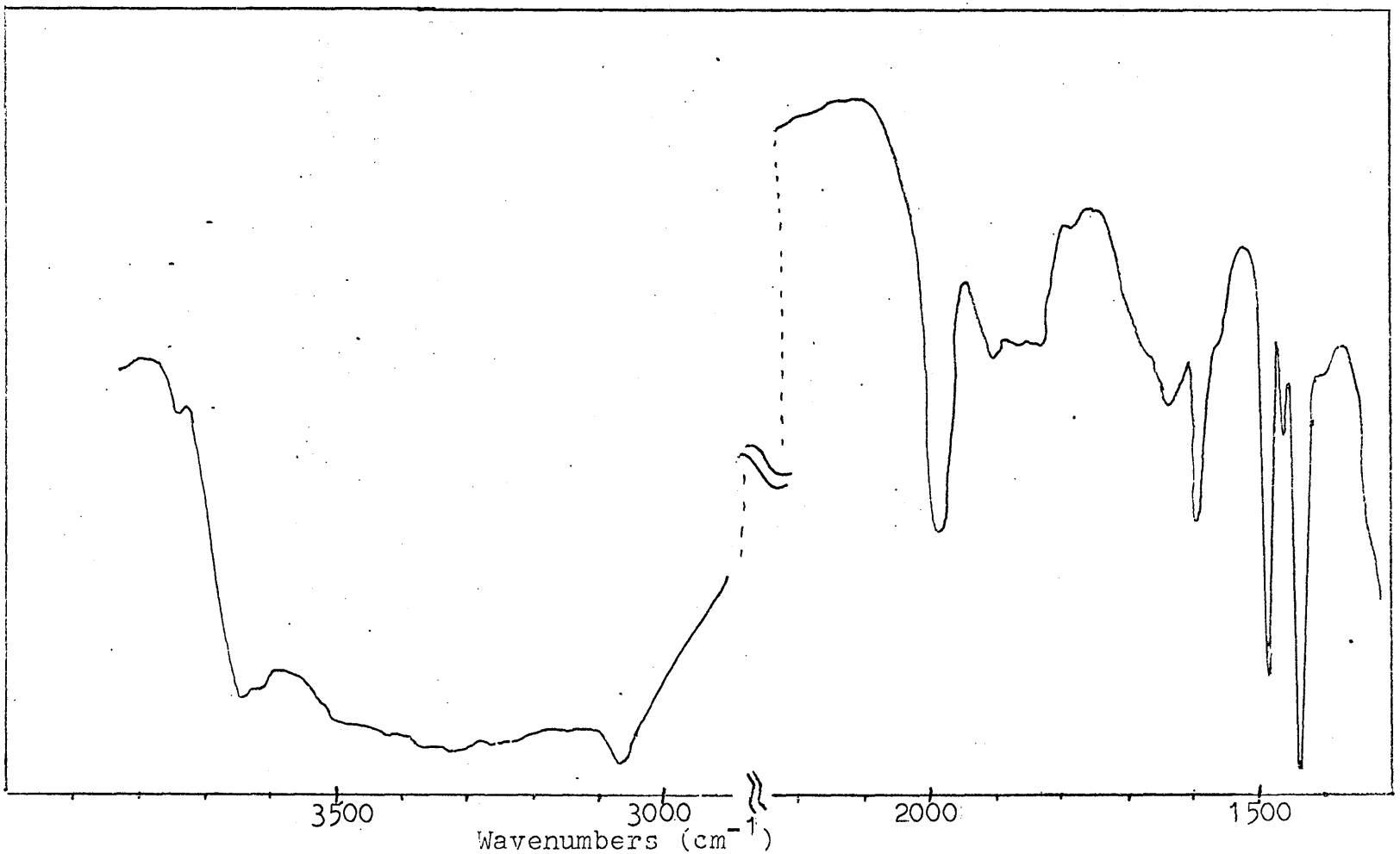

Fig. 9.3 Spectrum of silica supported tristriphenylphosphine rhodium chloride

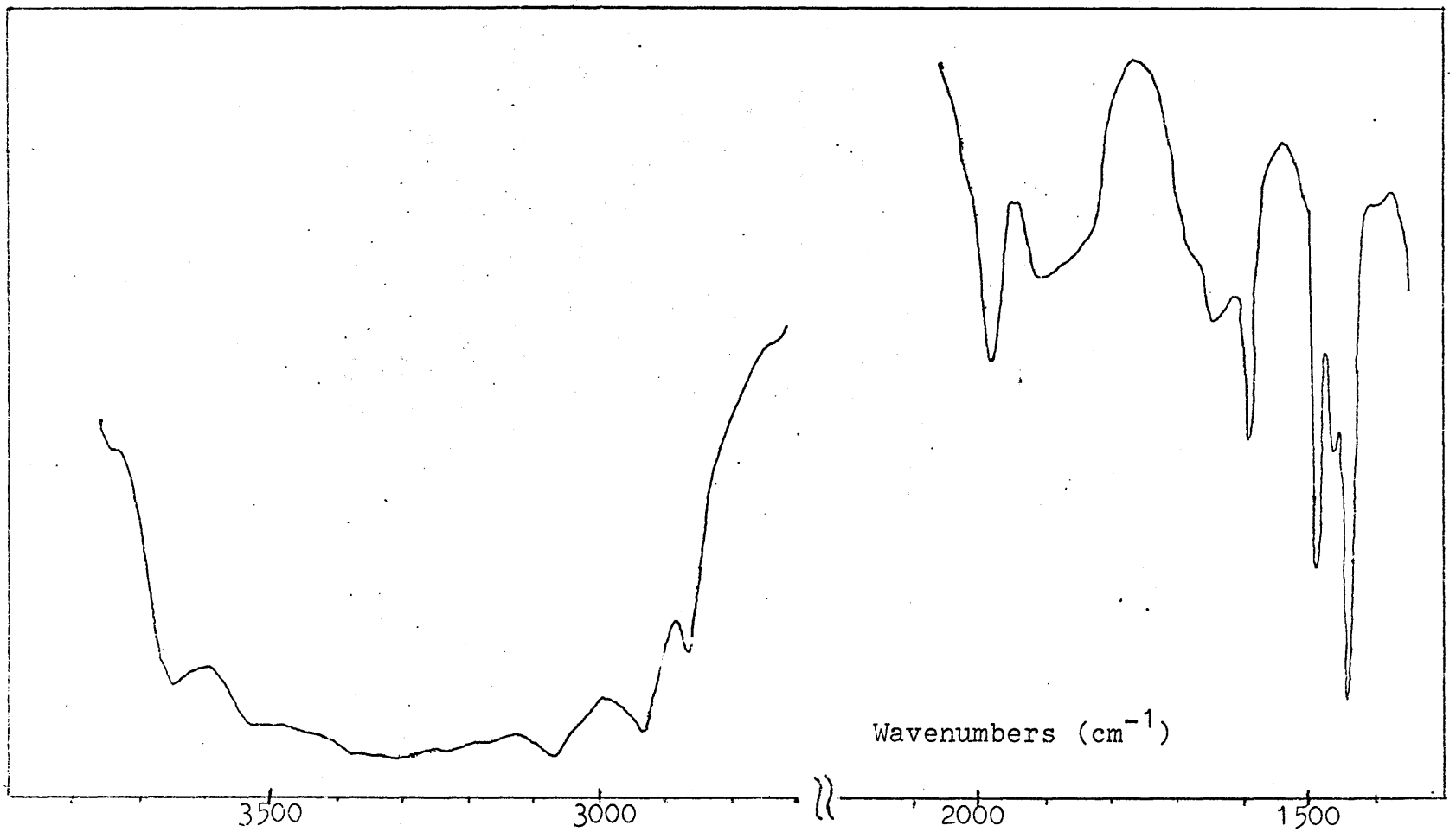

Fig. 9.4 Spectrum of silica supported tristriphenylphosphine rhodium chloride

DISCUSSION SECTION

CHAPTER 10

REACTIONS OVER THE SILICA SUPPORTED TRIMERIC METAL DODECACARBONYLS

The ensuing discussion of the properties of the supported triruthenium dodecacarbonyl and triosmium dodecacarbonyl will be approached from two aspects. First, the information obtained about the physical characteristics of the catalysts will be summarised with a view to explaining the changes in the supported complex under different conditions. Second, an attempt will be made to correlate the information obtained about the hydrogenation, isomerisation and deuterium exchange of but-1-ene over these catalysts, thereafter to consider further the implications of the features of these reactions and to offer explanations for these features in terms of reaction mechanism. Finally, by looking at the conclusions drawn from these approaches, an attempt will be made to identify the supported species active in catalysis.

10.1 The Natures of the Supported Complexes

10.1.1 Physical Properties

The structures of triruthenium and triosmium dodecacarbonyl are well established. Both compounds have the metal-metal bonded structure shown in Fig. 10.1 (112). In the solid state and when dissolved in organic solvents, these ~~solvents~~ complexes are stable on exposure to air and to light. Tr~~i~~these ~~solvents~~ complexes are stable on exposure to air and to light. structure shown in Fig. 10.2 (113). Comparisons between the chemical properties of this complex and those of triruthenium dodecacarbonyl (114) have indicated that in the former compound, the metal-metal bonds are easily broken and that only under the mildest conditions is the triiron cluster relatively stable. The ruthenium trimer, on the other hand, is much more robust while the osmium cluster is extremely stable.

Low resolution studies by infra-red spectroscopy of triruthenium dodecacarbonyl in the solid state and in carbon tetrachloride have shown that the ν(CO) absorptions lie around 2060, 2030 and 2010 cm^{-1} (115,116), while for triosmium dodecacarbonyl in cyclohexane solution, ν(CO) is 2068, 2035, 2014 and 2002 cm^{-1} (117). The orders of these bands are normal for a cis-$[M(CO)_4L_2]$ species (118).

Apart from a slight lowering of resolution, probably caused by the superimposition of the spectrum of silica, the infra-red spectrum of the silica supported triruthenium dodecacarbonyl is similar to the spectrum of the complex

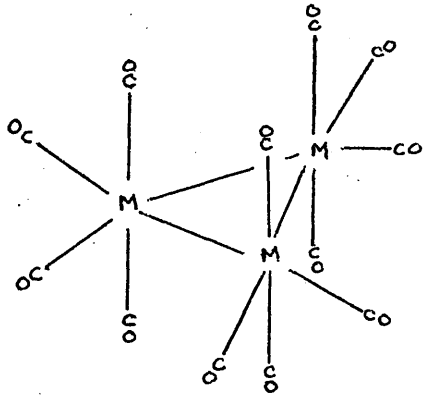

Fig. 10.1 Structure of Triruthenium and Triosmium Dodecacarbonyl

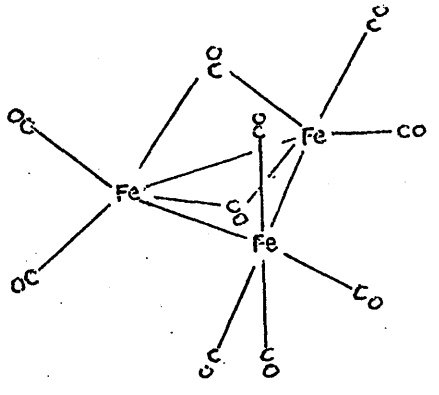

Fig. 10.2 Structure of Triiron Dodecacarbonyl

in a solution of methylene dichloride. It is probable that any small shifts in the absorption bands of the carbonyl are due to a solvent effect (118) and so it is further probable that the triruthenium dodecacarbonyl undergoes no chemical change when it is initially placed in contact with the support material. Neither the spectrum nor the colour of the supported complex changes when it is stored under dry nitrogen, indicating that the complex does not decompose under these conditions.

The corresponding supported triosmium complex is also yellow in colour and this colour persists when the complex is stored under dry nitrogen. Since the triosmium complex is extremely stable, it is likely that it too undergoes no chemical change on coming in contact with silica. The relatively less stable iron complex, on the other hand, decomposes almost immediately on contact with the silica, showing that the support is not just an inert carrier but that it has a definite chemical action upon the complex.

The observation of colour changes and changes in infra-red spectrum undergone by the silica supported triruthenium complex show that it undergoes a series of chemical transitions during its heat treatment and exposure to air. The transition from the yellow to the pink form on heating must be caused by some change in

symmetry of the complex due to a change in its structure. By exposure of the yellow or pink forms to air, there is a gradual loss of carbon monoxide in the transition to the grey form, since the spectrum of this grey form shows no carbonyl absorptions. In the case of the pink form, this decomposition is fast and it passes through an intermediate white form, whose spectrum differs from those of both the yellow and pink forms. It has also been found that the spectrum of the white form may be reproduced by heating the yellow form in air (Fig. 6.4), and there is no evidence for the pink form being an intermediate in this case. It is probable that heating the yellow form in air simply accelerates the transition to the white form and that at room temperature, this transition was not observed over a relatively short time.

Such changes in colour and spectrum could be due to one or more of the following chemical transitions or a combination of two or more:

(i) loss of one or more molecules of carbon monoxide;

(ii) breakage of ruthenium-ruthenium bonds;

(iii) substitution of one of the carbonyl ligands by a better π - acceptor or σ-donor;

(iv) oxidation of the metal.

That carbon monoxide is lost during the activation of the supported complex is substantiated by the results

obtained from the radiochemical examination of the 10% w/w sample. Furthermore, these experiments also indicate that only a certain number of carbon monoxide molecules may be removed at a given temperature and that further carbon monoxide is lost only when the temperature is increased. Thus, one may conclude that by removing x carbonyl ligands from the complex at T°C, a new species, $Ru_3(CO)_{12-x}$, which is more stable than supported $Ru_3(CO)_{12}$ at that temperature, may be formed. The appearance of the absorption band at $2000cm^{-1}$ in the activated species and in the species exposed to air is evidence for the substitution of one of the ligands by a better π-acceptor or σ-donor, as the lowering of $\tilde{\nu}(CO)$ is indicative of a smaller back-donation of electrons into the π^* orbitals of one or more of the carbonyl ligands by a trans-effect, and these electrons are drawn instead to the better π-electron acceptor. This new band might also be explained by the oxidation of the metal, again producing a smaller back-donation of electrons to the carbonyl ligand.

Recently, Eady and co-workers (119) have reported the formation of ruthenium and osmium carbonyl hydrides from the reaction of water with triruthenium and triosmium dodecacarbonyl. These complexes, which are three-dimensional clusters of six, seven or eight metal atoms, are relatively stable. It is conceivable that a similar

reaction might occur on the silica, which contains surface hydroxyl groups, to produce such metal carbonyl hydride cluster compounds. The formation of complexes of this kind would explain the appearance of the new peaks at 2050 and 1970 cm^{-1} in the spectrum of the pink form as being metal-hydride absorptions. This could be tested by using silica with deuterium-exchanged surface hydroxyl groups. While such compounds might be stable in an inert atmosphere, they could be sensitive to the presence of oxygen and decompose when exposed to air to produce the white form.

The experiments to find the activation energies of the hydrogenation and isomerisation reactions over samples of the supported complex with different histories show that each of the different forms of the supported complex has different catalytic properties and give further evidence that exposure of the freshly prepared supported complex to light, heat and the atmosphere causes changes in the chemistry of the system.

Thus, the yellow and pink forms, which are stable in an inert atmosphere and in the dark, decompose in the presence of light and oxygen. Although the ruthenium and osmium complexes on their own are stable to these conditions, when supported on silica, they become extremely sensitive. Any further discussion of the mechanisms of

these transitions must, therefore, take account of the role of the support in the activation of the complexes to catalyse the hydrogenation and isomerisation of but-1-ene.

It is also interesting to note the lack of any X-ray or electron diffraction pattern from both the freshly prepared and used samples of the supported complex. (The used sample, having been exposed to air, showed no carbonyl absorption in its infra-red spectrum.) From this evidence, one must conclude that there is no crystalline material present on the surface of the silica, or that any particles are very small ($<$10-20 Å) and that in the discussion of the active species, one can consider the catalyst 'particles' to be on or approaching the molecular scale.

10.1.2 The Active Catalyst

L'Eplattenier et al. (120,121) have postulated that $RuH_2(CO)_4$ is an intermediate in the homogeneous hydrogenation of nitrobenzene by triruthenium dodecacarbonyl. They have also postulated that the lower activity of triosmium dodecacarbonyl towards hydrogenation reactions is because of the greater stability of the intermediate osmium hydridocarbonyl. On the other hand, Davie and co-workers (100) have postulated the species active in the disproportionation of propene on supported molybdenum hexacarbonyl to be a sub-carbonyl complex of the form

$Mo(CO)_{6-x}$, while a later report by Howe et al. (101) has claimed that the active catalyst is, in fact, molybdenum in a high oxidation state. From the arguments outlined in section 10.1.1, however, one is led to believe that the active species in the present study is a sub-carbonyl complex of the form

$$\left[L_xRu(CO)_{4-x}\right]_n$$

and that activation, which does not occur unless the support is present, involves the displacement of carbonyl ligands by the support itself acting as a ligand through an -O-Si- group. Hydride ligands, transferred from the surface hydroxyl groups on the silica, might also cause the displacement of carbon monoxide or the breakage of a metal-metal bond.

Replacement of a ruthenium-carbon bond with a ruthenium-hydride bond and/or with a highly polar ruthenium-oxygen bond could render the complex extremely sensitive to attack by molecular oxygen, leading eventually to the complete decomposition of the active complex. Thus, on prolonged exposure of the yellow form to air at ambient temperature or on heating the yellow form in air, the active pink species would be formed transiently but would be readily attacked by molecular oxygen to produce initially the white form containing no hydride ligands and finally the metal itself.

10.1.3 Summary

The conclusions drawn above may be summarised as follows. First, when freshly supported, the complexes retain their molecular structure as the yellow form. Second, when the yellow form is heated in an inert atmosphere, the complex and support react to form a hydrido-species which is attached to the surface through a metal-oxygen bond (the pink form); this species is sensitive to attack by molecular oxygen and on exposure to air, it rapidly reacts to produce the white form, which is believed to be similar in structure to the pink form but containing no hydride ligands. Further exposure of the white form to air produces the grey form, which is believed to be extremely finely divided metal particles on the support. The yellow form also decomposes to the metal upon prolonged exposure to air. Finally, it is believed that the relatively unstable pink hydrido-species is the catalyst which is active in the hydrogenation and isomerisation of but-1-ene.

10.2 Reactions of But-1-ene

10.2.1 The Hydrogenation of But-1-ene on Silica Supported Triruthenium Dodecacarbonyl

As was outlined in section 1.4, the mechanism generally

accepted for the hydrogenation of olefins requires the addition of a hydrogen atom to an adsorbed olefin molecule to form the "half-hydrogenated" state (54), in this case an adsorbed butyl radical. There are two principal mechanisms by which this species may be formed. First, the Langmuir-Hinshelwood mechanism, in which the adsorbed butene combines with dissociatively adsorbed hydrogen, viz.,

Reaction Scheme A.

$$C_4H_8(g) + (*) \rightleftharpoons C_4H_8(a) \qquad (a,a')$$

$$H_2(g) + 2(*) \rightleftharpoons 2H(a) \qquad (b,b')$$

$$C_4H_8(a) + H(a) \rightleftharpoons C_4H_9(a) + (*) \qquad (1,-1)$$

$$C_4H_9(a) + H(a) \longrightarrow C_4H_{10}(g) + 2(*) \qquad (2)$$

The kinetics of the reaction are consistent with one in which the catalyst surface is completely covered with olefin and hydrogen is comparatively weakly adsorbed. Assuming competative adsorption, the surface coverages, Θ, of but-1-ene and hydrogen are given by the Langmuir adsorption isotherms:

$$\Theta_B = \frac{b_B p_B}{1 + b_B p_B + b_{H_2}^{\frac{1}{2}} p_{H_2}^{\frac{1}{2}}};$$

$$\Theta_H = \frac{b_{H_2}^{\frac{1}{2}} p_{H_2}^{\frac{1}{2}}}{1 + b_B p_B + b_{H_2}^{\frac{1}{2}} p_{H_2}^{\frac{1}{2}}},$$

where $B = C_4H_8$. Under conditions where the olefin is adsorbed much more strongly than hydrogen, these

equations simplify to $\Theta_{C_4H_8} = 1$, and $\Theta_H \propto p_{H_2}^{\frac{1}{2}}$.

If the addition of an adsorbed hydrogen atom to the butyl radical (step 2) is rate determining, then the rate expression is

$$\text{rate} = k_2 \Theta_{C_4H_9} \cdot \Theta_H .$$

A steady state analysis shows that

$$\Theta_{C_4H_9} = \frac{k_1 \Theta_{C_4H_8} \Theta_H}{k_2 \Theta_H + k_{-1}}$$

and when this is substituted into the rate expression, the rate of reaction is given by

$$\text{rate} = \frac{k_1 k_2 \Theta_{C_4H_8} \Theta_H^2}{k_2 \Theta_H + k_{-1}} .$$

Thus, if Θ_H and k_2 are small compared with k_{-1} such that $k_{-1} >> k_2 \Theta_H$, the rate expression reduces to rate = Kp_{H_2}, which agrees with the observed kinetics.

The Rideal-Eley mechanism, on the other hand, visualises the formation of the butyl radical from the reaction of an adsorbed butene molecule with molecular hydrogen, viz.,

Reaction Scheme B.

$$C_4H_8(g) + (*) \rightleftharpoons C_4H_8(a) \qquad (a,a')$$

$$C_4H_8(a) + H_2\text{--}* + (*) \rightleftharpoons C_4H_9(a) + H(a) \qquad (1,2)$$

$$C_4H_8(a) + H(a) \rightleftharpoons C_4H_9(a) + (*) \qquad (3,4)$$

$$C_4H_9(a) + H(a) \longrightarrow C_4H_{10}(g) + 2(*) \qquad (5)$$

The determination of the surface coverages of the intermediate species by a steady state analysis shows that

$$\theta_{C_4H_9} = \left[\frac{k_1 k_3 p_{H_2}}{k_4(k_2 + k_5)}\right]^{\frac{1}{2}}$$

and

$$\theta_H = \left[\frac{k_1 k_4 p_{H_2}}{k_3(k_2 + k_5)}\right]^{\frac{1}{2}}$$

Thus, if step 5 is rate determining, the order of the reaction with respect to hydrogen is unity. If, on the other hand, the rate limiting step is step 1, then

$$\text{rate} = k_1 \theta_{C_4H_8} \cdot p_{H_2}.$$

The initial order of unity in hydrogen for the addition reaction is, therefore, compatible with both the Langmuir-Hinshelwood and Rideal-Eley mechanisms and it is impossible to distinguish between them on kinetic evidence alone. Further consideration will be given to the relative merits of each of these mechanisms in conjunction with the discussion of the isomerisation and exchange reactions.

10.2.2 The Isomerisation of But-1-ene on Silica Supported Triruthenium Dodecacarbonyl

In the discussion of the isomerisation reaction of but-1-ene, consideration must be given both to the mechanism involving an alkyl intermediate and to that involving

the interconversion between an adsorbed olefin and a π-allyl intermediate as have been outlined in section 1.4.3.

Since both the mechanisms described above for the hydrogenation of but-1-ene require the formation of butyl radicals on the catalyst, there exists the possibility that alkyl reversal is responsible for double-bond migration. However, if this is the case, olefin desorption (step a') would be expected to be the rate limiting step, since in both schemes A and B, $\Theta_H \propto p_{H_2}^{\frac{1}{2}}$ and any other step would lead to an order of 0.5 or unity with respect to hydrogen.

The kinetics of the interconversion reaction show that the order of this reaction with respect to but-1-ene is equal to unity. By inspection of the Langmuir isotherm for the adsorption of but-1-ene, it may be seen that in order to fulfil this requirement, the surface coverage of but-1-ene, Θ_B, must be very small, as $b_B p_B \ll 1$. However, it has been argued in the previous section that the kinetic evidence from the hydrogenation reaction strongly suggests that Θ_B is very large, because the order of this reaction with respect to but-1-ene is zero. These observations are inconsistent with the same species being an intermediate in both the hydrogenation and isomerisation reactions. From kinetic evidence alone,

therefore, it would appear that these reactions occur via different intermediates and that they do not occur on the same surface site.

The alternative mechanism for isomerisation involves the formation of a 1-methyl-π-allyl intermediate. Furthermore, it might be expected that this step would be rate determining, as it requires the rupture of a carbon-hydrogen bond. The rate expression may then be written as rate = $k\Theta_{C_4H_8}$, which is independent of hydrogen coverage and so is in agreement with the observed zero order with respect to hydrogen.

A postulate that the mechanism for double-bond migration involves a 1-methyl-π-allyl intermediate has several important implications. First, the butyl intermediate produced in the hydrogenation reaction must be predominantly 1-butyl rather than 2-butyl as the latter would give rise to isomerisation. Thus, the exchange of but-1-ene would be independent of the isomerisation reaction and the deuterated but-2-enes would be produced predominantly by the isomerisation of deuterated but-1-ene. It is highly significant, therefore, that in reaction series L carried out at 90°C, approximately 50% of the but-1-ene underwent isomerisation to cis and trans but-2-ene during the induction period, and yet very little exchanged product was observed. This effect, however, will be

considered more fully in the discussion of the exchange reactions.

A second feature of the π-allyl mechanism is that isomerisation should occur in the absence of molecular hydrogen by inter- or intra-molecular hydrogen transfer, whereas the alkyl exchange mechanism cannot be initiated without a source of hydrogen atoms. Test reactions in the pulse-flow reactor on supported triruthenium dodecacarbonyl, which had never been in contact with molecular hydrogen, have shown that but-1-ene readily undergoes isomerisation in the absence of hydrogen and, although no precise quantitative data are available for these reactions, it is nevertheless firm evidence in favour of a π-allyl intermediate.

Third, the distributions of the but-2-enes will depend upon the relative stabilities of the syn- and anti-conformations of the adsorbed 1-methyl-π-allyl intermediate, rather than upon the conformation of an adsorbed 2-butyl radical. Assuming approximately equal interaction energies for Me-Me and Me-surface, the latter approach predicts that the minimum initial trans/cis ratio be unity and that the trans/cis ratio decrease with increasing temperature (29). In this case, however, although the trans/cis ratio is never less than unity, there is no obvious trend in the variation of this ratio

with temperature. The observation that the trans/cis ratio is always greater than unity is paralleled by the fact that syn-π-1-methylallyl cobalt tricarbonyl is more stable than the anti-isomer and that the former may be obtained from the latter by equilibration at 80°C (122).

The results of series B for the hydrogenation of cis but-2-ene show that the trans/cis butene ratio is fairly constant at $\simeq$0.6 ($\pm$ 0.07) over a wide range of conversions to n-butane and that this ratio starts to tend towards its equilibrium value only at 80% conversion. Furthermore, the initial rate of hydrogenation of cis but-2-ene was found to be about twice that for but-1-ene. As a 2-butyl species must be an intermediate in the hydrogenation of a but-2-ene, it is probable that this is also the major intermediate in its isomerisation. A 1-methyl-π-allyl intermediate would be unlikely in this case as the adsorbed cis but-2-ene would tend to form the anti-conformation of the π-allyl intermediate and addition of a hydrogen atom to this would result in the formation of cis but-2-ene, giving no net reaction. This observation implies that the adsorbed 2-butyl species undergoes relatively rapid hydrogenation to n-butane, while loss of a hydrogen atom to reform but-2-ene occurs much less readily.

If the isomerisation of but-1-ene were to involve

a 2-butyl species as an intermediate in an alkyl reversal mechanism, therefore, it would be expected that this intermediate would undergo relatively rapid addition of a further hydrogen atom to form n-butane. Thus, it is to be expected that the hydrogenation reaction would proceed at a measurable rate from the onset of the isomerisation process. Experimental observations show, however, that at 90°C approximately 50% of the reactant but-1-ene undergoes isomerisation before the onset of the hydrogenation reaction can be detected. Furthermore, the most distinctive features present in all the distribution curves for the hydrogenation of but-1-ene are (a) the minimum in each of the curves for but-1-ene and the corresponding maxima in those for cis and trans but-2-ene and (b) the butene distributions do not tend towards their equilibrium values even at 75% conversion to n-butane. These features suggest that cis and trans but-2-ene hydrogenate significantly faster than but-1-ene and this is supported by the experimental observation that cis but-2-ene hydrogenates more rapidly than but-1-ene over the same catalyst sample. Furthermore, they are evidence in favour of the proposal that hydrogenation and isomerisation occur independently on different sites.

The differences in the rates of hydrogenation of but-1-ene and the but-2-enes can be explained by a

difference in their relative strengths of adsorption, produced by a combination of two effects; first, by an inductive effect whereby electrons from an α-alkyl group 'migrate' towards the olefinic bond, resulting in a reduction in the π-electron back donation from the metal atom to the olefin and hence weakening the olefin-metal bond (as the contribution from a methyl group is approximately the same as that from an ethyl group, this effect would be almost twice as great in the but-2-enes as in but-1-ene); and second, by a steric effect, whereby the sheer bulk of the two α-methyl groups hinders the approach of the olefin to an already sterically crowded metal atom. Parallels to these effects have been found in coordination chemistry and it has been shown (59) that ethylene coordinates so strongly to tristriphenylphosphine rhodium(1)chloride that the hydrogenation reaction is poisoned, whereas with propylene, which is more weakly bound, the hydrogenation reaction proceeds smoothly.

10.2.3 The Reaction of But-1-ene with Deuterium on Silica Supported Triruthenium Dodecacarbonyl

A number of features of the hydrogenation and the isomerisation reactions have been discussed in relation to the possible reaction mechanisms, but it is still not clear which mechanism for each of these is operative in

this system. The results of the exchange reactions will, therefore, be considered with the following aims in view:

(a) to characterise the exchange of but-1-ene with deuterium on the supported complex;

(b) to establish whether the results are consistent with one or other of the proposed mechanisms for isomerisation; and

(c) to determine if the results are consistent with one or other of the proposed mechanisms for hydrogenation.

The principal features of the deutero-butene distributions for the reactions over silica supported triruthenium dodecacarbonyl are that initially, the but-2-enes have a slightly higher deuterium content than has but-1-ene and, as the reaction proceeds, the deuterium content of the product butenes increases more rapidly than that of the reactant. The distributions for cis and trans but-2-ene are generally similar. At low conversions, the n-butane contains a mean of less than two deuterium atoms per molecule, indicating considerable addition of exchanged hydrogen.

It is reasonable to assume that the exchange reaction occurs via an adsorbed alkyl intermediate, as has been postulated for the hydrogenation reaction, viz.,

$$C_4H_8(g) + (*) \rightleftharpoons C_4H_8(a) \qquad (a,a')$$

$$\left\{ \begin{array}{l} D_2(g) + 2(*) \rightleftharpoons 2D(a) \qquad (b,b') \\ \qquad\qquad \text{OR} \\ C_4H_8(a) + D_2\text{--}(*) \rightleftharpoons C_4H_8D(a) + D(a) \qquad (1,-1) \end{array} \right.$$

$$D(a) + C_4H_8(a) \rightleftharpoons C_4H_8D(a) + (*) \qquad (2,-2)$$

Now, if the rate of exchange is defined as

$$r_e = \frac{\sum_1^8 (\text{partial pressure of but-1-ene-}d_0)}{\text{reaction time}},$$

then the initial rates of exchange of but-1-ene at each temperature may be calculatcd (54). These are shown in table 10.1.

TABLE 10.1

Summary of Initial Rates of Reaction of But-1-ene at Various Temperatures

Reaction	Temp. (°C)	r_d	r_i (mm.min^{-1})	r_e(BUT-1)	D.N.(BUT-1)
L/S	90	0.43	11.1	0.11	0.12
M/S	110	0.63	16.9	0.15	0.17
K/4	130	1.63	61.6	1.45	0.40

By plotting the logarithm of the initial deuterium number for deutero-but-1-ene against the reciprocal of the absolute temperature, a good approximation to the value of

the term ($E_{oe} - E_h$), where E_{oe} is the activation energy for the exchange of but-1-ene, may be derived from the slope of the straight line obtained (123). This value is found to be 10Kcal.mol.$^{-1}$. Earlier arguments on the hydrogenation reaction, however, have led one to propose that even in the initial stages of the hydrogenation reaction, the but-2-enes are hydrogenated significantly faster than but-1-ene. It is considered, therefore, that the value of 12Kcal.mol.$^{-1}$ already obtained for E_h does not refer solely to but-1-ene and that substitution of this value for E_h in the above expression would not give the true value of E_{oe} for but-1-ene.

It is to be expected that in the initial stages of the reaction, the but-2-enes would contain more deuterium than would but-1-ene, as all the isomerised molecules would have been in contact with the surface at least once and also had the opportunity to exchange, while a large proportion of the reactant molecules would never have been adsorbed. If exchange were to occur via a 2-butyl intermediate, then it would be expected that this would be accompanied by isomerisation and that the initial product of this reaction would be but-2-ene-d_1 with the deuterium atom on the 1-methyl group unless multiple reactions occur. Thus, the exchange and isomerisation reactions would occur by the same mechanism

and it would be expected that every isomerised but-2-ene would contain at least one deuterium atom. It is apparent, however, from the initially high percentage of but-2-ene-d_0 that isomerisation occurs mainly without the incorporation of a deuterium atom and this is firm evidence in favour of the view that exchange of but-1-ene does not proceed via a 2-butyl intermediate.

If exchange were to occur via a 1-butyl intermediate, which could not lead to isomerisation, the resulting but-1-ene-d_1 would contain the deuterium atom on the 2-position. Isomerisation of this species by loss of an α-hydrogen atom would produce a 1-methyl-π-allyl-d_1 species which could then gain a further deuterium atom or a hydrogen atom to form deutero-but-2-ene. The initial high proportion of but-2-ene-d_0 is firm evidence in favour of inter- or intra-molecular hydrogen transfer. A feature of this mechanism for the incorporation of deuterium into the but-2-enes is that one would expect the but-2-ene deuterium content to reflect the change in that of but-1-ene but at a slower rate: this is clearly not the case and other factors must be considered to explain this observation.

It was suggested in section 10.2.2 that but-1-ene was relatively strongly adsorbed on the catalyst surface. Support for this view is given by the estimate for the

value of ($E_{oe} - E_h$) of 10Kcal.mol.$^{-1}$ (indicating that the activation energy for the exchange process is relatively high compared with that for hydrogenation) and by the relatively low rates of exchange obtained for but-1-ene. Thus, these features could be due to the relatively high strength of adsorption of but-1-ene, or be the result of an extremely low coverage of the surface by deuterium or be due to a combination of both of these effects.

The observed results may be explained in terms of a difference in strengths of adsorption of the butenes as follows. If but-1-ene were relatively strongly adsorbed on the catalyst, then it would form the 1-butyl species comparatively slowly, as this would require the disruption of a stable metal-olefin bond. Not only would this effect give rise to a slow rate of olefin exchange, but at low temperatures the but-1-ene could partially poison the sites for but-2-ene adsorption. The extent of poisoning would not necessarily be so great at higher temperatures because of the higher energy and hence higher mobility imparted to the molecules. As the isomerisation process is extremely fast relative to hydrogenation, there is a rapid build up of the but-2-enes and the chance of their finding a vacant site is high. If the postulate that the but-2-enes are only relatively weakly adsorbed

is accurate, then they would undergo a fast addition of hydrogen to produce the 2-butyl species which, by addition of another hydrogen atom could form n-butane or alternatively, by loss of a hydrogen atom could isomerise or revert to its original form. Because the trans/cis ratio does not increase particularly rapidly with conversion, one is led to the view that the addition of a second hydrogen atom to the 2-butyl species is the more important of the two processes but that exchange of the but-2-enes is still significantly faster than exchange of but-1-ene. Thus, the observed initial rate of the hydrogenation reaction would be dependent to some extent upon the initial rate of isomerisation, in that hydrogenation would not occur to a measurable extent until a sufficiently high concentration of but-2-ene was available.

Now, because $(E_{oe} - E_h)$ is greater than zero, the rate limiting step for hydrogenation is unlikely to be the same as that for exchange. Furthermore, the reversible formation of the adsorbed 1-butyl species cannot be rapid compared with the addition of a further 'hydrogen' atom to form n-butane, as predicted by the Langmuir-Hinshelwood theory, or $(E_{oe} - E_h)$ would be expected to be less than zero. These implications can, however, be explained in terms of a relatively low surface coverage of deuterium and the slow formation of the 1-butyl species by the

reaction of physically adsorbed molecular deuterium with an adsorbed but-1-ene molecule, viz.

$$C_4H_8(a) + D_2\text{--}* \underset{-1}{\overset{1}{\rightleftharpoons}} C_4H_8D(a) + D(a) \quad (A)$$

The resulting 1-butyl could now react with another adsorbed 'hydrogen' atom by step 2 to form deutero-n-butane or alternatively lose a 'hydrogen' atom by step (-1) to produce but-1-ene-d_1:

$$C_4H_8D(a) + \text{'H'}(a) \xrightarrow{2} C_4H_9D + 2*$$

In this system, the slow step for hydrogenation might be either of steps 1 or 2, depending upon the relative energies of the left and right hand sides of equilibrium A but in any case, $E_{RHS} < E_{LHS}$, otherwise $(E_{oe} - E_h) \leqslant 0$. Thus, the slow step in the exchange reaction must be step (-1).

By invoking such a mechanism for the activation of molecular hydrogen, one is able to visualise a new explanation for the relatively slow rate of interconversion of cis and trans but-2-ene compared with their rates of hydrogenation. If the term $(E_{oe} - E_h)$ for these isomers be also greater than unity, and it is reasonable to assume that this is so, then, by a similar reasoning to the above, it should be more favourable for another 'hydrogen' atom to add to the intermediate 2-butyl species to form n-butane than for the 2-butyl species to lose a 'hydrogen' atom to revert to but-2-ene. This argument does not,

however, satisfactorily explain why some exchanged but-1-ene appeared during the induction period and it must be assumed that some hydrogenation did occur at this stage but at a rate so slow as to be imperceptible.

Consideration of the relative values for the activation energies of the three processes provides further evidence in favour of the π-allyl mechanism being operative in the isomerisation reaction. The activation energy for the hydrogenation of but-1-ene (E_h) has already been shown to equal 12Kcal.mol^{-1}. Now, if the exchange and isomerisation of but-1-ene both occur via a 1-butyl species, the value obtained for E_i (15Kcal.mol^{-1}) would be expected to equal E_{oe}. However, it has already been shown that the term ($E_{oe} - E_h$) for but-1-ene is equal to 10Kcal.mol^{-1} indicating that $E_{oe} \geqslant$ 22Kcal.mol^{-1}. It must, therefore, be concluded that isomerisation and exchange do not occur via the same reaction intermediate.

10.2.4. Conclusions

By correlation of the postulates which have been proposed in the preceding sections, it is now possible to formulate the complete picture of the reactions of but-1-ene with hydrogen over silica-supported triruthenium dodecacarbonyl.

It has been concluded that the rate of hydrogenation

of but-1-ene is relatively slow compared with the rates of hydrogenation of cis and trans but-2-ene. Although it has not been possible to identify the slow step in the hydrogenation reaction, considerations of the relative activation energies for hydrogenation and olefin exchange have led one to conclude that these reactions proceed by a Rideal-Eley mechanism and that the activation of molecular hydrogen occurs by its reaction with an adsorbed olefin molecule to form a butyl intermediate and an adsorbed hydrogen atom. If this latter step is rate-determining, then the relative strengths of adsorption of the butenes will determine their relative rates of hydrogenation. If, on the other hand, the addition of a further hydrogen atom to the butyl intermediate is rate-limiting, the relative rates of hydrogenation of but-1-ene and the but-2-enes will be determined by the relative stabilities of the adsorbed 1-butyl and 2-butyl intermediates respectively.

Evidence from the isomerisation and exchange reactions has led one to believe that hydrogenation and isomerisation do not occur on the same surface sites. While the surface coverage of olefin on the sites for hydrogenation has been shown to be high, the kinetics of the isomerisation reaction are consistent with the surface coverage being low on the sites active for isomerisation. (These kinetics might also be explained by there being very few sites

on the surface available for this process and by their number increasing with increasing pressure of but-1-ene. Partial blocking of these sites by adsorbed hydrogen would also explain the slightly negative order obtained for hydrogen in isomerisation.) Furthermore, a comparison of the relative values of the activation energies for the exchange and isomerisation of but-1-ene indicates that these reactions do not proceed by the same mechanism. It is, therefore, considered that the principal mechanism for the isomerisation of but-1-ene is via a 1-methyl-π-allyl intermediate by inter- or intra-molecular hydrogen transfer.

From the results of the exchange reaction, it has been concluded that the slow step in the exchange of the butenes is the loss of a hydrogen atom from the adsorbed butyl intermediate. It is believed that the activation energy for this process is lower in the case of the but-2-enes than for but-1-ene and that the relative rates of exchange of the butenes ~~is~~ are determined by the relative stabilities of the appropriate butyl intermediates.

10.2.5 Reactions over Silica Supported Triosmium Dodecacarbonyl

Because no kinetic data are available for the hydrogenation and isomerisation of but-1-ene on this catalyst,

discussion of the mechanisms is severely restricted. However, a number of interesting features of the isomerisation reaction did appear from this study. First, at temperatures at which hydrogenation occurred (ca. 200°C) no isomerisation of but-1-ene in the absence of hydrogen was observed in the test reactions: this may be because the reaction was too slow to be detected in the pulse-flow system. Second, the butene distribution curves show a continuous trend towards the equilibrium values. Although both these features contrast with those of the reactions over the ruthenium complex, they do not rule out the possibility that a similar mechanism is operative; since the reactions were so slow, the results could simply be indicative of thermodynamic control being operative at this temperature, rather than the kinetic or geometric control which was postulated for the ruthenium complex.

The product distributions of the exchange reactions are also in contrast with those over the ruthenium complex and the proportions of exchanged butenes were shown to be similar at all conversions. An important similarity with the reactions over the ruthenium complex, however, is the high proportion of d_0-butenes at low conversion.

If one assumes that the same mechanism is operative over both complexes and that exchange occurs principally via a 1-butyl intermediate, then the differences in product

distributions must be due to a smaller difference in the strengths of adsorption either of but-1-ene and the but-2-enes or of the 1-butyl and 2-butyl intermediates. Thus, at an elevated temperature, thermodynamic control of the reaction would predominate and the geometric factors would lessen in importance. This being so, the strengths of adsorption of the three butenes on this catalyst might be similar.

Thus, if in this case exchange occurs mainly via 1-butyl, the but-1-ene-d_1, being the most abundant exchanged species, will contain the deuterium atom on the 2-position unless multiple reactions occur. Isomerisation of this species by loss of an α -hydrogen atom produces a C_4H_7-d_1 species which may then gain a further deuterium atom or a hydrogen atom. These results, therefore, are consistent with the same mechanisms being operative in both systems.

10.3 The Olefin-Metal Complex

The first step in the reaction of but-1-ene on the active catalyst must be its adsorption or coordination to the complex to form an intermediate. In view of the discussion in section 10.1 as to the nature of the active species, this intermediate might be of the form (A)

$$\left[(C_4H_8)Ru(CO)_{4-x}L_{x-1}\right]_n \qquad \text{Form (A)}$$

in which the olefin is coordinated to the metal via a π-bond and in which L would be a hydride ligand or some link to the surface of the silica. One other species which might be considered is one in which the olefin acts as a bridging ligand similar to a σ-diadsorbed species to produce a structure of the form (B):

$$\left[L_{x-1}(CO)_{4-x}Ru(C_4H_8)Ru(CO)_{4-x}L_{x-1}\right] \qquad \text{Form (B)}$$

It is considered, however, that such a complex might be too stable to react further and would play little part in the reaction.

Considering form (A), we have two alternatives for the next step in the reaction: addition of hydrogen to form a butyl species (where the hydrogen may have come either from the support or from the gas phase via the metal or alternatively from the reaction of molecular hydrogen); or the loss of a hydrogen atom from the butene to form a π-allyl complex. Exchanged but-1-ene, therefore, would be formed by the loss of a hydrogen atom from a 1-butyl intermediate, while isomerisation would proceed by the addition of hydrogen to the π-allyl complex. These steps could be further complicated by the possibility that hydrogen might be lost from or donated to adjacent

metal atoms.

Migration of hydrogen from the support, which has been invoked for the reaction of buta-1,3-diene with deuterium on alumina supported gold (124), would have important implications which were not considered in section 10.2. First, the high proportion of d_0 and d_1 n-butane might be produced by the addition of hydrogen which had migrated from the support and second, the initial distributions of deutero-but-2-enes might be explained by postulating the addition of migratory hydrogen to but-1-ene to form a 2-butyl species which might then isomerise, thus precluding the necessity for a special site for isomerisation. Migratory hydrogen used up in this way could then be replaced by the adsorption of hydrogen from the reaction mixture. It is considered, however, that this second implication is unlikely, as it explains neither the difference in rates of hydrogenation of the butenes nor the induction period before the onset of hydrogenation: further evidence for this viewpoint, however, could only be provided by experiments using a support with deuterium-exchanged hydroxyl groups.

Having decided that there are two different sites on the catalyst surface, there still remains the question of why this should be. From the lack of diffraction patterns of the supported complex, it is unlikely that

this question may be answered by reference to lattice sites. It might, however, be explained by the structure of the active complex. If, for the sake of simplicity, one considers that the active complex retains the metal trimer, this structure might be asymmetrical, such that only one or two of the metal atoms are bound to the surface. Similarly, not all three metal atoms require to be bound to a hydride ligand. If this is the case, then at least two distinct types of environment are possible and the environment of each particular metal atom would determine its catalytic characteristics.

10.4 Conclusions

The results of these experiments show that by supporting a transition metal carbonyl on silica, a catalyst active in the hydrogenation and isomerisation of butenes may be prepared. Since neither the complex nor the support alone is active in these reactions, both must be essential constituents of the system. Furthermore, a prerequisite of activation of the supported complex is its loss of some carbon monoxide. From these observations, it is concluded that the support acts as a catalyst in the activation of the complex.

The results of the hydroisomerisation, isomerisation and exchange reactions lead one to the conclusion that

the isomerisation reaction proceeds via a 1-methyl-π-allyl intermediate; this mechanism satisfactorily explains most of the characteristics of the reaction and its product distributions and there is no evidence which contradicts this postulate. Similarly, one concludes that but-1-ene coordinates to the catalyst much more strongly than the but-2-enes and that it undergoes exchange more slowly than these isomers.

It is believed that hydrogenation occurs by a Rideal-Eley mechanism and that activation of hydrogen proceeds by the reaction of physically adsorbed molecular hydrogen with an adsorbed butene molecule.

Finally, it is concluded that two distinct 'sites' exist on this catalyst: one of these being active in the isomerisation reaction and the other in the hydrogenation and exchange reactions.

CHAPTER 11

DISCUSSION OF THE OTHER SUPPORTED SYSTEMS

In this chapter, the results of the other systems which were studied will be discussed. Particular attention will be given to silica supported rhodium trichloride and tristriphenylphosphine rhodium chloride. The natures of the supported complexes and the abilities of the supported complexes to catalyse the isomerisation of but-1-ene will be discussed in terms of the structures and the stabilities of the complexes.

11.1 Silica Supported Rhodium Trichloride

Because of the lack of information on the physical characteristics of the supported complex, it is not possible to postulate the structure of the active form of this catalyst. However, from the evidence that the colour of the supported complex darkens on heating from pink to brick red, one might speculate that this reversible transition could be caused by an increase in the ligand field splitting of the d-orbitals of the metal ion. Such an increase could be due to the participation of the support in the transition by becoming weakly coordinated to the rhodium atom by the displacement of coordinated water. Such participation would be analogous to that postulated for solvent molecules in the isomerisation of terminal

olefins catalysed by rhodium complexes in the homogeneous phase (64,65).

The principal features to emerge from the studies of the isomerisation of but-1-ene to cis and trans but-2-ene are that at each of the three temperatures, the percentage conversion decreased with increasing injection number, as did the trans/cis ratio which, in the run at 70°C, fell below unity. Thus as the activity of the catalyst decreased, formation of the cis isomer became more favourable relative to the trans isomer.

The homogeneous isomerisation of olefins by rhodium complexes has already been described in section 1.5.3 and Fig. 1.7 and it has been postulated that an alkyl species is the intermediate in this reaction (65). It has also been suggested that the alcoholic solvent would be the source of hydrogen to produce this species.

In the supported system, the only source of hydrogen is the support itself and, if an alkyl reversal mechanism is operative in this case, one may postulate the participation of the support in the activation of the complex for catalysis. Such participation would require the migration of hydrogen atoms from surface hydroxyl groups of the support to the rhodium atom to form an intermediate hydride complex. By direct transfer of this hydrogen atom to the coordinated olefin, an intermediate alkyl

species would be produced. This species, by loss of a hydrogen atom, could then revert to but-1-ene or isomerise to cis or trans but-2-ene.

If a 1-methyl-π-allyl species is the intermediate, no such participation of the support need be involved. A coordinated but-1-ene molecule would form the π-allylic intermediate by loss of a hydrogen atom, which could coordinate to rhodium. Addition of this hydrogen atom to the π-allyl species could result in the production of cis or trans but-2-ene.

Because of the lack of available kinetic data, it is not possible to choose between the merits of these mechanisms in this instance. Powerful evidence might be obtained by studying a system in which the surface of the support had been previously deuterated and determining the extent of deuterium incorporation, if any, into the product hydrocarbons.

The effect of injecting successive pulses of but-1-ene at each of the three temperatures is shown in table 5.1. The deactivation is greatest between the first and second pulses of but-1-ene and this is greater at lower temperatures. Since there were no signs of the presence of rhodium metal on the catalyst, even after multiple injections of but-1-ene, the deactivation is unlikely to have been due to the reduction of the complex. It

is reasonable to assume, therefore, that the deactivation was caused by the accumulation on the surface of very strongly coordinated hydrocarbon species, which could reduce the number of sites available for the adsorption of the reactant in successive pulses. These observations suggest that in the experiments by Acres and co-workers (95) on the isomerisation of pent-1-ene to cis and trans pent-2-ene catalysed by a supported solution of rhodium trichloride, reduction of the salt was probably caused not by the olefin but by the solvent.

The decrease in the trans/cis ratio of the product but-2-enes might be explained by postulating that there are at least two types of site on the catalyst: on one of these, cis but-2-ene would be formed preferentially and on the other, the major product would be trans but-2 ene. If the site on which cis but-2-ene is formed preferentially were to be deactivated at a slower rate than that for trans but-2-ene, then the trans/cis ratio would be expected to decrease with loss of activity. It is significant, therefore, that evidence has been found elsewhere for the preferential formation of the cis isomer in the rhodium trichloride catalysed isomerisation of hex-1-ene (65a).

11.2 Silica Supported Tristriphenylphosphine Rhodium Chloride

It is apparent from the infra-red data obtained in this study that, by placing the complex in intimate contact with the support, the complex undergoes a structural rearrangement such that two new bands appear at 1460 and 1990 cm^{-1}. The band at 1990 cm^{-1} appears in the region where one expects to see metal-hydride and carbonyl absorptions and it may be deduced that the process resulting in the new species is one of the following:

(a) addition of carbon monoxide to the metal from an organic carbonyl impurity in the solvent;

(b) transfer of hydrogen to the metal from the support;

(c) intra-molecular hydrogen transfer to the metal from a ligand;

(d) addition of hydrogen to the metal from the solvent or impurities therein.

The observation that the new peaks are present in the spectra of the complex supported from spectroscopic grade benzene and from very pure deuterochloroform eliminates alternatives (a) and (d). The spectroscopic evidence does not, however, allow a clear distinction to be made between alternatives (b) and (c).

If a hydride ligand is provided by the support, then it is to be expected that the spectrum of the complex supported on the deuterated surface would show a decrease

in intensity of the band at 1990 cm^{-1} and the appearance of a new band at 1407 cm^{-1}, corresponding to ν(Rh-D). Although the former feature is observed, the latter is not. If, on the other hand, the hydride ligand is provided by intra-molecular hydrogen transfer, one expects no reduction at all in the intensity of the peak at 1990cm^{-1}.

The peak at 1460 cm^{-1}, however, which appears in the region for ν(C-H) may indicate a change in the symmetry of one of the benzenoid rings, caused by the loss of a hydrogen atom. The resulting complex might be of the form (A) containing a rhodium-carbon σ-bond (Fig. 11.1). A similar structure has been postulated by Bennett and Miller to explain the spectra of some iridium-triphenylphosphine complexes (125).

A complex formed by the transfer of hydride from the support, however, would be expected to be bound to the surface and to be of the form (B). The spectrum of this complex would not be expected to show a peak at 1460 cm^{-1}. (See Fig. 11.1)

Since the supported complex is active in neither the isomerisation nor the hydrogenation of but-1-ene, then this must have a relatively stable structure. This is in distinct contrast with the corresponding homogeneous system where the triphenylphosphine is relatively labile and the replacement of one of these ligands with a solvent

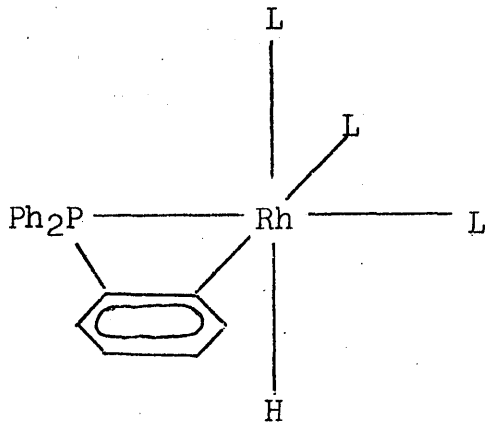

Structure (A) Formed by intra-molecular hydrogen transfer.

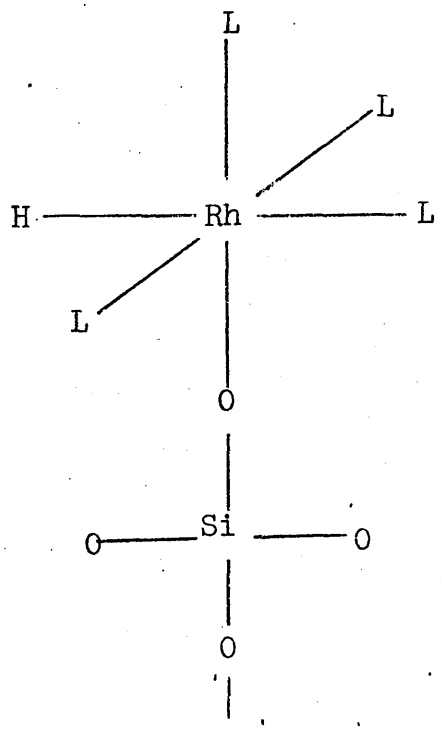

L = Ph_3P or Cl

Structure (B) Formed by transfer of hydrogen from the support.

Fig. 11.1

molecule during the hydrogenation of olefins is considered to be an integral part of the reaction mechanism (59). If the earlier postulates are valid and interaction of the support with the complex produces hydride complexes similar to (B), these complexes might also be expected to be catalytically active. This is further evidence in favour of structure (A) which might be structurally stable. Intensive spectroscopic investigation is required, however, before any more definite conclusions may be drawn.

11.3 Potassium Ethylene Trichloroplatinate and Ethylene Palladous Chloride

Although potassium ethylene trichloroplatinate is monomeric and ionic whereas ethylene palladous chloride is dimeric and covalent, both compounds will be considered together because of their common property of containing a metal-olefin π-bond. Of the compounds examined in the present study, these were the only complexes containing an olefin ligand. It is the lability of this ligand which renders these complexes extremely sensitive to nucleophilic attack by water leading to their decomposition to the metal (80,126).

It was observed that these complexes decomposed on contact with the dry support under a stream of dry nitrogen.

In previous sections it was suggested that surface hydroxyl groups on the support are capable of interacting with the supported metal complexes and it is envisaged that the decomposition of these complexes is the result of such interaction. Nucleophilic attack by the oxygen atom of a surface hydroxyl group could lead to the displacement of ethylene from the complex: a coordinated oxygen atom would tend to pull electrons from the metal-olefin bond, which would be weakened due to the decrease in π-electron back-donation from the metal to the olefin. The resulting transitory species would be unstable and would decompose to the metal.

Hayes (96) has reported that it is possible to successfully support ethylene platinous chloride on alumina and has used this system as a catalyst in the hydrogenation of ethylene to ethane. Thus the platinum complex is probably more robust than the analogous palladium complex and it appears that the relative stabilities of the complexes must be the critical factor in their abilities to be supported.

CHAPTER 12

GENERAL CONCLUSIONS

From the studies reported in this thesis, it is apparent that the support/complex systems may be arranged into three general categories, each of which contains at least two sub-groups. These are listed below.

(i) Complex retains its structure on the support.

(a) System inactive in the hydrogenation or isomerisation of olefins, e.g.

$(C_5H_5)_2TiCl_2/SiO_2$.

(b) System active in the hydrogenation and/or isomerisation of olefins, e.g.

$[(C_2H_4)PtCl_2]_2/Al_2O_3$ (96).

(ii) Complex undergoes change of structure on the support.

(a) System inactive in the hydrogenation or isomerisation of olefins, e.g.

$(Ph_3P)_3RhCl/SiO_2$.

(b) System active in the hydrogenation and/or isomerisation of olefins, e.g.

activated $Ru_3(CO)_{12}/SiO_2$.

(iii) Complex decomposes to the metal on contact with the support, e.g. $Fe_3(CO)_{12}/SiO_2$.

The most important factors contributing to the catalytic activity of transition metal complexes in the homogeneous

phase have been described in section 1.5.1 and it is believed that these factors are similarly important in the activity of the support/complex systems. It is recognised that in homogeneous systems, the solvent may not always be just a dispersant for the catalyst molecules but be able to act as a co-catalyst by being a source of hydrogen, for example in the isomerisation of olefins by alcoholic solutions of rhodium trichloride (65, 65a). Similarly, while it is believed that the alumina in the ethylene platinous chloride/alumina system (96) acts only as a dispersant, it is believed that the silica in the rhodium trichloride/silica system acts also as a co-catalyst by providing a "pool" of hydrogen atoms. The feature in the complex/support system of the dispersant acting in the destabilisation of some complexes to produce an active catalyst by causing a change in structure of the complex, as in the case of $Ru_3(CO)_{12}/SiO_2$, is also paralleled in homogeneous catalysis by the role of the solvent in the activity of tristriphenylphosphine rhodium chloride as a hydrogenation catalyst.

Parallels may also be drawn between complex/support and metal/support systems, although these are not always clear. Until recently, it was believed that the support played only a passive role in catalysis by a metal/support system, but various investigations (124,127,128,129) have produced evidence for the view that the support

does indeed provide a "pool" of hydrogen atoms which take part in catalytic reactions. The support may also interact chemically with the metal, thereby modifying the properties of the latter (130,131) and it may exert an influence on the structure of the metal (124).

In view of the many attempts to correlate the results of homogeneously and heterogeneously catalysed reactions, the kind of system used in the present study provides useful information on the properties of active catalysts and for the elucidation of reaction mechanisms. Because of the presence of ligands on the metal atom, it has been shown possible to observe directly changes in structure of the catalyst while studying reactions in the heterogeneous phase. Furthermore, it provides a method of observing reactions catalysed heterogeneously by single metal atoms in a complex.

Finally, from the results of the present study, it is believed that, by careful selection of complexes, it may prove possible to prepare highly selective and specific heterogeneous catalysts.

APPENDIX A

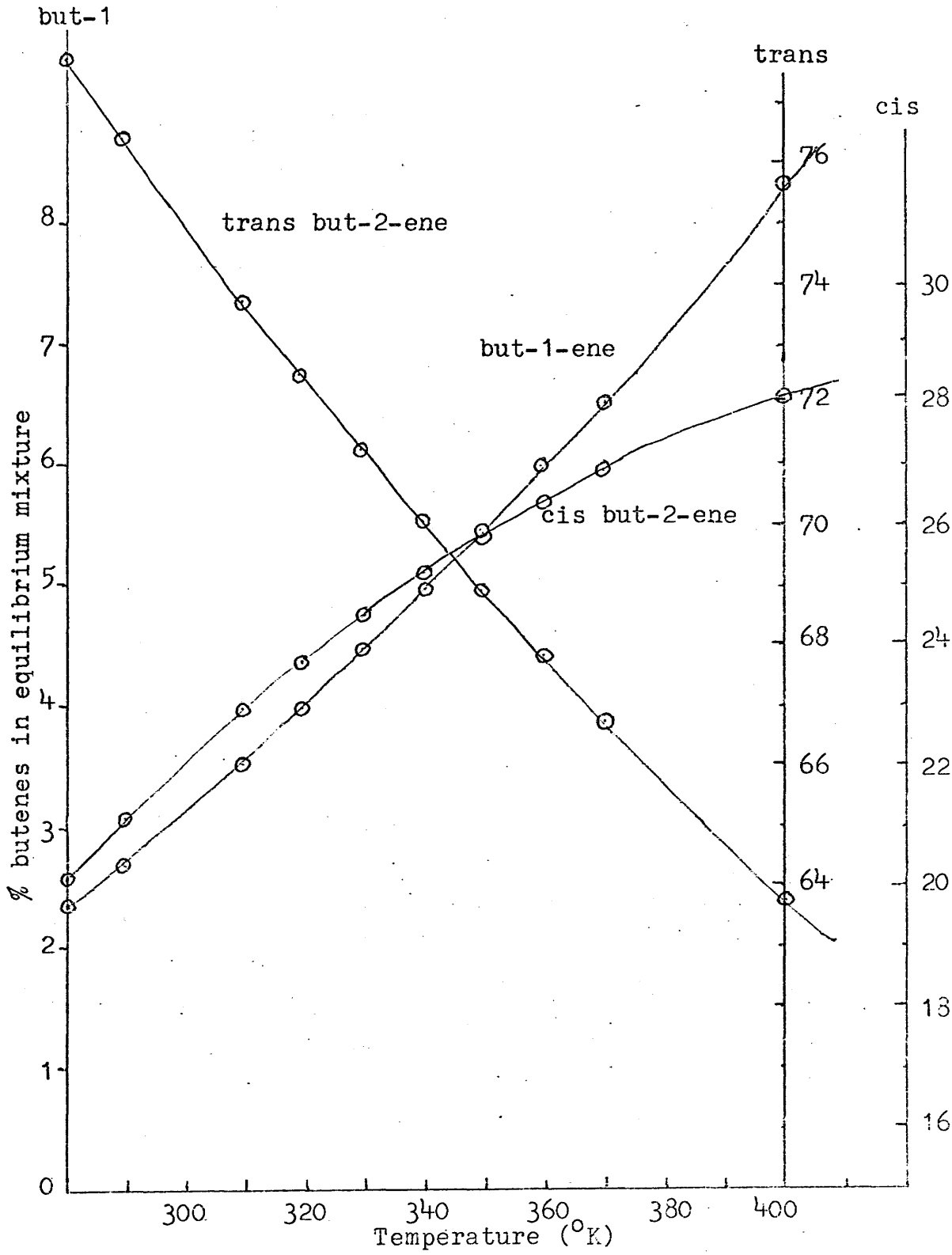

Equilibrium Distributions of the Butenes at Various Temperatures between 280 and 400°K.

APPENDIX B

Equations for calculation of parent ion concentration in mass spectrometric analyses.

The reason for the need to correct the measured intensity of each mass for the fragmentation of higher masses has been described. The full equations are listed below.

X = parent ion concentration (X = A,B,C,....etc.)
x = measured positive ion current (x = a,b,c,...etc.)
X' = parent ion concentration after correction for C^{13}
(X' = A',B',C',...etc.)

f_1 and f_2 are the fractions of the first and second fragments respectively.

A. n-Butane

m/e

68 A = a

67 B = b

66 $C = c - f_1(A + .10B)$

65 $D = d - f_1(.90B + .20C)$

64 $E = e - f_1(.80C + .30D) - f_2(A + .200B + .022C$

63 $G = g - f_1(.70D + .40E) - f_2(.80B + .356C + .067D)$

62 $H = h - f_1(.60E + .50G) - f_2(.623C + .467D + .133E)$

61 $I = i - f_1(.50G + .60H) - f_2(.467D + .534E + .222G)$

60 $J = j - f_1(.40H + .70I) - f_2(.333E + .556G + .333H)$

59 $K = k - f_1(.30I + .80J) - f_2(.222G + .534H + .467I)$

58 $L = l - f_1(.20J + .90K) - f_2(.133H + .467I + .623J)$

57 $M = m - f_1(.10K + L) - f_2(.067I + .356J + .800K)$

56 $N = n - f_2(.022J + .20K + L)$

Correction for C^{13}.

$L' = L$

$K' = K - 0.044L'$

$J' = J - 0.044K'$

etc.

B. n-Butenes

m/e

64 $A = a$

63 $B = b$

62 $C = c - f_1(A + .125B)$

61 $D = d - f_1(.875B + .25C)$

60 $E = e - f_1(.375D + .750C) - f_2(.250B + .036C + A)$

59 $G = g - f_1(.500E + .625D) - f_2(.107D + .429C + .750B)$

58 $H = h - f_1(.625G + .500E) - f_2(.214E + .536D + .536C)$

57 $I = i - f_1(.750H + .375G) - f_2(.357G + .572E + .357D)$

56 $J = j - f_1(.875I + .250H) - f_2(.536H + .536G + .214E)$

55 $(K = k - f_1(J + .125I) - f_2(.750I + .429H + .107G))$

54 $(L = l - f_1(J + .2501 + .036H))$

Correction for C^{13}.

$$J' = J$$

$$I' = I - 0.044J'$$

$$H' = H - 0.044I'$$

etc.

REFERENCES

1. I. Langmuir, J. Amer. Chem. Soc., 34, 1310 (1912).
2. J.E. Lennard-Jones, Trans. Faraday Soc., 28, 333 (1932)
3. H.S. Taylor, J. Amer. Chem. Soc., 53, 578 (1931)
4. H.S. Taylor, Proc. R. Soc., A108, 105 (1925)
5. G. Halsey and H.S. Taylor, J. Chem. Phys., 15, 624 (1947)
6. R.N. Pease, J. Amer. Chem. Soc., 45, 2296 (1923)
7. R.N. Pease and L. Stewart, J. Amer. Chem. Soc., 47, 1235 (1925)
8. P.M. Gundry and F.C. Tompkins, Quart. Rev., 14, 247 (1960)
9. L. Pauling, Proc. R. Soc., A196, 343 (1949)
10. A.A. Balandin, Z. Phys. Chem., 126, 267 (1927)
    " " B2, 289 (1928)
11. P.H. Emmett and N. Skau, J. Amer. Chem. Soc., 65, 1029 (1943)
12. P.H. Emmett, "New Approaches to the Study of Catalysis", Ch.3 (Priestly Lecture). The Pennsylvania State University, University Park (1962)
13. O. Beeck and A.W. Ritchie, Disc. Faraday Soc., 8, 159, (1950)
14. O. Beeck, Disc. Faraday Soc., 8, 118 (1950)
15. O. Beeck, A.E. Smith and A. Wheeler, Proc. R. Soc., A177, 62, (1940)
16. A.T. Gwathmey and R.E. Cunningham, Adv. Catalysis, 10, 57 (1958)
17. H.E. Farnsworth, Adv. Catalysis, 15, 31, (1964)
18. G.C. Bond, Disc. Faraday Soc., 41, 200 (1966)

19. G.C. Bond, Proc. 4th Intern. Cong. Catalysis (Moscow), 266 (1968)

20. R. Van Hardeveld and F. Hartog, Adv. Catalysis, 22, 75 (1972)

21. R. Van Hardeveld and A. Van Montfoort, Surface Sci., 4, 396 (1966)

22. R. Van Hardeveld and A. Van Montfoort, Surface Sci., 17, 90 (1969)

23. M. Boudart, J. Amer. Chem. Soc., 72, 1040 (1950)

24. G.M. Schwab, Disc. Faraday Soc., 8, 166 (1950)

25. A. Couper and D.D. Eley, Disc. Faraday Soc., 8, 689 (1950)

26. W.H.M. Sachtler, Discovery, 26, 16 (1965)

27. C.N. Hinshelwood, "The Kinetics of Chemical Change", Clarendon Press, Oxford (1966)

28. E.K. Rideal, Proc. Cambridge Phil. Soc., 35, 130 (1939)

29. J.I. Macnab and G. Webb, J. Catalysis, 10, 19 (1968)

30. G.I. Jenkins and E.K. Rideal, J. Chem. Soc., 2490, 2496 (1955)

31. S.J. Stephens, J. Phys. Chem., 63, 512 (1959)

32. B.M.W. Trapnell, Trans Faraday Soc., 48, 160 (1952)

33. P.W. Selwood, J. Amer. Chem. Soc., 79, 3346 (1957); Proc. 2nd Intern. Congress on Catalysis (Editions Technip, Paris 1961), 2, 1795

34. K. Morikawa, W.S. Benedict and H.S. Taylor, J. Amer. Chem. Soc., 57, 592 (1935)

35. K. Morikawa, N.R. Trenner and H.S. Taylor, J. Amer. Chem. Soc., 59, 1103 (1937)

36. J. Horiuti, G. Ogden and M. Polanyi, Trans. Faraday Soc., 30, 663 (1934)

37. J. Horiuti and M. Polanyi, Trans. Faraday Soc., 30, 1164 (1934)

38. G.K.T. Conn and G.H. Twigg, Proc. R. Soc., A171, 55 (1939)

39. G.C. Bond and P.B. Wells, Proc. 2nd Intern. Congress on Catalysis (Editions Technip, Paris 1961), 1, 1159

40. G.C. Bond, "Catalysis by Metals", Academic Press, London (1962)

41. F.C. Gault, J.J. Rooney and C. Kemball, J. Catalysis, 1, 255 (1962)

42. J.J. Rooney, J. Catalysis, 2, 53 (1963)

43. J.J. Rooney and G. Webb, J. Catalysis, 3, 488 (1964)

44. R.G. Guy and B.L. Shaw, Adv. Inorg. Chem. and Radiochem., 4, 77 (1962)

45. M.A. Bennett, Chem. Rev., 62, 611 (1962)

46. G.C. Bond and G. Webb, Platinum Metals Rev., 6, 12 (1962)

47. J.C. Brown and C.A. Brown, J. Amer. Chem. Soc., 85, 1003 (1963)

48. N.F. Foster and R.J. Cretanovic, J. Amer. Chem. Soc., 82, 4274 (1960)

49. J.E. Douglas and B.S. Rabinovitch, J. Amer. Chem. Soc., 74, 2486 (1952)

50. G.C. Bond and J. Turkevich, Trans. Faraday Soc., 49, 281 (1953)

51. G.H. Twigg, Disc. Faraday Soc., 8, 152 (1950)

52. J. Halpern, J.F. Harrod and B.R. James, J. Amer. Chem. Soc., 83, 753 (1961)

53. J. Halpern, B.R. James and A.L.W. Kemp, J. Amer. Chem. Soc., 83, 4097 (1961)

54. J.I. Macnab and G. Webb, J. Catalysis, 26, 226 (1972)

55. S. Carra and R. Ugo, Inorg. Chim. Act. Rev., 1, 49 (1967)

56. J. Halpern, Adv. Chem. Series, 70, 1 (1968)

57. B.R. James, Inorg. Chim. Act. Rev., 4, 73 (1970)

58. J. Halpern, J.F. Harrod and B.R. James, J. Amer. Chem. Soc., 88, 5150 (1966)

59. J.A. Osborn, F.H. Jardine, J.F. Young and G. Wilkinson, J. Chem. Soc., 1711 (1966)

60. J. Kwiatek, I.L. Mador and J.K. Seyler, Adv. Chem. Series, 37, 201 (1963)

61. J.C. Bailar Jr. and H. Italani, J. Amer. Chem. Soc., 89, 1592 (1967)

62. R.D. Cramer, E.L. Jenner, R.V. Lindsey Jr. and U.G. Stolberg, J. Amer. Chem. Soc., 85, 1691 (1963)

63. H.A. Tayim and J.C. Bailar Jr., J. Amer. Chem. Soc., 89, 3420 (1967)

64. R. Cramer, J. Amer. Chem. Soc., 88, 2272 (1966)

65. J.F. Harrod and A.J. Chalk, J. Amer. Chem. Soc., 88, 3491 (1966)

65a. J.F. Harrod and A.J. Chalk, J. Amer. Chem. Soc., 86, 1776 (1964)

66. L. Roos and M. Orchin, J. Amer. Chem. Soc., 87, 5502 (1965)

67. G.C. Bond and M. Hellier, J. Catalysis, 7, 217 (1967)

68. R. Cramer and R.V. Lindsey Jr., J. Amer. Chem. Soc., 88, 3534 (1966)

69. R. Cramer, J. Amer. Chem. Soc., 87, 4717 (1965)

70. see, e.g., A.J. Canale, W.A. Hewett, T.M. Shryne and E.A. Youngman, Chem. Ind. (London), 1054 (1962)

71. see, e.g., J.A. Osborn, G. Wilkinson and J.F. Young, Chem. Comm., 17 (1965)

72. see, e.g., P.M. Henry, Adv. Chem. Series, 70, 126 (1966)

73. F. Cariati, R. Ugo and F. Bonati, Inorg. Chem., 5, 1128 (1966)

74. P. Collman and W.R. Roper, J. Amer. Chem. Soc., 87, 4008 (1965)

75. J. Halpern, Am. Rev. Phys. Chem., 16, 103 (1965)

76. N.R. Davies, Australian J. Chem., 17, 212 (1964)

77. R.E. Rinehart and J.S. Lasky, J. Amer. Chem. Soc., 86, 2519 (1964)

78. M. Orchin, Adv. Catalysis, 16, 2 (1966)

79. G. Wilke, Angew. Chem., Intern. Ed., 2, 105 (1963)

80. G.E. Coates, M.L.H. Green, P. Powell and K. Wade, "Principles of Organometallic Chemistry" Methuen (1962)

81. J. Halpern and B.R. James, Can. J. Chem., 44, 671 (1966)

82. see, e.g., M.G. Burnett, P.J. Connolly and C. Kemball J. Chem. Soc. (A), 800 (1967)

83. L. Vaska and J.W. DiLuzio, J. Amer. Chem. Soc., 84, 670 (1962)

84. E.N. Frankel, E.A. Emken, H.M. Peters, V.L. Davidson and R.O. Butterfield, J. Org. Chem., 29, 3292 (1964)

85. E.N. Frankel, T.L. Mounts, R.O. Butterfield and H.J. Dutton, Adv. Chem. Series, 70, 177 (1968)

86. I. Ogata and A.Misono, Bull. Chem. Soc. Japan, 37, 439, 900 (1964)

87. L. Marko, Proc. Chem. Soc., 67 (1962)

88. L. Marko, Chem. Ind. (London), 260 (1962)

89. L. Vaska and R.E. Rhodes, J. Amer. Chem. Soc., 87, 4970 (1965)

90. J. Halpern, Proc. 3rd Intern. Cong. Catalysis, (Amsterdam, 1965)

91. R.S. Nyholm, ibid.

92. G.C. Bond, Adv. Chem. Series, 70, 25 (1968)

93. J.L. Garnett, Catalysis Rev., 5, 229 (1972)

94. G.C. Bond, J.J. Phillipson, P.B. Wells and J.M. Winterbottom, Trans. Faraday Soc., 62, 443 (1966)

95. G.J.K. Acres, G.C. Bond, B.J. Cooper and J.A. Dawson, J. Catalysis, 6, 139 (1966)

96. K.E. Hayes, Nature, 210, 412 (1966)

97. M. Misono, Y. Saito and Y. Yoneda, J. Catalysis, 10, 200 (1968)

98. R.L. Banks and G.C. Bailey, I. & E.C. Prod. Res. and Dev., 3, 170 (1964)

99. K.V. Williams and L. Turner, British Patent 1,116,243 (1968)

100. E.S. Davie, D.A. Whan and C. Kemball, J. Catalysis, 24, 272 (1972)

101. R.F. Howe, D.E. Davidson and D.A. Whan, J. Chem. Soc., Faraday Trans 1, 68, 2266 (1972)

102. M.L. Khidekel, A.D. Shebaldova and I.V. Kalechits, Russ. Chem. Rev., 40, 669 (1971)

103. J.L Dawes and J.D. Holmes, Inorg. Nucl. Chem. Letters, 7, 847 (1971)

104. R.J. Kokes, H. Tobin and P.H. Emmett, J. Amer. Chem. Soc., 77, 5360 (1955)

105. J.A. Hardy, J.I. Macnab and G. Webb, J. Sci. Instrum., 44, 959 (1967)

106. J.A. Hardy and G. Webb, Unpublished work

107. F. Schmidt-Bleek and F.S. Rowland, Anal. Chem., 36, 1696 (1964)

108. G.F. Taylor, Ph.D. Thesis, University of Glasgow (1967)

109. G.H. Twigg, Proc. R. Soc., A178, 106 (1941)

110. G. Webb, Ph.D. Thesis, University of Hull (1963)

111. F.H. Field and J.R. Franklin, "Electron Impact Phenomena" Academic Press, New York (1957)

112. C.W. Bradford, Platinum Metals Rev., 16, 50 (1972)

113. L.F. Dahl and J.F. Blount, Inorg. Chem., 4, 1373 (1965)

114. M.I. Bruce and F.G.A. Stone, Angew. Chem., Intern. Ed., 7, 428 (1968)

115. W. Beck and K. Lottes, Chem. Ber., 94, 2578 (1961)

116. H.P. Fritz and E.E. Paulus, Z. Naturforsch, 18b, 435 (1963)

117. D.K. Huggins, N. Flitcroft and H.D. Kaesz, Inorg. Chem., 4, 166 (1965)

118. D.M. Adams, "Metal Ligand and Related Vibrations", Arnold, London (1967)

119. C.R. Eady, B.F.G. Johnson and J. Lewis, J. Organometallic Chem., 57, C85 (1973)

120. F. L'Eplattenier and F. Calderazzo, Inorg. Chem., 6, 2092 (1967)

121. F. L'Eplattenier, P. Mathys and F. Calderazzo, Inorg. Chem., 9, 342 (1970)

122. D.W. Moore, H.B. Jonassen, T. Joyner and A.J. Bertrand, Chem. Ind., 1304 (1960)

123. G.C. Bond, J.J. Phillipson, P.B. Wells and J.M. Winterbottom, Trans Faraday Soc., 60, 1847 (1964)

124. D.A. Buchanan, Ph.D. Thesis, University of Glasgow (1972)

125. M.A. Bennett and D.L. Milner, J. Amer. Chem. Soc., 91, 6983 (1969)

126. J.S. Anderson, J. Chem. Soc., 971 (1934)

127. G.F. Taylor, S.J. Thomson and G. Webb, J. Catalysis, 12, 191 (1968)

128. J.A. Altham and G. Webb, J. Catalysis, 18, 133 (1970)

129. G.C. Bond, P.A. Sermon and J.B.P. Tipathi, Paper presented at Louvain meeting of Societe Chemique de Belgique, 1972

130. S.J. Thomson and G.A. Harvey, J. Catalysis, 22, 359 (1971)

131. F. Figueras, R. Gomez and M. Primet, Advan. Chem. Series, 121, 480 (1973)